4th International Conference on Magnetic Resonance Microscopy and Macroscopy

"Heidelberg Conference"

Division of Spatially Resolved Magnetic Resonance
of the
Groupement AMPERE

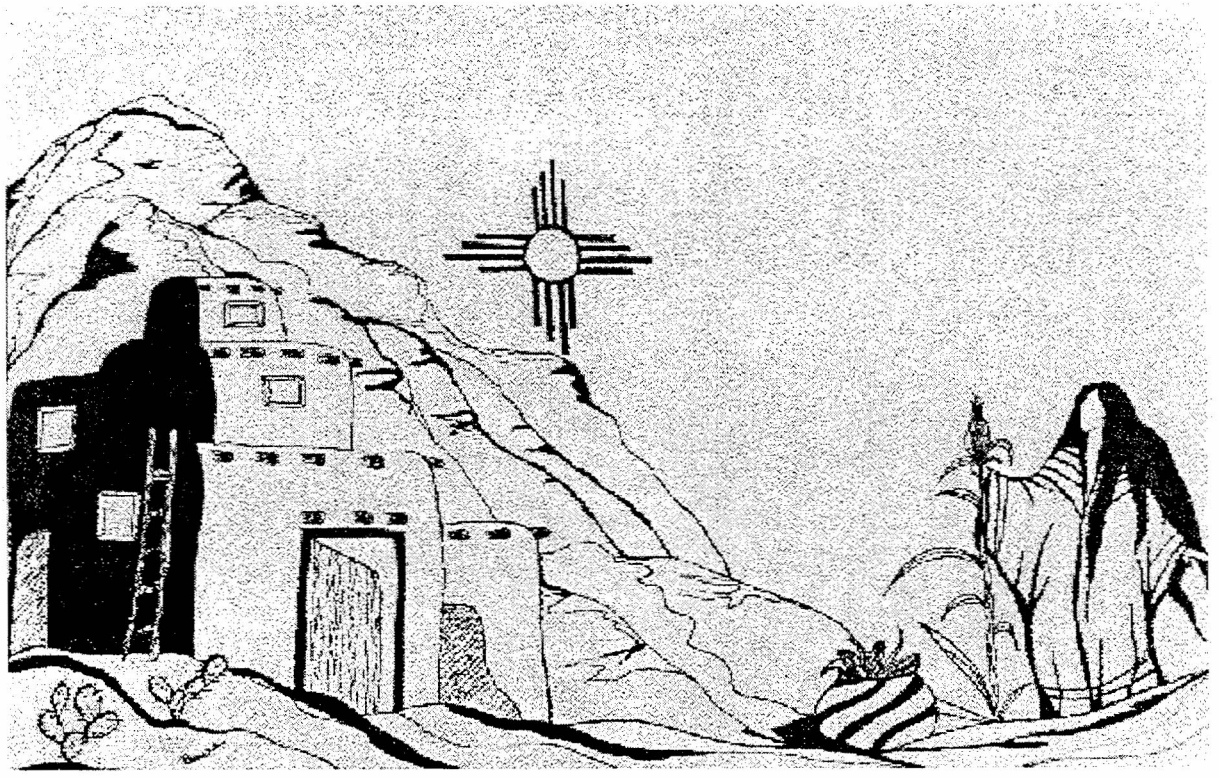

Albuquerque,New Mexico, USA

September 21-25, 1997

Book of Abstracts

Welcome to the 4th International Conference on Magnetic Resonance Microscopy (and Macroscopy) -- Heidelberg Conference. The inaugural conference was in Heidelberg in 1991, repeated in 1993, moved to Würzburg in 1995, jumped across the ocean to Albuquerque this year, and will return to Heidelberg in 1999. It is organized under the auspices of the "Division of Spatially Resolved Magnetic Resonance" of the AMPERE Society. An attraction is the introductory tutorial session which spans nearly two days. The scope of the conference has been broadened to include "macroscopy," reflecting the presence of features that are common to spatially resolved magnetic resonance that transcend physical scales.

SPECIAL EVENTS

- Saturday, September 20th -- Tutorial lectures followed by an informal social function.
- Sunday, September 21st -- Tutorial lectures, morning. Opening session at night with a special lecture by Paul Lauterbur.
- Monday, September 22nd -- Special Lecture by Jack Schmitt, Lunar Module Pilot on Apollo 17 and the only scientist/astronaut to ever walk on the moon.
- Tuesday, September 23rd -- Outing to Acoma Indian Pueblo in the afternoon. Special session "NMR and Internet" at night.
- Wednesday, September 24th -- General Assembly meets at 18:15.
- Thursday, September 25th -- Conference reception/party at Albuquerque Museum.

CONFERENCE OFFICE

The conference office will be located in the Kachina Room of the Sheraton. It will have an incoming telephone line for messages with the number to be available during the conference. It will also have terminals for accessing remote computers. A travel agent will be accessible by telephone.

SPONSORS: The financial assistance of the sponsors below is gratefully acknowledged.

- Bruker
- Doty
- Isotec
- Nalorac
- Siemens
- Smithkline Beecham
- Tecmag
- Varian

Division of Spatially Resolved Magnetic Resonance of the AMPERE Society: Officers

- W. Kuhn, Chair
- L. J. Berliner, Vice Chair
- B. Blümich, Secretary General
- G. A. Johnson, Vice Secretary General
- A. Haase, Treasurer
- E. Fukushima, Conference Chair
- E. R. Andrew, Senior Advisor

- L. D. Hall, Senior Advisor

Local Committee
Steve Altobelli, Beth Burns, Arvind Caprihan, Eiichi Fukushima, Alice Hannon, Jasper Jackson, Joe Seymour.

Conference art-work by Pam Trent.

Scientific Program

Schedule of Events
Saturday, September 20, 1997
Tutorial Session #1
10:00 - 11:00 Yang Xia, **"Introduction to magnetic resonance"**
11:30 - 12:30 Mark Haacke, **"Introduction to magnetic resonance imaging"**
12:00 - 14:00 Lunch
Tutorial Session #2
14:00 - 15:00 Paul Callaghan, **"Magnetic resonance microscopy"**
15:30 - 16:30 Al Garroway, **"Magnetic resonance macroscopy"**
17:00 - 19:00 Reception

Sunday, September 21, 1997
Tutorial Session #3
08:30 - 09:30 Larry Berliner, **"Introduction to electron spin imaging"**
10:00 - 11:00 Laurie Hall, **"Flow and diffusion measurements"**
11:30 - 12:30 Dave Cory, **"Solids Imaging"**

Opening Session (Chair: E. R. Andrew)
19:00 - 19:30 Welcome addresses and orientation
19:30 - 20:30 Opening lecture

Paul Lauterbur, *Biomedical Magnetic Resonance Laboratory, University of Illinois, Urbana, IL 61801, USA,* **"Notes on Gases, Gimmicks, Gels, and Gestation"**

Monday, September 22, 1997
08:30 - 10:15 Session #2: Biology I (Chair: M. Haacke)

08:30 - 09:15 M. von Kienlin and Axel Haase, *Institute of Physics, University of Würzburg, Germany*, **"Chemical Shift Microscopy"** (Siemens AG Lecture)

09:15 - 09:35 Y. Xia, *Physics Department, Oakland University, Rochester, MI 48309, USA*, **"Mapping T_1 and T_2 Anisotropy in Cartilage by Microscopic MRI (μMRI) at 14 μ m Pixel Resolution"**

09:35 - 09:55 R. Martin and M. Martin-Landrove, *Departamento de Fisica and Centro de Resonancia Magnetica, Facultad de Ciencias, Universidad Central de Venezuela, A.P. 47586, Caracas 1041-A, Venezuela*, **"A Novel Algorithm for Tumor Characterization by Analysis of Transversal Relaxation Rate Distributions in MRI"**

09:55-10:15 L. van der Weerd, T. Ruttink, D. van Dusschoten, F. Vergeldt, P. A. de Jager and H. Van As, *Wageningen Agricultural University, Dept. of Molecular Physics, Dreyenlaan 3, 6703 HA Wageningen, The Netherlands*, **"Imaging growth changes in plants during osmotic stress"**

10:45 - 12:30 Session #3: Solids I (Chair: R. Botto)

10:45 - 11:30 D. G. Cory, *Massachusetts Institute of Technology, NW14-4111, 150 Albany St., Cambridge, MA 02139*, **"NMR Microscopy and Pure NQR Imaging"**

11:30 - 12:00 S. Hafner, B. Traub and H.-W. Spiess, *Max-Planck Institut fur Polymerforschung, Postfach 3148, 55021 Mainz, Germany*, **"Magic Echo Imaging of Polymer Materials"**

12:00 - 12:30 R. Kimmich, *Universitat Ulm, Sektion Kernresonanzspektroskopie, 89069 Ulm, Germany*, **"Proton-detected ^{13}C Magnetic Resonance Imaging"**

12:30 - 14:00 Lunch (Executive Committee meets 12:30-14:00)

14:00 - 15:45 Session #4: Techniques (Chair: A. Haase)

14:00 - 14:25 W. S. Warren, *Princeton University, Department of Chemistry, Princeton, New Jersey*, **"MRI and fMRI using intermolecular zero-quantum coherences in solution"**

14:25 - 14:50 R. Bowtell and P. Robyr*, *Magnetic Resonance Centre, University of Nottingham, Nottingham, NG7 2RD, UK and *Department of Physical Chemistry, ETH-Zentrum, CH-8092, Zurich, Switzerland*, **"NMR Microscopy in Liquids Using the Dipolar Field"**

14:50 - 15:15 G. Zimmer, A. Guthausen, P. Blümler and B. Blümich, *Institut für Makromolekulare Chemie, RWTH Aachen, 52065 Aachen*, **"The NMR-MOUSE: NMR Relaxation Measurements on Soft Matter in Inhomogeneous Fields"**

15:15 - 15:30 H. Robert and D. Pusiol, *FaMAF, Universidad Nacional de Cordoba Ciudad Universitaria - 5000 Cordoba, Argentina*, **"Rotating-Frame NQR Imaging"**

15:30 - 15:45 Gorazd Planinsic[1] and Mark Symms[2], [1]*Physics Dept., University of Ljubljana, Jadranska 19, 1000 Ljubljana, Slovenia, ,* [2]*Institute of Neurology, London, WCIN 3BG, UK*, **"Spin-Echo in the Presence of Strong Gradient Field"**

16:15 - 18:00 Session #5: Electrons (Chair: L. J. Berliner)

16:15 - 16:45 G. R. Eaton, S. S. Eaton, and G. A. Rinard, *Departments of Chemistry and Biochemistry and Engineering, University of Denver, Denver, Colorado, 80208*, **"Frequency Dependence of EPR Sensitivity"**

16:45 - 17:15 S. Schlick, *Department of Chemistry, University of Detroit Mercy, Detroit, Michigan 48219, USA*, **"Electron Spin Resonance Imaging (ESRI) of Transport Processes in Polymers"**

17:15 - 17:40 J. L. Zweier, M. Chzhan, A. Samouilov and P. Kuppusamy, *Molecular and Cellular Biophysics Laboratories, Dept. of Medicine, and the EPR Center, Johns Hopkins University, Baltimore, MD 21224, USA*, **"Electron Paramagnetic Resonance Imaging of the Heart"**

17:40 - 18:00 P. C. Hammel[1], Z. Zhang[1], M. Midzor[2], M. L. Roukes[2] and J. L Childress[3], *[1]Los Alamos National Laboratory, Los Alamos, NM 87545, [2]California Institute of Technology, Pasadena, CA 91125, [3]University of Florida, Gainesville, FL 32611-2066,* **"Microscopic Characterization of Magnetic Materials Using Magnetic Resonance Force Microscopy"**

18:00 - 19:00 Special Lecture: (Chair: E. Fukushima)

Jack Schmitt , **"A scientist walks on the moon: The flight of Apollo 17"**

19:00 - 21:00 Poster reception

Tuesday, September 23, 1997

08:30 - 10:15 Session #6: Macroscopy I (Chair: A. N. Garroway)

08:30-09:15 R. L. Kleinberg, *Schlumberger-Doll Research, Ridgefield, Connecticut,* **"NMR Measurements of Crude Oils in Subsurface Earth Formations"**

09:15 - 09:45 A. De Los Santos and J. D. King, *Southwest Research Institute (SwRI), San Antonio, TX, USA,* **"Industrial Applications of NMR"**

09:45 - 10:15 L. J. Burnett, *Quantum Magnetics Inc., 7740 Kenamar Court, San Diego, CA 92121,* **"Several NDE Applications of NMR"**

10:45 - 12:30 Session #7: Biology II (Chair: Y. Kanazawa)

10:45 - 11:15 G. Navon[1], Y. Sharf[2], U. Eliav[1] and Y. Seo[3], *Schools of Chemistry[1] and Physics[2], Tel Aviv University, Tel Aviv 69978, Israel, [2]Dept. of Physiology, Kyoto Prefectural University of Medicine, Kamigyo-ku, Kyoto 602, Japan,* **"Histology and Strain Images of Blood Vessel Walls Using ^{2}H Double Quantum-Filtered MRI"**

11:15 - 11:45 Y. Seo[1], H. Takamiya[2], H. Ishikawa[3], T. Nakashima[3], Y. Sharf[4] and G. Navon[4], *[1]Dept. of Physiology, [2]Dept. of Orthopaedic Surgery & [3]Dept. of Medicine III Kyoto Prefectural Univ. of Medicine Kamigyo-ku, Kyoto 602, Japan [4]Schl. of Chemistry Tel Aviv Univ., Ramat Aviv, Tel Aviv, 69978 Israel,* **"NMR Imaging of Rigid Biological Tissues"**

11:45 - 12:05 J. Ruff, F. Wiesmann, K.-H. Hiller, S. Neubauer[1], W. R. Bauer[2], and A. Haase, *Physikalisches Inst., Universität Würzburg, [1] Med. Universitätsklinik, 97074 Würzburg, Germany, [2]II. Medizinische Universitätsklinik Mannheim/Heidelberg, 61835 Mannheim Germany,* **"Capability of Microscopic NMR imaging for In Vivo Quantification of Myocardial Function and Mass in Young (10g) Mice"**

12:05 - 12:30 W. Köckenberger[2], M. Heidenreich[1], A. Hudson[2], R. Bowtell[2] and R. Kimmich[1], *[1]Universitat Ulm, Sektion Kernresonanzspektroskopie, 89069 Ulm, Germany, [2]Magnetic Resonance Centre, University of Nottingham, Nottingham NG7 2RD, UK,* **"Investigation of the carbohydrate transport in plants by ^{1}H-detected ^{13}C spectroscopy and imaging by cyclic J cross polarisation"**

13:00 - 19:00 Conference outing to Acoma Pueblo

20:00 - 21:30 Session #8: Internet and NMR (Chair: D. Morris)

20:00 - 20:20 D. Morris, *Biomedical Magnetic Resonance Laboratory, University of Illinois U of I/BMRL 1307 West Park Street Urbana IL 61801*, **"Remote Microscopic NMR Imaging Via a Worldwide Web Interface to a Standard Imaging Spectrometer."**

20:30 - 20:50 Clinton Potter and Paul Lauterbur, *National Center for Supercomputing Applications, Biomedical Magnetic ResonanceLaboratory, and Beckman Institute. University of Illinois, Urbana IL USA,* **"ChickScope: WWW Control of an MRI for K-12 Education."**

21:00 - 21:20 Katsumi Kose, *Institute Of Applied Physics, University Of Tsukuba, Tsukuba-City 305 Japan*, **"Report on the Nuclear Magnetic Resonance Internet Conference Held in Japan."**

Wednesday, September 24, 1997
08:30 - 10:15 Session #9: Industrial Applications (Chair: J. Ripmeester)

08:30 - 09:00 Kevin R. Minard[1], Robert A. Wind [1], and Lee O. Dworjanyn[2], *[1]Pacific Northwest National Laboratory, P.O. Box 999, Richland, WA 99352, [2]Westinghouse Savannah River Co, Aiken, SC 29808*, **"MR Microscopy of Savannah River Tank Waste Simulants"**

09:00 - 09:30 D. Mueller, *BRUKER Analytik Silberstreifen, D-76287 Rheinstetten,* **"^{13}C Detection of Diamonds in Intact Stones"**

09:30 - 09:45 M. Szayna, R. Voelkel, L. Zedler, *BASF AG, 670~6 Ludwigshafen, Germany,* **"NMR microscopy in industrial research: polyurethane foams and poly (sodium acrylates)"**

09:45 - 10:00 S. N. Scrimgeour, G. Hunter, W. J. Harvey, C. H. Lloyd, D. Lane*, P. J. McDonald*, *Departments of Chemistry, Civil Engineering, and Dentistry, University of Dundee, Dundee DD1 4HN, Scotland, UK, *Department of Physics, University of Surrey, Guildford GU2 5XH, England, UK*, **"Stray Field Imaging (STRAFI) and Magnetic Resonance Microimaging (MRM) Studies of Water Intrusion/Stress Mobilisation in Dense Polymer Systems used in Construction"**

10:00 - 10:15 Nicole Black, Todd Vienneau[1], and Yong Pan, *Procter & Gamble Company, Miami Valley Laboratories, P. O. Box 538707, Cincinnati, OH 45253, [1]Procter & Gamble Pharmaceutical, 8700 Mason Montgomery, Mason, OH 45040*, **"NMR Microimaging, a Useful Tool to Study the Dissolution of Solids"**

10:45 - 12:30 Session #10: Macroscopy II (Chair: J. B. Miller)

10:45 - 11:30 O. A. Shushakov and V. M. Fomenko, *Inst. of Chem. Kinet. & Combust., 3, Institutskaya St., Novosibirsk 630090-RUSSIA*, **"Saturation of porous aquifers investigation using surface NMR"**

11:30 - 12:00 A. N. Garroway, M. L. Buess[+], J. B. Miller, K. J. McGrath, J. P.

Yesinowski, B. H. Suits[++] and G. R. Miller[*], *Code 6122, Chemistry Division, Naval Research Laboratory, Washington, DC 20375-5342 USA, [+]SFA, Inc., Landover MD, [++]Physics Department, Michigan Technological University, Houghton, MI 49931-1295, *University of Maryland, College Park, MD*, **"Nuclear Quadrupole Resonance (NQR) for detection of explosives and landmines"**

12:00 - 12:30 T. Rayner, A. D. Hibbs, B. Thorson, S. Beevor and L. J. Burnett, *Quantum Magnetics Inc., 7740 Kenamar Court, San Diego, CA 92121*, **"Quadrupole Resonance Explosive Detection Systems"**

12:30 - 14:00 Lunch (Division Committee meets 13:00-14:00)

14:00 - 15:45 Session #11: Flow and Diffusion I (Chair: J. Pope)

14:00 - 14:25 P. Blümler, K. Rombach, S. Laukemper-Ostendorf, and B. Blümich, *Institut für Makromolekulare Chemie and Zentrum für Magnetische Resonanz, Rheinisch-Westfälische Technische Hochschule Aachen, D-52074 Aachen, Germany*, **"Applications of Flow Imaging in Materials Science"**

14:25 - 14:45 M. M. Britton and P. T. Callaghan, *Department of Physics, Massey University, Palmerston North, New Zealand*, **"Non-Newtonian rheology as probed by NMR microscopy"**

14:45 - 15:05 K. Ogawa, M. Tobo, N. Iriguchi, S. Hirai, and K. Okazaki, *Research Center for Carbon Recycling & Utilization, Tokyo Inst. of Tech., 2-12-1 Ookayama, Meguro-ku, Tokyo 152*, **"Simultaneous Measurement of Temperature and Velocity Maps by Inversion Recovery Tagging Method"**

15:05 - 15:25 U. Goerke and R. Kimmich, *Sektion Kernresonanzspektroskopie, Universität Ulm, 89069 Ulm, Germany*, **"NMR-Imaging Techniques for Quantitative Characterization of Periodic Motions: 'Incoherent Averaging' and 'Spectral Side Band Analysis'"**

15:25 - 15:45 S. A. Altobelli[1] and L. Mondy[2], *[1]New Mexico Resonance, 2425 Ridgecrest Dr. SE, Albuquerque, NM 87108, USA, [2]Sandia National Laboratory, Albuquerque, NM*, **"Inversion Nulling in Slurry Flow Imaging"**

16:15 - 18:00 Session #12: Solids II (Chair: R. Botto)

16:15 - 16:35 E. W. Randall, *Queen Mary and Westfield College, University of London*, **"Advances in Stray Field-Gradient Techniques"**

16:35 - 17:00 D.M. Lane and P. J. McDonald, *Department of Physics, University of Surrey, GU2 SXH, UK*, **"Stray Field Imaging Of Solvent Ingress In Polymers"**

17:00 - 17:20 T. G. Nunes[1], P. R. Bodart[2], and E. W. Randall[3], *[1]ICTPOL/IST, Departmento de Engenharia de Materiais, Av. Rovisco Pais 1, 1096 Lisboa Codex, Portugal, [2]Dept. of Chemistry, Durham University, South Road, Durham DH1 3LE, UK, [3]Chemistry Dept. Queen Mary and Westfield College, Mile End Road, London, E14NS, UK*, **"Stray-Field Magnetic Resonance Imaging of Hardening Materials"**

17:20 - 17:40 W. Kuhn, *IIC Innovative Imaging Corp., Blieskastel, Germany*, **"Several industrial applications of NMR Microscopy"**

17:40 - 18:00 G. R. Davies, S. J. McCallum, I. Nicholson, D. J. Lurie, and J. M. S. Hutchison, *Department of Bio-medical Physics, University of Aberdeen, Forester Hill, Aberdeen, Scotland. AB25 2ZD*, **"CW MRI of Short T^2 Materials"**

18:15 - 18:45 General Assembly
19:00 - 21:00 Poster reception

Thursday, September 25, 1997
08:30 - 10:15 Session #13: Other Nuclei or Gas Imaging (Chair: G. D. Mateescu)

08:30 - 08:55 L. W. Hedlund, X. J. Chen, M. S. Chawla, H. E. Moeller, G. P. Cofer, J. R. MacFall and G. A. Johnson, *Center for In Vivo Microscopy, Department of Radiology, Duke University Medical Center, Durham, NC 27710*, **"Imaging the Lungs with Hyperpolarized Helium"**

08:55 - 09:15 D. O. Kuethe[1], A. Caprihan[2], E. Fukushima[2], H. M. Gach[3], and I. J. Lowe[3], *[1]Lovelace Respiratory Research Institute, Albuquerque, NM 87108, [2]New Mexico Resonance, Albuquerque NM 87108, [3]University of Pittsburgh*, **"Imaging Obstructed Ventilation in Lungs using Inert Fluorinated Gases"**

09:15 - 09:35 R. E. Gerald II, R. J. Klingler, J. W. Rathke and G. Sandi[1], *Chemical Technology and Chemistry Divisions[1], Argonne National Laboratory, 9700 S. Cass Ave., Argonne, IL 60439*, **"*In situ* imaging of charge carriers in an electrochemical cell"**

09:35 - 09:55 D. M. Gregory, R. E. Gerald II and R. E. Botto, *Chemistry Division, Argonne National Laboratory, Argonne, IL 60439*, **"^{129}Xe MRM of Gaseous Probes in Silica Aerogels"**

09:55 - 10:15 R. A. Komoroski[1-4], J. M. Pearce[1,2] and J. E. O. Newton[4,5], *Departments of [1]Radiology, [2]Pathology, [3]Biochemistry, [4]Psychiatry, and [5]Pediatrics, University of Arkansas for Medical Sciences4301 West Markham St., Little Rock, AR 72205*, **"Lithium Visibility In Rat Brain And Muscle *In Vivo* By ^{7}Li Nmr Imaging"**

10:45 - 12:30 Session #14: Instrumentation (Chair: J. Murphy-Boesch)

10:45 - 11:10 K. Kose and T. Haishi, *Institute of Applied Physics, University of Tsukuba, Tsukuba, Ibaraki 305, JAPAN*, **"A Flexible Pulse Programmer for MRI using a Commercial Digital Signal Processor Board"**

11:10 - 11:35 E.R. Andrew, M. Kempka and E. Szczesniak, *Departments of Physics and Radiology, University of Florida, Gainesville, FL 32611*, **"Novel Transverse Gradient Coils for Magnetic Resonance Microscopy"**

11:35 - 12:00 S. Crozier and D. M. Doddrell, *Centre for Magnetic Resonance, The University of Queensland, St. Lucia, Qld 4072, Australia*, **"A Compact Superconducting Magnet for MR Microscopy"**

12:00 - 12:15 K. Bartušek and Jaroslav Vojta, *Institute of Scientific Instruments, Královopolská 147, 612 64 Brno, Czech Republic*, **"Increase in the precision of the Gradient Magnetic Field Measurement"**

12:15 - 12:30 H. Liu, *University of Minnesota, Box 292, 420 Delaware, Minneapolis, MN 55455*, **"Spherical gradient coil for MR microscopy"**

12:30 - 14:00 Lunch

14:00 - 15:45 Session #15: Porous Media and Diffusion (Chair: P. Stilbs)

14:00 - 14:30 B. J. Balcom, *MRI Centre, Department of Physics, University of New Brunswick, P.O. Box 4400, Fredericton, N.B. Canada, E3B 5A3*, **"SPRITE Imaging of Short Relaxation Time Nuclei"**

14:30 - 14:55 I.V. Koptyug[1], R.Z. Sagdeev[1], V N. Parmon[2] and L Yu. Khitrina[3], *[1]Inernational Tomography Center, [2]Boreskov Institute of Catalysis, and [3]Novosibirsk State University, Novosibirsk 630090, Russia*, **"Drying of porous catalyst support bodies: a penetrating look"**

14:55 - 15:20 D. A. Doughty and L. Tomutsa, *BDM Petroleum Technologies, PO Box 2543, Bartlesville, OK 74005*, **"Pore Structure and Connectivity of Porous Rock by High Resolution NMR Microscopy"**

15:20 - 15:45 E. Vasina[1], V. Skirda[1], V. Volkov[2], A. Nechaev[2], B. Mchedlishvili[2], *[1]Dept. Molecular Physics, Kazan State University, Kremlevskaya str.181 Kazan 420008, Russia, [2]Shubnikov Institute of Crystallography, RAS, Moscow, Russia*, **"The translational self-diffusion of 1,3-propylene glycol in track etched membrane pores"**

16:15 - 18:00 Session #16: Flow and Diffusion II (Chair: L.D. Hall)

16:15 - 16:50 J. Stepišnik, *Physics Department, FMF, UL, Jadranska 19, Ljubljana, Slovenia*, **"Diffusion, Restricted Diffusion and Motion Correlation by Microimaging"**

16:50 - 17:20 K. Woelk, *Inst. Phys. Chem., University of Bonn, Wegelerstr. 12, D-53115 Bonn, Germany*, **"Imaging Diffusion in Gels, Polymers, and Solids"**

17:20 - 17:40 D. Ailion, *Department of Physics, University of Utah, Salt Lake City, Utah 84112, USA*, **"Translational Diffusion of Water Molecules in Lung"**

17:40 - 18:00 P. T. Callaghan, *Department of Physics, Massey University, Palmerston North, New Zealand*, **"A simple matrix formalism for spin echo analysis of restricted diffusion under generalised gradient waveforms"**

18:00 - 21:00 Conference dinner/reception at Albuquerque Museum

Posters

Posters are listed alphabetically by first author with presenting author underlined. Poster numbers refer to the broad categories, Biological (B), Materials (M), Solids (S) and Techniques and Instrumentation (T). Odd numbered posters will be presented during the Monday evening poster session and even numbered posters will be presented during the Wednesday evening poster session. Posters will remain up for the entire conference.

Poster: S1
R.J. Abbott, J.A. Chudek, G. Hunter, R.L. MacKay, L. Squires*, P.J. McDonald§, *Department of Chemistry, University of Dundee, Dundee DD1 4HN, Scotland, UK, *Non-wovens Division, Don and Low plc., Glamis Road, Forfar, Angus DD8 1EY, Scotland, UK, §Department of Physics, University of Surrey, Guildford GU2 5XH, England, UK*, **"Stray Field Imaging (STRAFI) and Magnetic Resonance Microimaging (MRM) Studies of the Anistropic Absorption of Solvents by Extruded Polypropylene"**

Poster: B1
E.W. Abel*, J.A. Chudek, G. Hunter, R.M. Lord*, R.L. MacKay, and R.P. Mills+, *Department of Chemistry, University of Dundee, Dundee. DD1 4HN, UK, *Dept. of Biomedical Engineering, University of Dundee, Dundee. DD1 4HN, UK, +ENT Department, Ninewells Hospital, Dundee. DD1 9SY, UK*, **"MRM in the modelling of the ossicular chain"**

Poster: M1
D. Airey, V. Chen*, J. Wu* and J. M. Pope, *Centre for Medical and Health Physics, Queensland University of Technology, GPO Box 2434 Brisbane, Australia 4001 and *UNESCO Centre for Membrane Science and Technology, University of New South Wales, Sydney, Australia 2052*, **"Concentration Polarisation: An *in situ* study"**

Poster: T2
B.J. Balcom, M. Shea, S. D. Beyea, *MRI Centre, Department of Physics, University of New Brunswick, Fredericton, NB, E3B 5A3, Canada*, **"Single Point MR Measurements of Gradient Waveform"**

Poster: M2
Bernard Baldwin, *Phillips Petroleum Co., 103 GB, Bartlesville, OK 74004*, **"Capillary Pressure Curves from MRI Images of Centrifuged Reservoir Rock"**

Poster: M3
Alfonso Benavides*, Sigifredo Gonzalez, Damaris Barrantes and Miguel Martin-Landrove, *Departamento de Fisica and Centro de Resonancia Magnetica, Facultad de Ciencias, Universidad Central de Venezuela , A.P. 47586, Caracas 1041-A, Venezuela and *Instituto de Ciencias de la Tierra , Facultad de Ciencias, Universidad Central de Venezuela, A.P. 47586, Caracas 1041-A, Venezuela*, **"Simulated relaxation rate and local magnetic field distributions in porous systems"**

Poster: M4

S.D. Beyea, B.J. Balcom, P.J. Prado, R.L. Armstrong and T.W. Bremner[1], *Magnetic Resonance Imaging Centre and [1]Department of Civil Engineering, University of New Brunswick, Fredericton, NB, E3B 5A3, Canada*, **"Moisture Profiles of Drying Concrete using Single-Point Imaging (SPI)"**

Poster: M5
S.D. Beyea[1], B.J. Balcom[1], P.J. Prado[1], R.L. Armstrong[1], T.W. Bremner[2] and P.E. Grattan-Bellew[3], *[1]Magnetic Resonance Imaging Centre and [2]Department of Civil Engineering, University of New Brunswick, Fredericton, NB, E3B 5A3, Canada, [3]Institute for Research in Construction, NRC, Ottawa, ON, K1A 0R6 Canada*, **"3D microscopy of moisture at the paste/aggregate transition zone in hardened concrete using SPRITE"**

Poster: B2
Stephen J Blackband, *University of Florida, PO Box 100245, Gainesville, FL 32610*, **"Diffusion weighted MR microscopy of isolated brain slices"**

Poster: M6
A.J. Bohris[+], P.J. McDonald[+], M. Mulheron[*], B. Newling[+] and B. LePage[*], *Departments of Physics[+] and Civil Engineering[*], University of Surrey, Guildford, Surrey, GU2 5XH, UK*, **"A broad line magnetic resonance imaging study of water transport in cementitious building materials"**

Poster: T3
A. J. Bohris[*], D. A. Faux[*], D. G. Gillies[+] and P. J. McDonald[*], *Departments of [*]Physics and [+]Chemistry, University of Surrey, GU2 5XH, UK*, **"The analysis and development of pulse sequences for self diffusion weighted stray field imaging"**

Poster: B16
Sudeep Chandra, Konstantin Gurbanov, Robert Strittmatter, Eliot H. Ohlstein, Giora Z. Feuerstein and Susanta K. Sarkar, *SmithKline Beecham Pharmaceuticals, 709 Swedeland Road, King of Prussia, PA-19406*, **"High resolution in vivo magnetic resonance microscopy of the rat heart at 4.7 T using a local RF transceiver coil"**

Poster: S2
J.A. Chudek, G. Hunter, F. Mohd. Som, P.J. McDonald*, B. Newling*, *Department of Chemistry, University of Dundee, Dundee DD1 4HN, Scotland, UK, *Department of Physics, University of Surrey, Guildford GU2 5XH, England, UK*, **"Stray field imaging (STRAFI) and magnetic resonance microimaging (MRM) studies of high impact polystyrene, an elastomer-toughened material"**

Poster: B3
J.A. Chudek, I.E. Geoghegan#, G. Hunter, R.L. MacKay, M.E.N. Majerus+, S. Moritz, R.J. McNicoll# and A.N.E. Birch#, *Department of Chemistry, University of Dundee, Dundee, DD1 4HN, UK, #Scottish Crop Research Institute, Invergowrie, Dundee. DD2 5DA, UK, +Dept. of*

Genetics, University of Cambridge, Cambridge, CB2 3EH, UK, **"MRM, an alternative approach to the study of host/parasitoid relationships in insects"**

Poster: T4
Sarah L. Codd and Paul T. Callaghan, *Department of Physics, Massey University, Palmerston North, New Zealand*, **"Generalised Treatment of Modulated Gradient Spin Echo Attenuation for Restricted Diffusion in Spherical Pores"**

Poster: B4
G. J. Cowin, I. A. Leditschke, S. Crozier* and Z.H. Endre, *Dept. of Medicine and *Centre for Magnetic Resonance, The University of Queensland, St. Lucia, Qld 4072, Australia*,**"Does hypoxia produce alterations in cortical and medullary osmolyte concentrations? An assessment by volume localised ^{1}H magnetic resonance microspectroscop (MRS)"**

Poster: T5
S. Crozier, W. U. Roffman and D. M. Doddrell, *Centre for Magnetic Resonance, The University of Queensland, St. Lucia, Qld 4072, Australia*, **"Novel, asymmetric gradient coil sets for MRM"**

Poster: B5
Yoshihiro Doi and Yoko Kanazawa, *Faculty of Pharmaceutical Sciences, Kyushu University, Fukuoka 812-82, JAPAN*, **"^{19}F chemical shift imaging of F-nuc formed from 5-FU in mouse tumor: Fast spin echo vs. spin echo for a short T_2 signal"**

Poster: T6
A. Duh[1], J. Stepisnik[2,3], A. Mohoric[2] and I. Sersa[3], *[1]Institute of Mathematics and Physics, University of Maribor, Faculty of Electrical Engineering and Computer Science, Smetanova 17, 2000 Maribor, Slovenia, [2]Physics Dept., University of Ljubljana, Jadranska 19, 1000 Ljubljana, Slovenia, , [3]J. Stefan Institute, Jamova 39, 1000, Ljubljana, Slovenia*, **"Diffusive edge enhancement in NMR microscopy"**

Poster: T7
K.V. Ermolaev, N.N. Volkova, V.A. Dubovitskij and L.N. Erofeev, *Institute for Chemical Physics, Chernoglovka, Moscow, Russia,* **"Nongradient NMR Imaging of Solid Polymers"**

Poster: M7
Colin A. Fyfe, Almira I. Blazek, Hiltrud Grondey, Brian J. Fahie[1], Avinash Nagia[1] and Sham K. Chopra[1], *Department of Chemistry, University of British Columbia, 2036 Main Mall, Vancouver, B.C., Canada V6T 1Z1, [1]Pharmaceutical Sciences Division, Glaxo Wellcome Inc., 7333 Mississauga Road, Mississauga, Ontario, Canada L5N 6L4*, **"NMR Imaging in the Development of Formulations for the Controlled Release of Drugs"**

Poster: S3

C. A. Fyfe, Z. Mei and H. Grondey, *Chemistry Department, University of British Columbia, Vancouver, B.C., Canada, V6T lZl*, **"Investigation of blowing agents in insulating polymer foams by ^{19}F microscopic NMR imaging"**

Poster: B6
Roland Giesen, *Inst. für Makromol. Chemie, RWTH Aachen, Worringer Weg 1, D 52074 Aachen, Germany,* **"Application of PFG NMR to biological and porous materials"**

Poster: M8
John A. Golightly, Ken J. Packer, Roger N. Ibbett, *Department of Chemistry, University of Nottingham, Nottingham, UK, NG7 2RD, Courtaulds, Lockhurst Lane, Coventry, UK*, **"NMR characterisation of PAN solutions and their non-solvent induced phase separation"**

Poster: S4
A. Guthausen, *Institut fur Makromol. Chemie, RWTH Aachen, Worringer Weg 1, 52054 Aachen, Germany*, **"NMR relaxation measurements on soft matter by the NMR MOUSE"**

Poster: T8
Tomoyuki Haishi, Katsumi Kose, *Institute of Applied Physics, University of Tsukuba, Tsukuba, Ibaraki 305, Japan*, **"A real time NMR image reconstruction-display system using a high-speed personal computer"**

Poster: T9
R. Haken, P. Blümler, B. Blümich, *MARC, Magnetic Resonance Center, Worringerweg 1, D-52056 Aachen, Germany, BIOMAT, Interdisciplinary Centre for Clinical Research, RWTH Aachen, Germany*, **"The NMR-Endoscope"**

Poster: S5
Uwe Heuert, Manfred Knörgen, Horst Schneider, *University Halle, Dept. of Physics, Friedemann-Bach-Platz 6, D-06108 Halle, Germany*, **"Comparison of different NMR imaging sequences to map material properties by using the transversal relaxation in polymer networks"**

Poster: M9
J. H. Iwamiya, S. W. Sinton, and A. W. Chow, *Advanced Technology Center, Lockheed Martin Missiles & Space, Mail Stop O/H1-32, B/204, 3251 Hanover Street, Palo Alto, CA 94304*, **"Magnetic resonance imaging of the flow behavior of highly filled materials"**

Poster: T10
R. Kimmlingen, H. Adolf and A. Haase, *Institute of Physics, University of Würzburg, 97074 Würzburg, Germany*, **"Analytical gradient coil design: A practical approach towards optimized construction of NMR microscopy systems"**

Poster: S6

Manfred Knörgen, Uwe Heuert, Horst Schneider, *University Halle, Dept. of Physics, Friedemann-Bach-Platz 6, D-06108 Halle, Germany*, **"The influence of thermal aging on different filled elastomers shown by NMR microscopy"**

Poster: M10
M. E. Komlosh and P. T. Callaghan, *Department of Physics, Massey University, Palmerston North, New Zealand*, **"NMR evidence for reptation dynamics in semi-dilute polymers?"**

Poster: S7
D. Lane*, S.N. Scrimgeour[+], C.H. Lloyd[+], G. Hunter[+], P.J. McDonald*, [+]*Dentistry and Chemistry Depts, University of Dundee, Dundee DD1 4HN, Scotland, *Department of Physics, University of Surrey, Guildford GU2 5XH, Surrey, England*, **"The Application of Stray Field Imaging (STRAFI) to Dental Materials Science"**

Poster: T11
John J. Lee[1], David J. Schneider[2], Jack H. Freed[3], Paul C. Lauterbur[1], [1]*Biomedical Magnetic Resonance Laboratory, University of Illinois at Urbana-Champaign, Urbana, IL 61801,* [2]*Cornell Theory Center, Cornell University, Ithaca, NY 14853,* [3]*Baker Laboratory of Chemistry, Cornell University, Ithaca, NY 14853*, **"Physical and Computational Models for Magnetic Resonance Imaging by Populations"**

Poster: M11
Johannes Leisen, Haskell W. Beckham and W. W. Carr, *School of Textile & Fiber Engineering, Georgia Institute of Technology, Atlanta, GA, 30332-0295 U.S.A.*, **"Observation of Water Distribution and Diffusion during the Drying Process in Textiles"**

Poster: M12
R. Mair*+, C.H. Tseng*+, G.P. Wong*, R.L. Walsworth*, M. Hurlimann#, L. Schwartz# and S. Patz+, **Harvard-Smithsonian Center for Astrophysics, Cambridge, MA, #Schlumberger-Doll Research, Ridgefield, CT, + Brigham and Womens Hospital and Harvard Medical School, Boston, MA*, **"Noble gas NMR of model porous media"**

Poster: M13
I.V. Mastikhin, V.S. Teslenko, V.A. Morosov, G.S. Ananchenko, S.I. Dikalov, *International Tomography Center, SB RAS, International Tomography Center, Institutskaya 3a st., Novosibirsk, 630090, Russia*, **"Initiation of chemical reactions in liquid by weak shock waves"**

Poster: T12
G. D. Mateescu, *Department of Chemistry, Case Western Reserve University, Cleveland, Ohio 44106, USA*, **"Oxygen-17 MRI and MRS: Old and New"**

Poster: M14
Patrick McConville[#], James M. Pope[#] and Joseph W. Huff*, [#]*Centre for Medical and Health Physics, School of Physical Sciences, Queensland University of Technology, GPO Box 2434*

*Brisbane, Australia 4001, *Cornea and Contact Lens Research Unit, School of Optometry and Cooperative Research Centre for Eye Research and Technology, University of New South Wales, Sydney, Australia,* **"NMR Relaxivity and Diffusional Studies of Water in Contact Lens Hydrogels"**

Poster: B7
B. A. Moffat[#], R. J. W. Truscott* , M. H. J. Sweeney*, and J. M. Pope[#], [#]*Centre for Medical and Health Physics, Q.U.T., Queensland, Australia, 4000, *Australian Cataract Research Foundation, Department of Chemistry, University of Wollongong, NSW, Australia, 2522,* **"Application of NMR Microimaging to the Study of Water Transport in Eye Lenses"**

Poster: M15
A. Mohoric, J. Stepisnik, M. Kos and G. Planinsic, *Physics Dept., University of Ljubljana, Jadranska 19, 1000 Ljubljana, Slovenia,* **"Natural convection and self-diffusion measurements by NMR"**

Poster: B8
P. Mullins, S. Polley, D. Bradely, P. Hockings, A. Dhiri, D. Middleton, D. Reid and J. Connelly, *University of Queensland Analytical Sciences, SmithKline Beecham, The Frythe , Herts. U.K. AL6 9AR,* **"*In vivo* histology: MRI in the study of kidney toxins"**

Poster: B9
D. Pereira*, C. Zambrano and M. Martin-Landrove, *Departamento de Fisica and Centro de Resonancia Magnetica, Facultad de Ciencias, Universidad Central de Venezuela, A.P. 47586, Caracas 1041-A, Venezuela and *Departamento de Fisica Aplicada, Facultad de Ingenieria, Universidad Central de Venezuela, Caracas, Venezuela,* **"Characterization of malignancy in tumors of the central nervous system through fractal analysis"**

Poster: T13
Delia Perez, Alfonso Benavides* and Miguel Martin-Landrove, *Departamento de Fisica and Centro de Resonancia Magnetica, Facultad de Ciencias, Universidad Central de Venezuela, A.P. 47586, Caracas 1041-A, Venezuela and *Instituto de Ciencias de la Tierra, Facultad de Ciencias, Universidad Central de Venezuela, Caracas, Venezuela,* **"Relaxation-Diffusion Processes and Local Magnetic Field Distributions in Natural Porous Media"**

Poster: B10
K. Potter[*], E. Petersen[*], J. Butler[†], R. Balakir[†], P. Precht[†], K.W. Fishbein[*], W.E. Horton[†] and R.G.S. Spencer[*], *NMR Unit[*] and Cartilage Biology Unit[†], National Institute on Aging, National Institutes of Health, 4940 Eastern Ave., Baltimore, MD 21224,* **"Morphometric analysis of cartilage grown in a HFBR using NMR microscopy"**

Poster: T14
P.J. Prado, B.J. Balcom and R.L. Armstrong, *MRI Centre, Department of Physics, University of New Brunswick, Fredericton, NB, E3B 5A3, Canada,* **"Gas Phase Imaging Using a Rapid SPI Method (SPRITE)"**

Poster: B11
K. Saito[1,3], N. Kataoka[2], P. Bluemler[3], B. Bluemich[3] and Y. Sawada[2], *[1]Advanced Technology Research Laboratories, Nippon Steel Corporation, 3-35-1 Ida Nakahara-ku, Kawasaki City 211, Japan, [2]Research Institute of Electrical Communication, Tohoku University, Sendai, Japan, [3]Magnetic Resonance Center MARC, RWTH-Aachcn, D-52056 Aachen, Germany*, **"NMR microimaging of cell sorting process in Three dimensional dissociated cell aggregates"**

Poster: T15
T. W. J. Scheenen, D. van Dusschoten, P. A. de Jager and H. Van As, *Wageningen Agricultural University, Dept. of Molecular Physics, Dreyenlaan 3, 6703 HA Wageningen, The Netherlands*, **"Fast spatially resolved displacement-imaging in (bio)systems"**

Poster: T16
D. M. Schmidt[1], J. S. George[1], S. I. Penttila[1], A. Caprihan[2], and E.F. Fukushima[2], *[1]Los Alamos National Laboratory, Los Alamos, NM 87545, [2]New Mexico Resonance, Albuquerque, NM 87108*, **"Diffusion Imaging with Hyper-Polarized ^{3}He Gas"**

Poster: B12
S. N. Scrimgeour*, C. H. Lloyd*, G. Hunter[+], J. A. Chudek[+] And R. L. Mackay[+], *Dental School* and Chemistry Department[+], University of Dundee, Dundee DD1 4HN, Scotland, UK*, **"Magnetic Resonance Microimaging (MRM) Of Teeth"**

Poster: B13
Y. Seki, Naruse S[1], Seo Y[2], Murakami M, Ozaki T[3], Kitagawa M, Ishiguro H, Nakae Y, Hayakawa T[1], *Internal Medicine II, Nagoya University[1], Tsurumai 65, Showa-ku, Nagoya 466; Physiology I, Kyoto Prefectural University of Medicine[2], Kawaramachi-Hirokoji, Kamigyo-ku, Kyoto 602; and National Institute for Physiological Sciences[3], Myoudaiji, Okazaki 444, Japan*, **"Analysis of esophageal motility by fast MR imaging"**

Poster: T17
P. Shkarin and R. G. S. Spencer, *National Institutes of Health, National Institute on Aging, 4940 Eastern Avenue, Baltimore, MD 21224*, **"Efficient simulation of NMR imaging sequences by isochromat summation"**

Poster: S8
A. Spyros, N. Chandrakumar and R. Kimmich, *Sektion Kernresonanzspektroskopie, Universitat Ulm, Albert Einstein Allee 11, 89069 Ulm, Germany*, **"J-Cross Polarization ^{13}C Edited Imaging of Elastomers"**

Poster: S9
A. Spyros and R. Kimmich, *Sektion Kernresonanzspektroskopie, Universitat Ulm, Albert Einstein Allee 11, 89069 Ulm, Germany*, **"Application of imaging to the study of enzymatic degradation of poly(ß-Hydroxybutyrate), a biodegradable polymer"**

Poster: S10
Ronald Dean Stoddard, *Washington University, Department of Physics, 11051 Brookings Dr., St. Louis, MO 63130*, **"Monitor Degree of Cure of Carbon/Epoxy Composites with the NMR Relaxation Time T_2"**

Poster: B14
H. Takamiya*, Y. Kusaka*, Y. Seo**, T. Morimoto**, Y. Hirasawa*, **Dept. of Orthop. Surg. & **Dept. of Physiol., Kyoto Pref. Univ. of Med., Kyoto 602 Japan*, **"MR image of cortical bone using constant-time-imaging method"**

Poster: S11
B. Traub, D. Maring, S. Hafner, H. W. Spiess, *Max-Planck-Institut für Polymerforschung, Ackermannweg 10, 55128 Mainz, Germany*, **"NMR imaging of mechanically treated polymers"**

Poster: M16
R. A. Waggoner,* M. Nakagawa,[†] J. Glass,[††] M. Reece,[†]*, And E. Fukushima**, **The Institute of Physical and Chemical Research(RIKEN), Saitama, Japan, [†]Colorado School of Mines, Golden, CO., [††, †]*Sandia National Laboratories, Albuquerque, NM 87185, **New Mexico Resonance, Albuquerque, NM 87108*, **"Particle compaction as observed by MRI"**

Poster: M17
W. Wang[†], J.H. Walton[§], M.J. Mccarthy[†] & K.L. Mccarthy[†], *[†]Dept. of Food Science and Technology and [§]NMR Facility, University of California, Davis, CA 95616*, **"Evaluation of mixing profiles of power law fluids in scraped surface heat exchanger geometry using MRI"**

Poster: B15
Su Xu[1], E. K. Jordan[1], W. Li[2], S. Brocke[3], J. W. M. Bulte[1], L. Quigley[3], N. Tresser[3], Y. Yang[1], J. L. Ostuni[1], S. A. Chesnick[4], H. Def. Webster[2], H. F. Mcfarland[3], J. A. Frank[1], *Laboratory of Diagnostic Radiology Research[1], OD, OIR, Laboratory of Experimental Neuropathology[2], NINDS, Neuroimmunology Branch[3], NINDS, Laboratory of Cardiac Energetics[4], NHLBI, National Institutes of Health, Bethesda,MD 20892, USA, Bldg.10, Room B1N-256, LDRR, National Institutes of Health, Bethsda, MD 20892*, **"Detection of experimental allergic encephalomyelitis mouse model using *in vivo* MR microscopy"**

TALKS

Notes on Gases, Gimmicks, Gels, and Gestation

Paul Lauterbur

Biomedical Magnetic Resonance Laboratory,
University of Illinois, Urbana, IL 61801, USA

(1)Fluorinated gases with normal nuclear polarizations and very short 19F T1 and T2 values can be used for lung ventilation imaging. Studies on phantoms and a live dog will be described. (2) Detection of small magnetically-perturbing objects, singly and collectively, can be enhanced by a variation on the old DEFT esperiment. (3)Gels that respond to their environment by changing their volumes or shapes are sometimes called "smart" polymers. Some that we are trying to train to be contrast agents must then also be described as hyperactive, neurotic, or even psychotic. (4) On a saner note, 3D microscopic MRI can be an effective tool for routine anatomical studies of human and animal embryos. Practical approaches to this goal will be illustrated.

Chemical Shift Microscopy

Markus von Kienlin, Axel Haase
Institute of Physics, University of Würzburg, Germany

Introduction

Chemical Shift Microscopy attempts to measure the spatial distribution of specific chemical compounds with the best possible (spatial *and* spectral) resolution. The main factor which limits the obtainable resolution is sensitivity, which is influenced by the instrumentation, by the NMR pulse sequence and the acquisition parameters, and also by the data analysis. In this contribution, we will present our current research activities in the field of NMR spectroscopic imaging (SI) on a microscopic scale.

Instrumentation

Unlike for *in vivo* measurements on a macroscopic scale (where noise is dominated from the sample), the noise in microscopic NMR examinations arises mostly from losses in the reception coil. Every care has to be taken to minimize these losses, which can be either resistive or radiative, or due to the electric or magnetic fields. The design of a superconducting probehead and initial results which demonstrate an approx. fivefold gain in SNR at 7T will be shown[1]. Sensitivity can be further increased with quadrature coils, which until today have been hardly used in NMR microscopy[2].

NMR Methodology

The signal-to-noise ratio (SNR) depends on the parameters of the pulse sequence (repetition time, flip angle) and the data acquisition (acquisition time, with or without gradient, bandwidth). A simple strategy how these parameters can be optimized will be presented. State-of-the-art method in NMR is Fourier imaging. Due to the limited resolution of SI, however, the spatial response function (SRF) of conventional Fourier methods is poor and leads to signal contamination between voxels. Better strategies like "acquisition weighting[3]" and "radial spectroscopic imaging[4]" will be explained.

Current Applications

We apply chemical shift microscopy to study high-energy phosphate metabolism in the isolated rat heart[5] (^{31}P: 54 µl voxels in 60 min at 11.75 T) and in *ricinus communis* seedlings[6] (^{1}H: 17.5 nl voxel volume in 3.5 h at 11.75 T). Spectral resolution can be drastically improved with correlation spectroscopy techniques, which yield a two-dimensional spectrum in every pixel of the spectroscopic image[7]. This has been applied in plants[8] and in rat brain. Exemplary results of these applications will be shown.

References

1. F. Odoj et al., *13th ESMRMB* 144, 1996; 2. T. Lanz et al., *13th ESMRMB* 653, 1996; 3. T.H. Mareci et al., *JMR* 57:157, 1984; 4. M. Meininger et al., *JMR* 125:325, 1997;
5. C. Rösch et al., *5th ISMRM, Vancouver* 1997; 6. A. Metzler et al., *JMRB* 105:249, 1994;
7. A. Ziegler et al., *JMRB* 112:141, 1996; 8. A. Metzler et al., *PNAS.* 92 (25):11912, 1995.

MAPPING T_1 AND T_2 ANISOTROPY IN CARTILAGE BY MICROSCOPIC MRI (μMRI) AT 14 μM PIXEL RESOLUTION

YANG XIA
Physics Department
Oakland University
Rochester, MI 48309, USA

Articular cartilage is the connective tissue coated on the ends of bones in joints. Cartilage is highly specialized in both the molecular and spatial struclures to provide a smooth surface for joint motion and to cushion the joint against shock impact. Study of cartilage by MRI is motivated by the role of cartilage in various stages of osteoarthritis, one of the most common diseases in adults. In a highly organized biological tissue such as cartilage, relaxation times of the tissue will depend not only on the chemical compositions and structures of the molecules, but also on the physical structure of the tissue. If the tissue structure exhibits any macroscopic anisotropy, water molecules in the tissue could have different rotational rates about different molecular axes. This will result in non-zero averaging of the dipolar spin Hamiltonian (H_D) and a consequent orientational dependence of T_2. Relaxation times can therefore be used to probe the physical structure of the tissue as well as any structural change due to diseases in the tissue.

In this study, imaging experiments at 14~m pixel resolution were conducted by obtaining 2D T_1 and T_2 relaxation maps of canine articular cartilage placed at a series of orientations with respect to the external magnetic field (-35°, 3°, 25°, 40°, 57° and 85°). The selected orientations form a series of discrete sampling points for the geometrical factor ($3\cos^2\theta$ - 1) that dominates the non-zero Hamiltonian.

In the T_1 mapping experiments, the proton intensity images of cartilage were influenced strongly by the cartilage orientation in the magnetic field. However, no orientational dependence of T_1 was observed in the quantitative T_1 maps of cartilage. The T_1 profiles are essentially identical, and fairly uniform as a function of the cartilage tissue depth.

In the T_2 mapping experiments, a distinct orientational dependence of T_2 was observed in cartilage. The T_2 characteristic of cartilage exhibits three unique regions: the first region occupies about 10% of the cartilage thickness and exhibits a tissue-depth-dependent T_2 anisotropy; the second region occupie.s about 13% of the cartilage thickness and exhibits an isotropic and depth independent T_2; and the third region occupies about 77% of the cartilage thickness and exhibits a distinct T_2 anisotropy. These three unique regions in, μ MR images correspond approximately to the three histological zones in cartilage tissue. These findings are consistent with the understanding that collagen fibrils are oriented randomly in the transition zone and are perpendicular to the articular surface in the deep zone. A movie is available to illustrate the T_2 characteristic in cartilage as a function of the tissue orientation.

In summary, relaxation characteristics in canine cartilage have been examined accurately and at microscopic resolution. The correlation between the T_2 anisotropy and the curve of $\{ 3\cos^2\theta - 1 \}$ suggests that water molecules that are closely associated with proteoglycans are confined within the collagen network in articular cartilage. The T_2 anisotropy provides an indirect but sensitive indicator for the orientational structures of collagen fibrils and proteoglycan macromolecules in cartilage. The ability to visualize such structures is important because of the direct connection between the proteoglycans / collagen matrices and the mechanical characteristics of the cartilage tissue.

A NOVEL ALGORITHM FOR TUMOR CHARACTERIZATION BY ANALYSIS OF TRANSVERSAL RELAXATION RATE DISTRIBUTIONS IN MRI

RAFAEL MARTIN AND MIGUEL MARTIN-LANDROVE
Departamento de Fisica and Centro de Resonancia Magnetica
Facultad de Ciencias
Universidad Central de Venezuela
A.P. 47586, Caracas 1041-A, Venezuela

In complex and heterogeneous systems, as for instance living tissues, the proton transversal magnetization decay is not governed by a single relaxation rate but by a superposition of different relaxation rates, each one corresponding to different dynamical environments. In general, this situation is represented by a continuous distribution function and the measured decay corresponds to its Laplace transform. In the present work a novel algorithm is developed and used to invert the Laplace transform in order to obtain the relaxation rate distribution fi~nction from the experimental decay. The methodology is applied to a variety of tumors, with different degrees of malignancy as well as to healthy tissue. Using the standard CarrPurcell-Meiboom-Gill (CPMG~ pulse sequence, images for different echoes are registered and then for the same region of interest in each image, the pixel intensity is averaged in order to obtain the decay curve of average intensity for that specific region. The number of regions selected for each tumor depended on the size and heterogeneity as observed on the nmr image. The decays so obtained were processed by the proposed algorithm and correlated to results obtained by biopsies. The results show that when there is malignancy it occurs in a very defined relaxation rate window and outside of it only liquid or benign neoplasic tissue are present. Other parameters of the relaxation rate distribution are also under study to correlate them with clinical data. The methodology developed in this work can be implemented easily in any type of scanner working at any magnetic field and can be extended to study other pathologies.

Imaging growth changes in plants during osmotic stress

L. van der Weerd, T. Ruttink, D. van Dusschoten, F. Vergeldt, P.A. de Jager, H. Van As
Wageningen Agricultural University
Dept. of Molecular Physics
Dreyenlaan 3, 6703 HA Wageningen, The Netherlands

Osmotic stress studies on intact plants using NMR Imaging have been reported previously (1). Here growth studies on water cultured Maize plants during osmotic stress are presented.
The shoot apex growth rate was studied using an open access 0.5 T electro magnet with full environmental control of the leaf area, imaging longitudinal cross-sections of the plant stem at the growing zone. Quantitative T_2 imaging by a PFG-CPMG like imaging sequence was combined with chlorophyl fluorescence and water uptake measurements.

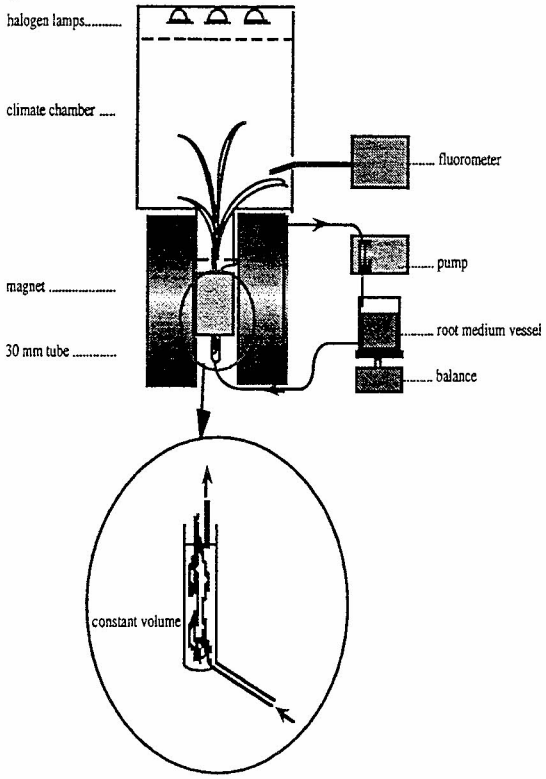

Five weeks old water culture plants of *Zea mays* L, cv. LG 11 were studied during osmotic stress induced by replacing the normal root medium by a well aerated PEG-6000 medium, with a water potential of -0.25 Mpa, under high light (100 Lux) conditions. Water uptake was measured by weighting the root medium vessel outside the magnet (see Figure). A multiple spin-echo imaging sequence was applied with TR=1.8 s, TE=4.6 ms, SW=50 kHz, and 64 echoes per echo train, resulting in a 48*128*128 matrix of complex data. T2 and amplitude images were calculated from the decay of the intensity of the echo images on a pixel by pixel base. The field-of-view was 50 mm in the longitudinal and 30 mm in the transversal direction and the slice thickness 2.5 mm. One measurement took 15 min. Photosynthetic activity was measured on the second top leaf in a fixed position using a modulated fluorometer (Waltz PAM 2000).

The results revealed a high correlation between stress periods and stem apex growth. It was striking that though the NMR parameters, the water uptake and the photosynthetic activity hardly changed during stress periods, growth of the stem apex stopped completely during these periods. These measurements support the theory that maize is not able to redistribute water to vital organs as the growing zones during osmotic stress.

References:

1. H. Van As, D. van Dusschoten, S. Nagarajan, F. Vergeldt and P.A. de Jager, Book of abstracts 3rd International Conference on Magnetic Resonance Microscopy, Wurzburg, Germany, August 27-31, 1995, p. 15.

NMR MICROSCOPY AND PURE NQR IMAGING

D. G. CORY
Massachusetts Institute of Technology
NW14-4111, 150 Albany St.
Cambridge, MA 02139

Abstract

This talk will touch on two related topics:

1. high resolution NMR microscopy,
2. pure Nuclear Quadrupole Resonance Imaging.

Both will be discussed in terms of methods for obtaining a sharp and spatially uniform point spread function.

The first part will focus on Constant Time Imaging approaches to NMR microscopy. The resolution in Nuclear Magnetic Resonance (NMR) microscopy is limited by a combination of the inherent low sensitivity of NMR, the destruction of spin magnetization gratings by molecular diffusion, and variations in the local magnetic field strength introduced by spatial variations of the bulk susceptibility. While none of these may be completely overcome, constant time imaging methods are the optimal approach to recording images when the above factors are important. This method aims to instantaneously create a spin magnetization grating and then to efficiently sample the spatially invariant portion of this - corresponding to a selected Fourier component of the sample distribution. The method is introduced, analyzed in the presence of molecular diffusion and demonstrated to yield high resolution images. To implement the method, a microscopy probe was constructed for a standard bore 600 MHz NMR spectrometer, and this is described, along with some high resolution examples.

Pure NQR imaging depends on creating a magnetization grating via RF gradients, and the greatest challenge is to control the complex spin dynamics in this heterogeneous system. We will discuss unique probe designs and methods that convert this into a linear imaging system.

MAGIC ECHO IMAGING OF POLYMER MATERIALS

S. HAFNER, B. TRAUB, H.W. SPIESS
Max-Planck Institut für Polymerforschung
Postfach 3148
D-55021 Mainz, Germany

Two different strategies can be employed to overcome the broad lines in rigid polymers or other solids. The first is to use the strong gradients found in the stray field of the static magnetic field while the other relies on the application of line-narrowing techniques. The most promising imaging techniques of the latter type are based on multiple-pulse line-narrowing or constant-time phase-encoding techniques. The use of magic echoes proved to be particularly successful for both cases (1) because magic echoes allow relatively long evolution intervals during which the spatial encoding can take place.

Spin-density images of polymers alone however give seldom access to structural information in polymers since the variation of the (spin) density usually manifests on a much smaller length scale as could be resolved by NMR microscopy. As already shown for soft solids, in such cases spectroscopic or relaxometric information has to be incorporated into the imaging technique. Microscopic material properties can then be measured via the corresponding parameters, while the macroscopic distribution of these properties is accessible by imaging.

The main topic of this contribution thus is the introduction of material-specific information into the solid-state imaging experiment. After a short outline of the magic-echo technique, we therefore concentrate on a 2D variant that allows the incorporation of spectroscopic or relaxometric information. It consists in its imaging part of a constant time phase-encoding magic-echo sequence followed by a multiple-magic echo imaging sequence for frequency-encoding. Prior to the imaging sequence a filter sequence is applied, the length of which is varied for determining the corresponding relaxation parameter.

This imaging sequence is applied to polymer samples which have been drawn under various conditions. Whereas the pure spin density image proved to be insensitive to the resulting changes in the material, relaxation-time images clearly distinguish between regions of different mobilities resulting from the mechanical treatment.

References:

(1)S. Hafner, D.E. Demco, R. Kimmich, Solid State NMR 6 (1996), 275-293
(2)F. Weigand, S. Hafner, H.W. Spiess, J. Magn. Reson. A 120 (1996), 201-205

PROTON-DETECTED ^{13}C MAGNETIC RESONANCE IMAGING

RAINER KIMMICH
Universitat Ulm, Sektion Kernresonanzspektroskopie
89069 Ulm, Germany

^{13}C has scarcely been considered as a nucleus for magnetic resonance imaging. The reasons are the low natural abundance and the low gyromagnetic ratio so that the sensitivity appears to be not particularly promising.

The latter problem can be overcome by recording proton signals edited in such a way that only hydrogen nuclei coupled to ^{13}C are detected whereas signals due to all other groups are suppressed. Several pulse schemes developed for this purpose can be found in the literature. Here we are referring to the cyclic cross polarization (CYCLCROP) indirect ^{13}C imaging scheme [1,2] which turned out to be a very reliable tool.

The principle is a cyclic rotating-frame cross-polarization pathway from protons to ^{13}C and back to protons. While the polarization is concentrated on the ^{13}C side, all proton coherences are spoiled, so that only the subsequently repolarized protons contribute to the signal.

The low natural abundance of ^{13}C may even be considered as an advantageous feature permitting the experimenter to carry out particularly specific investigations. ^{13}C enriched compounds are chemically practically indistinguishable from their counterparts with natural isotope composition. Substances labeled in this way are therefore ideal probes for the detection of local transport, metabolism and material properties.

1. C. Kunze and R. Kimmich, *Magn. Reson. Imaging 12,* 805 (1994).
2. R. Kimmich, *NMR-Tomography, Diffusometry, Relaxometry,* Springer, Berlin, 1997.

MRI AND FMRI USING INTERMOLECULAR ZERO-QUANTUM COHERENCES IN SOLUTION

WARREN S. WARREN
Princeton University
Department of Chemistry
Princeton, New Jersey

Abstract:

A new method for MRI and functional MRI is presented, with contrast generated by detection of signal from intermolecular zero-quantum coherences (iZQCs) in solution. Such a signal would not be observable in the conventional framework of magnetic resonance; it originates in long range dipolar couplings in solution, which are traditionally ignored but have now been extensively investigated in spectroscopic applications [1,2]. These coherences correspond to detecting the signal produced by simutaneously flipping two water spins in opposite directions on molecules separated by 10μm-10 mm. Unlike conventional MRI, where contrast is based on variations in spin density and relaxation times (often with injected contrast agents), contrast in iZQC images comes from variations in the susceptibility over a distance dictated by gradient strength. This contrast should prove useful in detection of small tumors and in fMRI, since in both cases local variations in oxygen concentration are important, and susceptibility depends on oxygen concentration. Experimental demonstrations of contrast enhancment at 4T and 9.4T will be presented.

1. W. S. Warren, W. Richter, A. H. Andreotti and S. Farmer, Science 262, 2005 (1993); W. Richter, S. Lee, W. S. Warren, and Q. He, Science 267, 654 (1995); S. Vathyam, S. Lee and W. S. Warren, Science 272, 92 (1996)
2. S. Lee, W. Richter, S. Vathyam and W. S. Warren, J. Chem. Phys. 105, 874 (1996)

NMR Microscopy in Liquids Using the Dipolar Field

R. Bowtell and P. Robyr*

Magnetic Resonance Centre, University of Nottingham, Nottingham, NG7 2RD, UK
and Department of Physical Chemistry, ETH-Zentrum, CH-8092, Zurich, Switzerland*

Introduction

The dipolar magnetic field generated by the nuclei themselves is generally neglected in liquid state NMR experiments because it is many orders of magnitude weaker than any applied magnetic fields. In highly polarised samples the dipolar field can, however, give rise to significant effects, particularly when the magnetisation is spatially modulated via the use of magnetic field gradients. These effects include the formation of unexpected multiple quantum coherences in 2D NMR experiments (1) and the generation of multiple spin echoes (MSE) after the application of just two RF pulses (2).

Method

It has been shown that through manipulation of the magnetisation, MSE can be used to extract structural information (3-6) from liquid samples. This is possible because in the presence of spatially modulated magnetisation, the dipolar field experienced by a particular nuclear spin mainly results from the local magnetisation found within a distance less than the spatial period of modulation (3). By adjusting this period structure can be probed at varying length scales. All the magnetisation contributes to the NMR signal in such experiments irrespective of the period of modulation. Consequently there is no reduction in sensitivity on moving to finer resolution, and the achievable resolution is set by diffusion effects rather than by the direct signal to noise ratio considerations which usually limit conventional NMR microscopy experiments. In water, diffusion restricts the resolution to the order of 10 mm, but in less mobile liquids sub-micron resolution may be achieved.

Implementation of NMR microscopy using the dipolar field requires experimental sequences in which spatially modulated transverse magnetisation evolves in the presence of modulated longitudinal magnetisation. The amplitude of the resulting MSE then provides structural information. Such sequences can also allow the measurement of diffusion coefficients in an experiment that only requires a single gradient pulse (7). Using the Fourier space representation of the dipolar field, we have recently established a simple and direct relation between the variation of the MSE amplitude as a function of the degree of spatial modulation and the structure under investigation (4-5). This allows structural parameters to be extracted from systems when a simple model is available. Further work has shown that under certain circumstances the Patterson function describing the structure under investigation can be directly calculated via a Hankel transform of the MSE data (6).

Results and Discussion

Experiments have been carried out using an 11.7 T NMR microscope. The generation of spatially modulated magnetisation in some experiments was facilitated by the use of specially designed multi-layer gradient coil, which can generate a gradient of 50 Tm^{-1} when carrying a current of 30 A (8). Samples consisted of 5 mm NMR tubes containing water surrounding randomly packed polystyrene micro-spheres (Duke Scientific, Palo Alto, CA) of three different radii (200, 100 and 50 mm). The resulting experimental data are in good agreement with the theoretical predictions resulting from a sample model, comprising a linear mixture of cubic primitive and face-centred lattices. The Patterson functions calculated from these data well approximate those expected from the sample model down to a length scale of about 15 mm. At 11.7 T, the strength of the signal generated by the dipolar field in these sort of samples is about one order of magnitude less than that given by conventional NMR experiments. The results described above indicate the feasibility of measuring structural information using dipolar field effects in model systems. Future work will be directed towards the application of these techniques to more interesting samples such as emulsions, polymer melts and biological systems.

We thank EPSRC for support of the NMR microscope.

References

1) W.S. Warren *et al*, Science, **262**, 2005, 1993.
2) R. Bowtell *et al*, J. Magn. Reson., **88**, 643, 1990.
3) W. Richter *et al*, Science, **267**, 654, 1995.
4) R. Bowtell and P. Robyr, Phys. Rev. Lett., **76**, 4971, 1996.
5) P. Robyr and R. Bowtell, J. Chem. Phys., **106**, 467, 1997.
6) P. Robyr and R. Bowtell, J. Chem. Phys., **107**, 702, 1997.
7) P. Robyr and R. Bowtell, J. Magn. Reson., **121**, 206, 1996.
8) R. Bowtell and P. Robyr, J. Magn. Reson (submitted).

THE NMR-MOUSE: NMR RELAXATION MEASUREMENTS ON SOFT MATTER IN INHOMOGENEOUS FIELDS

G. ZIMMER, A. GUTHAUSEN, P. BLÜMLER, AND B. BLÜMICH,
Institut für Makromolekulare Chemie
RWTH Aachen, 52065 Aachen

The MOUSE (MObile Universal Surface Explorer) is a novel NMR device designed for relaxation measurements in inhomogeneous magnetic fields. The polarizing B0 field is provided by two anti parallel magnetized permanent magnets, B1 is generated by a surface coil. As a consequence of the geometry of the MOUSE the fields are applied from the surface to arbitrarily large objects. Different applications make use of this arrangement: One example is the investigation of polymer coatings on ferromagnetic sheets, which is impossible for conventional NMR. The B0 gradient can also be used for measurements of molecular self diffusion in liquids as well as for water suppression in dispersions. In addition spatial resolution can be achieved by frequency encoding via the B0 gradient. Experimental results on soft materials like elastomers and biological tissue concerning these features will be presented.

ROTATING-FRAME NQR IMAGING METHODS

H. ROBERT AND D. PUSIOL
FaMAF, Universidad Nacional de Cordoba
Ciudad Universitaria - 5000 Cordoba, Argentina

A variety of techniques, based on Nuclear Quadrupole Resonance (NQR) methods, have recently been proposed and demostrated that enable the spatial discrimination and mapping of quadrupole nuclei in solid systems. The rotating-frame NQR imaging method is based on nutation frequency encoding of the spatial information with the aid of gradients of the radiofrequency amplitude. The absence of readout magnetic field gradients means that the full spectroscopic information is accesible. The technique is particularly suitable for the detection of spatial distributions of physical parameters influencing the NQR line shift. Examples are stress or presure and temperature gradients.

The original rotating-frame NQR imaging technique (1) involves a two-dimensional experiment for obtaining a 1D spin density profile. Recently, we proposed a one-shot 1D method to image a sample along the RF field gradient (2). The rapid rotating-frame technique involves magnetization sampling in the course of nutation by a train of RF gradient pulses separated by short acquisition intervals.

Two-dimensional spatial variation were first obtained simplely by recording a set of projections for different orientations of the sample with respect to the RF gradient direction (2,3). We have recently demonstrated (4) a 2D rotating-frame imaging method based on the application of a sequence of orthogonal RF linear gradients to the sample. Several variants of the technique were developed that do not involve rotation of the object and sample the spin density function on a Cartesian coordinate system.

For rapid 2D NQR imaging a new planar method is proposed that exploits the formation of rotary spin echoes. The Echo-Planar Rotating-Frame Imaging (EPROFI) technique employs two perpendicular RF gradients and continuous defocusing-refocusing of the magnetization for fast sampling of the reciprocal space. The high speed of the sequence will allow the visualization of time-dependent temperature and stress distributions in objects with powder geometry.

In this presentation the methods of producing NQR images are discussed and an outline of potentials applications is provided.

References

(1) E. Rommel, P. Nickel, R. Kimmich and D. Pusiol, J. Magn. Reson. 91, 630 (1990).
(2) H. Robert, A. Minuzzi, and D. Pusiol, J. Magn. Reson. A 118, 189 (1996).
(3) E. Rommel, R. Kimmich, H. Robert and D. Pusiol, Meas.Sci.Technol. 3, 446 (1992).
(4) H. Robert and D. Pusiol, J.Magn.Reson. (1997) in press.

SPIN-ECHO IN THE PRESENCE OF STRONG GRADIENT FIELD

GORAZD PLANINSIC[1], MARK SYMMS[2]
1-Physics Dept., University of Ljubljana
Jadranska 19, 1000
Ljubljana, SLOVENIA
2-Institute of Neurology
London, WClN 3BG, UK

Concomitant gradients are a known source of image distortion (1) in regimes where large gradients are used in conjunction with low static fields (on example DNP imaging (2,3) and low field MRI (4)). We are working for several years on MRI in the Earth's magnetic field. Weak field NMR methods provide a special conditions that can not be achieved in strong magnetic fields, such as strong gradient field on the size of the sample compared to the static magnetic field, and very fast gradient rise times compared to Larmor time. Here we show how the dephasing due to concomitant gradient fields can be rephased by a spin-echo sequence.

Consider the square sample with sides $2a$ placed in the coordinate center with the main field B_O applied along the z-axis and with a general field $B_G = (0, -Gyj, Gzk)$ which is switched on and off with rise/fall time t_R. If t_R is much longer than the Larmor time (practically always true), then the phase angle accumulated by a spin at (y,z) during gradient switch-on with an arbitrary gradient switch-on shape can be expressed in the following form

$$\Phi_{on} = \frac{2\pi\tau}{qt_0}\int_0^1 \sqrt{(yH(t')^2 + (q + zH(t'))^2}\,dt'$$

where $q=Bo/(Ga)$, $t_0 = 2\pi / (\gamma B_o)$, and y and z are normalized to a. The gradient switch shape function $H(t/\tau)$ should meet the boundary conditions $H(0)=0$, $H(1)=1$. It is easy to show that exactly equal phase is accumulated during gradient switch-off if corresponding symmetrical shape function $H(1-t/\tau)$ is used. This implies that total phase accumulated over any gradient pulse sequence formed from two parts that are symmetrical with respect to 180° pulse between them is zero at any point in the sample. The total phase of a spin at (y,z) accumulated during spin-echo sequence with bipolar gradient waveforms and one gradient switch shape function can be expressed in the form

$$\Phi_{tot}(y,z,t) = 2\Phi_{sw}(\tau) + \Phi_C(t_1) - \Phi_{sw}(\tau') - \Phi_C(t)$$

$$= \frac{2\pi}{qt_0}\left[(2\tau - \tau')P(y,z) + (t_1 - t)R(y,z)\right]$$

where P and R are functions of y and z only, index sw denotes gradient on/off switches and index C constant gradient intervals where $H(t)=1$. Time t is measured from the second gradient switch-on. From the last equation an important conclusion can be made: if $2\tau = \tau'$ all the spins in the observed slice will have phase zero at time $t=t_1$, so the completely refocused spin-echo will occur. This holds for an arbitrary shape function, as long as switch-on and switch-off shapes are symmetrical. The results of computer simulation confirm this prediction. Work is underway to confirm the predictions experimentally.

(l) D.G.Norris, J.M.S. Hutchison. Magn.Reson.Imag. 8, 33 (1990).
(2) D.J.Lurie et al, J.Magn.Reson. 84, 431 (1989).
(3) D.Grucker et al, Mag.Res.Med. 11, 691 (1993).
(4) J.Stepisnik et al, Mag.Res.Med. 15, 386 (1990).

FREQUENCY DEPENDENCE OF EPR SENSITIVITY

GARETH R. EATON, SANDRA S. EATON, AND GEORGE A. RINARD

Departments of Chemistry and Biochemistry and Engineering
University of Denver
Denver, Colorado, 80208

To obtain adequate depth penetration into large aqueous samples, EPR imaging is performed at frequencies between 250 MHz and 2 GHz. The feasibility of imaging physiologically significant signals at these frequencies is dependent upon obtaining adequate signal-to-noise (SN).

The issue of EPR signal intensity as a function of frequency has been confused for many years because of an unfortunate error in Poole's book, "Electron Spin Resonance: A Comprehensive Treatise on Experimental Technique". Experimental tests of the frequency dependence of SN have typically compared performance on extensively engineered X-band systems with results obtained on low-frequency EPR systems that have been built with minimal budget and/or for specialized purposes and are unlikely to approach ultimate sensitivity. The predictions and experimental results in the literature have provided a rather pessimistic picture.

We have re-derived the expressions for EPR signal intensity as a function of frequency and find a more optimistic picture, by a factor of ω. The following table summarizes the predicted frequency dependence of EPR signal intensity for 3 sets of assumptions concerning sample and resonator geometry for a lumped-element resonator such as a loop-gap resonator (LGR). When resonator and sample are scaled with wavelength and the microwave magnetic field, B,, is kept constant, the EPR signal varies as $\omega^{-1/4}$. Under these conditions EPR signal intensity, at constant extent of power saturation, is predicted to increase as frequency is reduced. If the sample and resonator size are held constant as would be done for sample-limited experiments, then EPR signal intensity varies as $\omega^{7/4}$.

The predictions in the table are consistent with the commonly-cited expressions for N~, when the same assumptions are made. The typical NMR case would be case 1, i.e. a constant sample size and constant loop size, for which the inductance L is constant. At NMR frequencies and for typical NMR coils, skin effects are likely to be small so the resistance would be constant for a constant loop size. The expression derived in the same way as the table entries gives an C~2 dependence where one factor of ~ comes from the magnetic susceptibility and the other from Lenz' s law.

	Case 1	Case 2	Case 3
	Constant sample size, constant LGR size	Sample size $\propto 1/\omega_o$, LGR size $\propto 1/\omega_o$	Constant sample size LGR size $\propto 1/\omega_o$
inductance	1	ω_o^{-1}	ω_o^{-1}
resistance	$\omega_o^{1/2}$	$\omega_o^{1/2}$	$\omega_o^{1/2}$
quality factor	$\omega_o^{1/2}$	$\omega_o^{-1/2}$	$\omega_o^{-1/2}$
filling factor	1	1	ω_o^{3}
$B_1/(P)^{1/2}$	$\omega_o^{-1/4}$	$\omega_o^{3/4}$	$\omega_o^{3/4}$
P for constant B_1	$\omega_o^{1/2}$	$\omega_o^{-3/2}$	$\omega_o^{-3/2}$
EPR signal, cost B_1	$\omega^{7/4}$	$\omega_o^{-1/4}$	$\omega_o^{11/4}$

ELECTRON SPIN RESONANCE IMAGING (ESRI) OF TRANSPORT PROCESSES IN POLYMERS

S. SCHLICK
Department of Chemistry
University of Detroit Mercy
Detroit, Michigan 48219, USA

2D (spectral-spatial) ESRI is applied in our lab for representation of distribution and dynamics of paramagnetic species in ion-containing polymers, crosslinked polymer gels and catalytic systems. Projections taken in a range of magnetic field gradients are used to reconstruct a 2D image that consists of the ESR spectrum along the chosen spatial coordinate. The method provides the concentration profiles and the lineshape of the ESR spectrum of the diffusant in each slice of the sample perpendicular to the direction of the gradient, thus making possible the determination of translational and rotational diffusion in one experiment. Four applications of this method will be presented here. 1. The diffusion coefficient, *D,* of nitroxide spin probes and spin-labelled poly(ethylene oxide) was measured by ESRI in hydrogels based on 2-hydroxyethyl-methacrylate (HEMA) and 2-(2-hydroxy-ethoxy)ethylmethacrylate (DEGMA) as monomers.[1] The gels are neutral, have excellent biological tolerance and good mechanical properties even at high water content (~60 %), and are especially useful for production of contact lenses. 2. Transport of a perdeuteriated nitroxide (PDTEMPONE) as tracer was measured in solutions of polystyrene (PS) in toluene and dimethylformamide (DMF), and in crosslinked polystyrene (cPS) networks swollen by the same solvents.[2] The D values were found to depend on the solvent, temperature and PS concentration in the solutions, and are significantly reduced by crosslinking. The temperature dependence of *D* shows an Arrhenius behavior, and the dependence on the polymer concentration in the solutions is consistent with the free volume theory. 3. ESRI based on paramagnetic MoV has been developed in order to avoid problems associated with "hyperfine artifacts". D values for MoV (as MoCl5) were measured at 300 K in solutions of poly(acrylic acid) in DMF as a function of polymer content,[3] and in perfluorinated ionomers swollen by ethanol.[4] ESRI based on MoV has the potential to measure transport properties, and temporal and spatial characteristics of reactions in catalytic systems. 4. The transport of spin probes has been measured in a self-assembled polymeric surfactant consisting of poly(ethylene oxide) (PEO) and poly(propylene oxide) (PPO) segments; probes that are known to intercalate in the hydrophobic regions, at the polymer-water interface, and in the water domains have significantly different diffusion coefficients.[5]

References

1. Schlick, S.; Pilar, *J.;* Kweon, S.-C.; Vacik, *J.;* Gao, Z.; Labsky, *J. Macromolecules* 199~, 28, 5780.
2. Gao, Z.; Pilar, *J.;* Schlick, S. *J. Phys. Chem.* 1996, 100, 8430.
3. Kruczala, K.; Gao, Z.; Schlick, S. *J. Phys. Chem.* 1996, 100, 11427.
4. Gao, Z.; Schlick, S. *J. Chem. Soc. Faraday Trans.* 1996, 92, 4239.
5. (a) Malka, K.; Schlick, S. *Macromolecules* 1997, 30, 456. (b) Zhou, L. Gao, Z.; Schlick, S., to be published.

Support: The Polymers Program of the National Science Foundation.

Electron Paramagnetic Resonance Imaging of the Heart

Jay L. Zweier, Michael Chzhan, Alexandre Samouilov, and Periannen Kuppusamy

Molecular and Cellular Biophysics Laboratories, Department of Medicine, and The EPR Center, John Hopkins University, 5502 Hopkins Bayview Circle, Baltimore, MD 21224

It has been hypothesized that free radical metabolism, oxygenation, and nitric oxide generation in biological organs such as the heart may vary over the spatially defined tissue structure. To address fundamental questions regarding the role of spatially localized alterations in radical metabolism, oxygenation, and nitric oxide in the pathophysiology of cellular injury during ischemia, we have developed instrumentation optimized for 3D spatial and 3D or 4D spectral-spatial imaging of free radicals in the isolated perfused rat heart at 1.2 Ghz. Using this instrumentation, high quality 3D spectral-spatial imaging of nitroxide metabolism was performed as well as spatially localized measurements of oxygen concentrations, derived from the oxygen dependent linewidth broadening. In these spectral-spatial images submillimeter resolution was observed enabling visualization of the left ventricular and right ventricular myocardium. With 3D spatial imaging using single-line labels, resolutions down to 100 mm were obtained enabling visualization of the ventricles, aortic root, and proximal coronary arteries. Using metal complexes which trap nitric oxide, measurement and imaging of nitric oxide generation during ischemia was performed. With the use of ^{15}N isotope labeling it was possible to map the metabolic pathway of this nitric oxide generation. Thus, EPR imaging is a powerful tool which can provide unique information regarding the spatial localization of free radicals, oxygen, and nitric oxide in biological organs and tissues.

MICROSCOPIC CHARACTERIZATION OF MAGNETIC MATERIALS USING MAGNETIC RESONANCE FORCE MICROSCOPY

P. C. HAMMEL[1], Z. ZHANG[1], M. MIDZOR[2], M.L. ROUKES[2] AND J.L. CHILDRESS[3]

[1]Los Alamos National Laboratory, Los Alamos, NM 87545
[2]California Institute of Technology, Pasadena, CA 91125
[3]University of Florida, Gainesville, FL 32611-2066

The Magnetic Resonance Force Microscope (MRFM) is a novel scanned probe instrument which combines the three-dimensional imaging capabilities of magnetic resonance imaging (MRI) with the high sensitivity and resolution of atomic force microscopy (AFM). This emerging technology holds clear potential for atomic scale resolution. When this potential is fully realized MRFM will enable non-destructive, chemical-specific, high-resolution microscopic studies and imaging of subsurface properties of a broad range of materials. We have observed the ferromagnetic resonance signal arising from a microscopic 20 X 40 micron particle of thin (3micron) yttrium iron garnet film using magnetic resonance force microscopy (MRFM). We have successfully obtained FMR signals from thin-film Co using MRFM techniques. These experiments point toward the promise of the MRFM as a microscopic probe of magnetic multilayer materials.

NMR MEASUREMENTS OF CRUDE OILS IN SUBSURFACE EARTH FORMATIONS

R. L. KLEINBERG
Schlumberger-Doll Research
Ridgefield, Connecticut

Petroleum reservoirs are usually sedimentary earth formations comprised of porous rock. Pore sizes may range over orders of magnitude within a single rock, and, in general, water, oil, and natural gas can coexist within each pore. In order to efficiently exploit a reservoir, it is necessary to know the location, quantities, and physical properties of the pore fluids. Well bore nuclear magnetic resonance measurements are now playing a substantial role in providing this information.

Transverse proton magnetization decays are measured by borehole NMR apparatus. Usually, these decays are analyzed in terms of distributions of relaxation times. In favorable cases, water and crude oil magnetizations are observed to decay with distinct relaxation times. However, many conditions can limit the NMR observability of hydrocarbons in reservoirs: (1) proton density is low, (2) there is substantial relaxation of magnetization within the dead time of the receiver, (3) water and oil signals decay at overlapping rates, making them difficult to distinguish, or (4) longitudinal relaxation time is sufficiently long that hydrocarbon spins cannot be fully polarized in the cycle time of the measurement.

A number of methods have been developed to detect the presence of oil in earth formations, even in unfavorable circumstances. Some are purely NMR methods, others employ combinations of physical measurements. Efficacy of these methods is demonstrated by oil well logs.

Industrial Applications of NMR

Armando De Los Santos, J. Derwin King
Southwest Research Institute (SwRI), San Antonio, TX, USA

Nuclear magnetic resonance (NMR) has been used successfully to monitor industrial processes on-line and at-line. NMR has typically been explored for those applications when other more common off-the-shelf technologies failed to provide the required results. Some of the NMR applications have demonstrated remarkable repeatability and stability. In many cases, it has been difficult to obtain the required accuracy and repeatability in the primary measurement techniques used for calibration. The instrumentation has proven to be rugged, dependable, accurate and useable to control a process. Savings due to reductions in out of specification product which is either recycled or disposed of has justified the cost of the on-line instrumentation.

Several applications will be described along with correlations to the physical parameters of interest. A brief overview of instrumentation for industrial applications developed by other organizations will also be presented.

Several NDE Applications of NMR

Lowell J. Burnett
Quantum Magnetics, Inc.
7740 Kenamar Court, San Diego, CA 92121

Over the past few years, Quantum Magnetics has developed a number of new and novel applications of nuclear magnetic resonance (NMR) for the non-destructive evaluation (NDE) of diverse items ranging from intercontinental ballistics missiles (ICBM) to people. While these NMR systems look very different qualitatively, there are a number of common features linking them together. This paper will describe several of these NDE applications of NMR, highlight the important design considerations, and summarize both the performance and the utility of the resulting systems

Histology and Strain Images of Blood Vessel Walls Using ^{2}H Double Quantum-Filtered MRI.

G. Navon[1], Y. Sharf [2], U. Eliav[1], and Y. Seo[3]
Schools of Chemistry[1] and Physics[2], Tel Aviv University, Tel Aviv 69978, Israel.
[2] Department of Physiology, Kyoto Prefectural University of Medicine, Kamigyo-ku, Kyoto 602, Japan.

The mechanical properties of blood vessel walls play a central roll in cardiovascular function. At normal blood pressure the length of the vessel is as much as 40% longer and its circumference is about 30% greater than in the unstressed condition. In the present study, we introduce a novel spectroscopic MRI method for displaying distinct tissue layers of the blood vessel wall as well as measuring its mechanical strain.

The observation of deuterium double quantum filtered (DQF) NMR signal is an indicator for the presence of anisotropic motion [1]. Recently we have reported the observation of ^{2}H DQF NMR signal of water in various large blood vessels. The anisotropic motion of the water molecules was later shown to be due to their interaction with the collagen fibers [2]. Furthermore, the deuterium DQF NMR spectrum was found to be highly sensitive to the composition of tissue layers as well as to the strain exerted on the vessel wall [3]. Our measurements of bovine carotid and coronary arteries indicated that the ^{2}H DQF NMR spectrum of the intermediate layer *tunica media* is insensitive to strain and is characterized by a relatively narrow signal and long relaxation times. On the other hand the spectral lineshape of the outer layer, the *tunica adventitia*, is much broader and is highly sensitive to strain; the residual quadrupolar interaction were found to gradually increase with elongation. Thus an imaging method based on ^{2}H DQF NMR can give us a map of both tissue composition and strain distribution within the blood vessel walls.

We obtained ^{2}H DQF 2D histological images of a cross section of an isolated, D_2O-hydrated, bovine coronary artery. By a proper use of the DQ creation time and the selection of the spectral frequency range different parts of the tissue can be highlighted. Spatially resolved DQF spectra were acquired for a fully relaxed and 55% elongated sample of a bovine coronary artery. In order to visualize the effect of elongation the average residual quadrupole splitting $\langle\Delta\nu_q\rangle$ was calculated for each pixel. The obtained ^{2}H quadrupolar splitting images are shown in the figure. On the basis of the calibration curve shown in the figure on the right hand side, which was previously done[2] for the outer layer of the coronary artery, these images can be interpreted as strain maps.

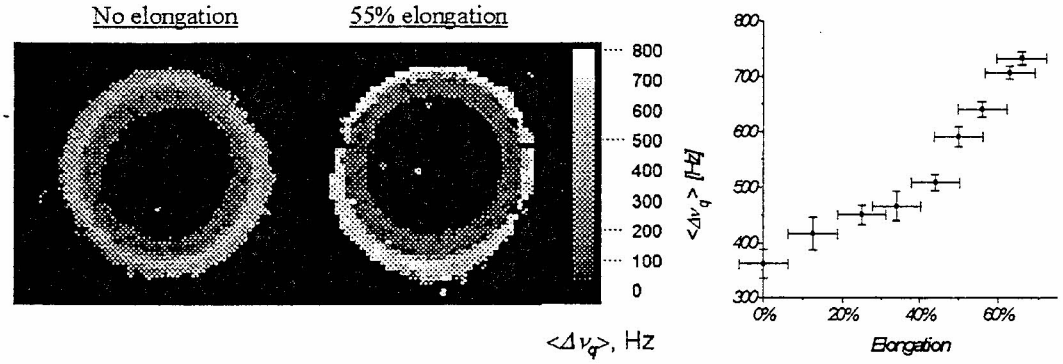

1. Y. Sharf et al., J. Magn. Reson., **B. 107** 60 (1995). 2. Y. Sharf et al., Magn. Reson. Med., **37,** 69 (1997). 3. Y. Sharf et al., Biophys. J., in press.

NMR IMAGING OF RIGID BIOLOGICAL TISSUES

Y. SEO[1], H. TAKAMIYA[2], H. ISHIKAWA[3], T. NAKASHIMA[3], Y. SHARF[4] AND G. NAVON[4]

[1]Dept. of Physiology, [2]Dept. of Orthopaedic Surgery & [3]Dept. of Medicine III
Kyoto Prefectural Univ. of Medicine
Kamigyo-ku, Kyoto 602, Japan
[4]Schl. of Chemistry
Tel Aviv Univ.
Ramat Aviv, Tel Aviv, 69978 Israel

Rigid biological tissues, such as bone, teeth, tendon and calculus, are usually depicted in almost "BLACK" by ordinary sequences of nuclear magnetic resonance imaging. There are several trials for getting imaging information form such rigid biological tissues. We summarized several attempts and results of imaging of bone, cartilage, teeth, tendon and calculus. All experiments were done at 7.05 T using an NMR spectrometer (AMX-300wb, Bruker) with a gradient control unit (BGUII, B.A.M.). A microimaging probe was used with a 12 mm diameter RF-coil (micro5.0, Spectrospin AG). The spectrometer was controlled by an X32/3 computer with a ParaVision/UXNMR software (Version 940510.B.6.1).

H-1 transverse relaxation times of teeth and cortical bone are ca. 100 us, and were the shortest T2 of the biological tissues. Gradient-echo (GE) and spin-echo (SE) imaging sequences can not depict teeth and cortical bone even used the shortest echo-time (ca. 1 ms). Constant-time-imaging (CTI) is a 3D-phase-encoding sequential point imaging method so that a single data point in the k-space is taken with a minimum echo-time (ca. 100 us). We can get images from teeth and cortical bone without any artifacts from chemical-shift and susceptibility differences in sample. The image is almost density image, and The CTI does not require any special instrumentation, but only cost time for data acquisition.

H-1 transverse relaxation times of tendon, cartilage and calculus are in the range of few milliseconds. Gradient-echo and spin-echo imaging sequence are valuable for these samples with relatively short T2 relaxation times. We can get 3D-GE images of gall bladder stones with a resolution of 63 um3.

The other direction of effort is getting NMR information from ordered biological tissues. Tendon consists of well ordered collagen fibers, and the ordered structure is essential for its physical strength. H-2 nuclei has been used as a molecular probe for detecting the order structure. The H-2 double-quantum-filter (DQF) NMR allows us to detect H-2 nuclei in the anisotropic slow motion condition. We have extended the H-2 DQF NMR to spectroscopic imaging (DQF-SI). In 1D-DQF-SI of the Achilles tendon and soleus muscle, the tendon raised a big residual quadrupolar splitting (nq ; ca. 2.5 kHz) at a short DQ creation time (400 us), and the muscle raised a small splitting (ca. 15 Hz) at a longer DQ creation time (6 ms). The DQF-SI also depicted that adenaturated part of tendon represented smaller nq which represented loss of order structure of collagen fibers.

These imaging techniques now open a new field to study the rigid biological tissues.

References

1. D.G. Cory, Ann. Rep. of NMR Spectr. 24, 114, 1992.
2. H. Sharf et al., Proc. SMRM, 4th Ann. Meeting, New York, 1241, 1996

Capability of Microscopic NMR Imaging for In Vivo Quantification of Myocardial Function and Mass in Young (10g) Mice

J. Ruff, F. Wiesmann, K.-H. Hiller, S. Neubauer[1], W. R. Bauer[2], A. Haase
Physikalisches Inst., Universität Würzburg, [1]Med. Universitätsklinik, 97074 Würzburg, Germany
[2]II. Medizinische Universitätsklinik Mannheim/Heidelberg, 61835 Mannheim, Germany

Introduction

Mice are rapidly gaining widespread popularity in studies of cardiac physiology. But the small size of the mouse heart and its ultrafast heart rate (up to 600 beats per minute) make it difficult to characterize cardiovascular pathophysiology by *in vivo* methods.

The purpose of this project was to investigate the capability of magnetic resonance imaging to study myocardial function and mass non invasively in the young mouse. Examination of young mice (21days;10g) which would be helpful for the investgation of developmental changes is highly challenging due to the "microscopic" heartsize.

Methods

NMR measurements were performed on a 7-T-Bruker BIOSPEC spectrometer with a microscopy gradient system ($\oslash$ 70mm; maximum field strength 870mT/m) and a Bruker Birdcage HF-coil.

5 male C57bl/6 mice (9.9±0.7g SD) were explored. Homebuilt echocardiogram (ECG) patches were attached to the front paws. A warming pad was used to maintain normothermia.

Scout images were obtained to define a short axis plane. An ECG-triggered cine-sequence was performed using segmented FLASH to acquire 12 images of different heart phases with the following parameters: TR $\approx$ 10ms (depending on RR-time), TE 1.6ms, 256×256 acquisition matrix, FOV 25×25mm^2, slice thickness 0.7-1.0mm. The resulting in plane resolution was 98×98μm^2 by a total acquisition time of 100s (1 slice, 12 images, 4 averages). 6-7 contiguous ventricular short axis slices were acquired.

The end diastolic (ED) and end systolic (ES) cine images were chosen to appoint the ED and ES volume of left ventricle (EDV, ESV) and left ventricular (LV) mass. To determine LV mass, the epicardial border was manually delineated. EDV and ESV could be evaluated automatically by a thresholding algorithm. The LV mass of the 5 mice was weighted post mortem.

Results

Cine images in all animals revealed clear definition of endo- and epicardial borders and high contrast between blood and myocardium (Fig.1). The short echo time prevented flow-artefacts, often leading to extrem signal loss inside the ventricles.

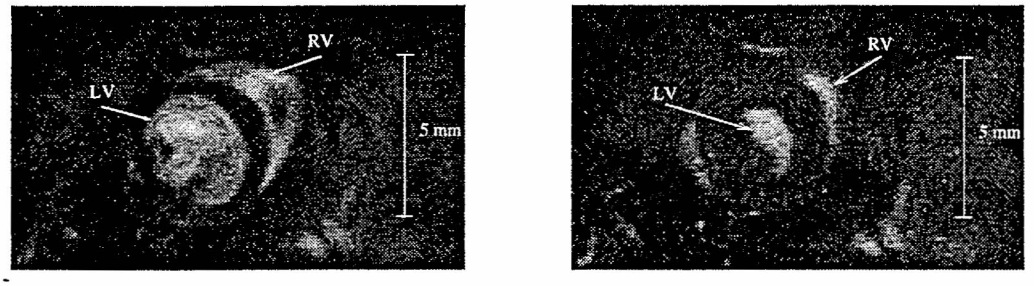

Fig.1. End diastolic and end systolic short axis image of the mouse heart (BW = 9.9g) .

The LV mass determined by MRI (42.1±2.1mg SD) and *ex vivo* (44.4±2.7mg) were in good agreement. LV function parameters were EDV 27.7±2.9μl, ESV 6.1±1.5μl and ejection fraction 78.0±5.4%. The interobserver variability was low: LV mass 4.0%, EDV 1.4%, ESV 6.6% and ejection fraction 2.2%.

Conclusion

In spite of the rapid movement of the small mouse heart, it was possible to obtain high quality cardiac images (Fig.1). It was possible to quantify cardiac function and mass in young mice accurately.

We are confident that improvement of spatial resolution will allow us to study even younger mice. Thus, NMR microscopic imaging is an ideal noninvasive tool to study the pathophysiology of heart diseases in the *in vivo* mouse model.

Investigation of the carbohydrate transport in plants by ^{1}H-detected ^{13}C spectroscopy and imaging by cyclic J cross polarisation

Walter Köckenberger[2*], Michael Heidenreich[1], Alex Hudson[2], Richard Bowtell[2], Rainer Kimmich[1]

[1]Universität Ulm, Sektion Kernresonanzspektroskopie, 89069 Ulm, Germany
[2]University of Nottingham, Magnetic Resonance Centre, Nottingham NG7 2RD, United Kingdom
*email: kocken@magres.nottingham.ac.uk, phone +44-115-9514751, fax +44-115-9515166

The major transport form of carbohydrates in plants is sucrose. The regulation and the mechanism of its transport over long distances is not well understood. NMR experiments using ^{13}C labelled compounds offer the possibility of non-invasive monitoring of carbohydrate transport, but are usually hampered by the low sensitivity of the ^{13}C nucleus. We report here on experiments with 6-days old castor bean seedlings in which we used indirect detection techniques to overcome the sensitivity problem, thus allowing measurements of sucrose metabolism and transport in vivo. In contrast to traditional destructive techniques used in plant physiology, our experimental design allows both the unambiguous identification of the transported compound and measurements of the undisturbed situation in intact plants.

Castor bean seedlings were grown hydroponically on the top of glass tubes which fitted in a specially designed insert for a micro-imaging probehead which operates in a 400 MHz widebore magnet. Position-labelled compounds ($^{13}C_1$-glucose and $^{13}C_1$-fructose) were supplied to the cotyledons. We observed uptake and further metabolic conversion of the two sugars to the disaccharide sucrose by directly detected ^{13}C spectroscopy on the intact plant. Cyclic J cross polarisation (CYCLCROP) was used to record rapidly spectra of both, the resonance of hydrogen coupled to the $^{13}C_1$ of the glucose moiety and the resonance of hydrogen coupled to the $^{13}C_1$ of the fructose moiety. The time resolution which could be achieved by repetition of the CYCLCROP experiment was sufficiently short (3 min) to follow directly the transport of the labelled sucrose in the plant stem. Furthermore spectra with the same time resolution have been obtained from three independent slices within the stem by using CYCLCROP with spatial localisation via one magnetic field gradient. After recording the transport of the labelled sucrose and its enrichment within the plant tissue by unloading from the vascular bundles for 8 hours the actual distribution of the labelled sucrose within the plant cross section was measured by acquiring a 128 × 16 ^{1}H-detected ^{13}C (spin echo) NMR image of C_1-sucrose resonance. The achieved spatial resolution was 54.7 μm × 437.5 μm in the transversal plane with 10 mm slice thickness set by the sensitive volume of the coil. The experimental time was 1.5 hours. Images with 128 × 128 point were reconstructed by zerofilling from the data matrix (fig1). The images revealed the unexpected result that the labelled sucrose is found mainly in the outer ring (the cortex parenchyma and the vascular bundles) and not within the centre of the plant stem.

fig1: ^{1}H-detected ^{13}C image of the C_1- sucrose resonance overlaid by a contour plot from a high resolution ^{1}H Image of the plant stem

The very encouraging results from these initial experiments indicate that indirect detection of ^{13}C via the ^{1}H NMR signal will open up a new range of applications of NMR in plant physiology.

[1]References:
Kunze C, Kimmich R (1994), MRI 12, No 5, pp 805-810
Kunze C, Kimmich R (1994), JMR B 105, pp 38-44

REMOTE MICROSCOPIC NMR IMAGING VIA A WORLDWIDE WEB INTERFACE TO A STANDARD IMAGING SPECTROMETER.

DOUG MORRIS
Biomedical Magnetic Resonance Laboratory, University of Illinois
U of I/BMRL 1307 West Park Street
Urbana IL 61801

We present an interface for remote microimaging operation of standard NMR spectrometers. The recent development of the World Wide Web (WWW) opens many opportunities for remote operation of inherently digital equipment such as modern NMR spectrometers and imagers. Gregory et. al. demonstrated the use of an MR imaging spectrometer via the WWW at the 1996 ENC.[1] We present a further development of this technology in which the imaging spectrometer, in this case a Varian INOVA system, itself contains the routines for control, acquisition, processing, and communicating NMR data over the Web. Highlights of this new development are: remote operation, accessibility to multiple operators, and an easily configured interface for users of varying expertise. We demonstrate the utility of the Web interface for imaging murine embryos with a variety of MRI procedures and hardware configurations. The new Web interface is of immediate utility to the micro - MRI community due to its standalone nature, educational flexibility, and ease of collaboration at a distance. Applications to education and collaboration will be discussed and demonstrated.

[1] C. D. Gregory, C. P. Potter, H. D. Morris, P. C. Lauterbur, Experimental Nuclear Magnetic Resonance Conference, The Asilomar Conference Center, Pacific Grove CA, March 17-22, 1996.

More information is available at the following URL:
http://bmrl.med.uiuc.edu:8080/WebNMR/ .

ChickScope: WWW control of an MRI for K-12 education.

Clinton Potter and Paul Lauterbur

National Center for Supercomputing Applications, Biomedical Magnetic ResonanceLaboratory, and Beckman Institute. University of Illinois, Urbana IL USA

The advance of remote control technology via the WWW allows the use of state-of-the-art research machinery in standard classroom based education. Chickscope is a demonstration project for this technology using a MRI to examine the development of a chicken embryo from fertilization until birth by school children ranging from kindergarten to high school. We report some of the finding from this initial exercise in multi-user concurrent operation of a MRI in an classroom setting.[1]

The remote control technology used in the Chickscope apparatus has been demonstrated elsewhere.[2] In short the WWW control system uses a RS-6000 computer to control network access and pass control information and data to a Surrey Medical Imaging Systems MRI console on a 4.0 T / 31 cm MR system. The imaging protocol instructions sent to the SMIS console are executed. Resultant imaging data is written to a shared network file system which is read and processed by the RS-6000 workstation. The processed image data and image acquisition parameters are written to an web accessible archive and passed along to the operators web browser. The operator is the connected web browser which initiated the imaging sequence. A number of web-browser may be connected at any one time and are equally capable of initiating a imaging experiment. Of course only one imaging experiment may run on the MRI at one time. Connected web browsers may be continuously updated to show the latest results without initiating a new acquisition.

Ten schools over a 100 mile area around Champaign,IL accessed the MRI twice a week to monitor the development of chick embryos maintained at the Beckman Institute. Local staff at the Beckman Institute and the University of Illinois prepared daily updates on the stages of development that were visible and physiological changes occurring. These updates were matched with MR images showing these changes. Student participation in online discussions and scrap books was performed using a WWW interface in addition to traditional classroom interactions.

Results, dynamics, and problems will be discussed. On-line documentation including the database of the project results is available.[3] A larger version of Chickscope is in the planning stages as a national or perhaps international demonstration project.

References:

[1] Submitted to the Chronicle of Higher Education.

[2] Presented at the 37th annual Experimental Nuclear Magnetic Resonance Conference, Pacific Grove, CA, p. 24 (March 1996).

[3] On-line references are available at
http://vizlab.beckman.uiuc.edu/ChickScope
http://bmrl.med.uiuc.edu:8080/NmrScope

REPORT ON THE NUCLEAR MAGNETIC RESONANCE INTERNET CONFERENCE HELD IN JAPAN

KATSUMI KOSE
Institute of Applied Physics
University of Tsukuba
Tsukuba-City 305 Japan

The strategic future planning committee of JSMRM held a symposium titled as "MRI & MRS in 21st century" in 1995. In this symposium, instructive lectures and exciting discussion were presented but the number of attendants was limited (<100) and there was no record for the valuable discussion. The chairpersons of the committee (Shoji Naruse, M.D. & Ph.D., and Masahiro Endo, Ph.D.) thus decided to have a symposium on the Internet because the meeting can be opened to many people and all of the discussion can be recorded. They planned to have the 1st JSMRM Internet meeting in January 1997 and organized the executive committee and technical committee in October 1996.

At first, the Internet meeting was planned only for domestic (Japanese) attendants, but afterwards, planned to have two parallel meetings performed in Japanese and in English (internationally). The meeting started January 27 and ended February 3 in 1997. About 30 papers were presented and hundreds of comments were posted (e-mailed) to the boards of the sessions displayed on the webpages of the meeting. All of the presentations and discussion were recorded on CD-ROM's and distributed in the 25th annual meeting of JSMRM held in Oomiya this September. If you are interested in this meeting, please contact
http://wwwbase.nacsis.ac.jp/jmrm/ic97/ss-index.html.

MR MICROSCOPY OF SAVANNAH RIVER TANK WASTE SIMULANTS

KEVIN R. MINARD[1], ROBERT A. WIND[1], AND LEE O. DWORJANYN[2]
[1]Pacific Northwest National Laboratory
P.O. Box 999
Richland, WA 99352
[2]Westinghouse Savannah River Co
Aiken, SC 29808

The production of fissionable materials for the nuclear weapons program led to the generation of significant amounts of highly radioactive nuclear waste, which needs to be processed so that it can be stored in a repository where it will have minimal impact on human health and the environment. At Savannah River Site, the In-Tank Precipitation (ITP) process presently in use employs tetraphenylborate ([B(Ph)4]-) (TBP) as the precipitation reagent for the removal of the soluble radioactive Cesium. It was found that various metallic species in the slurry, which can act as potential catalysts and supports for such catalysts, as well as the radiation that is present, resulted into a decomposition of the excess TBP leading to unexpected generation of benzene. This forced a shut-down of the ITP operations in order to gain a better understanding of the benzene generation, retention, and release, and to develop methodologies to control these processes. MR microscopy is one of the techniques that can been applied to investigate the benzene distribution in the waste slurries.

In this presentation the first MR microscopy results are given of such a study on simulated non-radioactive ITP slurries, carried out at PNNL. The slurries consisted of water, 4 wt% potassium tetraphenylborate (KTPB), and 5 M Na+, and were injected with up to 5 vol% benzene. The work was performed at 11.7 Tesla using a Varian UNITYplus spectrometer, extended with an imaging accessory and a microimaging probe manufactured by D.G. Cory and coworkers at the Massachusetts Institute of Technology (MIT). In this probe gradients up to 10 T/m can be generated. The experiments were performed on small samples with a volume of about 1 mm3, using a RF coil of both an inner diameter and a length of 1.7 mm. Total proton (i.e. benzene + water) MR micro-images were used to determine the distribution of the unobservable solid KTPB by virtue of its dark appearance in the images. Moreover, benzene-only images were generated by utilizing the significant differences between the water and benzene T1 values. 3D micro-images were obtained with a resolution of 10x10x10 cubic micrometers in the composite images and 20x20x20 cubic micrometers in the benzene-only images. Finally, restrictive diffusion experiments on ROI's in the samples selected with STEAM were used to detect the presence of small benzene-containing microstructures with sizes below the image resolution. In samples with 5 vol% added benzene it was found that the KTPB is more or less uniformly distributed throughout the sample, and that the benzene occurs in the form of relatively large droplets with sizes up to 200 micrometer, presumably surrounded by a layer of KTPB. It was also found that if the sample is shaken for a few hours, irreversible structural changes occur: the KTPB predominantly occurs in larger flake-like structures, whereas the benzene becomes part of KTPB/benzene agglomerates, and is present in structures with sizes of a few micrometers. Hence sample agitation might be a suitable technique to stabilize the benzene-containing slurries.

^{13}C Detection of Diamonds in Intact Stones

DETLEF MUELLER
BRUKER Analytik
Silberstreifen, D-76287 Rheinstetten

Abstract:

A major obstacle in the mining process of diamonds is the fact that embedding stones must be crushed down to the size of possible diamonds, thus also endangering potential larger gemstones. Therefore a detection method for diamonds within large intact stones is highly desirable. We have tested NMR and EPR for this purpose. EPR suffers significantly by the rather high dielectric losses of diamond carrying minerals, whereas the lower frequency ^{13}C NMR is not hopeless. On the other hand, the prohibitively long ^{13}C T1 values and magnetic inclusions in the surrounding Kimberlite complicate the situation significantly.

Methods to overcome these problems are discussed, among others:

- Ultrasonic shortening of T1
- Magnetisation transfer through pulsed DNP

The construction of a prototype system (throughput ~1to/hr) will be discussed and results from this system are presented. Current limitations, mostly due to inefficient spin diffusion, will be discussed.

NMR MICROSCOPY IN INDUSTRIAL RESEARCH: POLYURETHANE FOAMS AND POLY (SODIUM ACRYLATES)

M. SZAYNA, R. VOELKEL, L. ZEDLER
BASF AG
670~6 Ludwigshafen, Germany

One of the attractions of NMR microscopy is the ability to produce true 3D images Not only geometrical shapes but also chemical and physical properties can be spatially visualised by parameter selective techniques. Investigating "wet" systems which often are difficult to handle by other techniques poses no problem to NMR. However a direct transfer of well established NMR pulse sequences to real solids often results in serious problems due to short T_2 and long T_1 relaxation times. In such case indirect ways of measurement have to be chosen to circumvent limitations of the equipment, to improve the signal to noise ratio, and to shorten the duration of the experiment to an acceptable level.

Another requirement which is much desirable but so far has not been pursued sufficiently is the quantification of image data. Reducing the large amount of data to just a few parameters which characterise the sarnple is essential, if a correlation of image data with physical properties should be established, as is required in product development. An appropriate matching of spatial resolution and the size of structures under investigation is paramount.

An attempt has been made to study polyurethane foams and poly(sodium acrylates) by means of 3D NMR imaging by taking into account such considerations. Data are collected on a commercial microimaging system which is also equipped with a diffusion probe. Standard spin echo, gradient echo and diffusion pulse sequences are used for the acquisition of data. Images of a spatial resolution of up to 8 μ m in all three directions are obtained. Using standard as well as home-developed image processing programs statistical evaluations of the foam structure are made and the results compared t~ those from optical rnicroscopy. Good agreement between the two techniques is found as far as the statistics of the cell size is concerned. NMR data might be used for a further understanding of the mechanical properties of the foams which are used in the manufacturing of car seats etc.

The uptake of water in poly(sodium acrylate) material has also been studied. From a practical point of view its use as very potent water absorber in hygiene products makes such investigations important to industry.

STRAY FIELD IMAGING (STRAFI) AND MAGNETIC RESONANCE MICROIMAGING (MRM) STUDIES OF WATER INTRUSION/STRESS MOBILISATION IN DENSE POLYMER SYSTEMS USED IN CONSTRUCTION

S.N. SCRIMGEOUR, G. HUNTER, W.J. HARVEY, C.H. LLOYD, D. LANE*, P. J. MCDONALD*

Departments of Chemistry, Civil Engineering, and Dentistry,
University of Dundee
Dundee DD1 4HN, Scotland, UK
***Department of Physics**
University of Surrey
Guildford GU2 5XH, England, UK

Introduction:

High density and high modulus thermoset adhesives and stress transfer materials based on polyester and epoxide resins are increasingly being used in the construction industry. These substances are polar and as such have an affinity for water. Some epoxy adhesives are known to absorb water from the environment, a process which adversely affects their mechanical and physical properties. Water may also be preferentially absorbed at interfaces. Since the materials have high moduli, substantial swelling pressures can be expected and the resulting stresses have been implicated in the degradation of adhesive joints [1]. All applications involve bonding in situations which may be strain intolerant and, if a resin/polymer component undergoes significant dimensional change and the containment does not allow strain relaxation, then high localised stresses could result in distortion and/or failure of the component. At present the consequences of water absorption are not readily accounted for since the mechanisms for such movement into the bulk of such polymers systems are largely unknown.

Imaging Studies.

"Liquid" MRM and STRAFI [2] were used to study the actual distribution of sorbed water in intact polymer samples. CP/MAS spectroscopy was used to study polymer molecular chain dynamics. It was found that: (i) water penetration into bonded structures made from GRP composites occurs via the adhesive, not the GRP; (ii) changes in relative humidity during the mixing period of the adhesives make little difference to the strength of the bonded structures; (iii) all common epoxy adhesives contain large amounts of filler and these change the molecular chain dynamics of the polymer. This was previously unsuspected as fillers are normally regarded as chemically inert materials and are added to improve rheology and fracture toughness; (iv) water penetrated all the adhesives to a greater or less extent, but not their parent epoxies. The sorption is a two stage process. The first of these is anisotropic, water penetrating through cut or damaged surfaces but not through intact moulded or set surfaces. This has important implications for structures damaged in service. The second stage is Fickian; (v) Poisson's ratio remained the same even after 15 months' soaking, and while there were changes in Young's and bulk moduli, none indicated catastrophic loss of property. Mechanical failure in composite structures occurred at the GRP/adhesive interface after soaking, while in dry samples cohesive failure occurred in the GRP.

[1] R.C.L. Tai and Z. Szlarska-Smialowska, J. Mater. Sci., 28 (1993) 6199
[2] P.J. McDonald, Prog. NMR. Spectr., 30 (1997) 69

NMR MICROIMAGING, A USEFUL TOOL TO STUDY THE DISSOLUTION OF SOLIDS

NICOLE BLACK, TODD VIENNEAU[1], AND YONG PAN
Procter & Gamble Company
Miami Valley Laboratories
P.O. Box 538707
Cincinnati, OH 45253
[1]Procter & Gamble Pharmaceutical
8700 Mason Montgomery
Mason, OH 45040

Dissolution is an important issue to many consumer products. Factors that affect dissolution include the compound's intrinsic solubility, particle size, porosity, and molecular interactions. The dissolution rate of a solid tablet is normally controlled by one or more of the following steps: 1) water penetration to the tablet dry core, 2) disintegration of the tablet into small fragments or particles, 3) solubilization of the disintegrated particles, and 4) diffusion of the solubilized molecules into the homogeneous dissolution medium. The identification of the rate-controlling step is the key to controlling the release of actives.

Conventional methods for measuring water penetration require physical manipulation of samples, which may introduce considerable errors in measurement. NMR imaging provides a non-invasive method to examine the spatial distribution of mobile spins (protons) in a sample. The intensity in an image voxel reflects intrinsic NMR properties, namely, spin density, spin-lattice relaxation, and spin-spin relaxation. NMR imaging is an ideal tool to monitor a process like dissolution in real time. We have used NMR imaging to study the dissolution of a newly formulated pain reliever tablet.

The new pain reliever contains a sleep-aid in addition to an analgesic as active ingredients. The sleep-aid/analgesic tablets had a much slower release of both actives than the analgesic-only tablets in a standard dissolution test. We performed N~ imaging experiments on both of the tablets using a Bruker MSL-300 spectrometer. The tablet was placed in a 15 mm tube filled with a regular or deuterated dissolution medium at various pH. The images of a transverse plane were recorded every two minutes for four hours using a spin-echo imaging pulse sequence. The dry core area over time was measured using a macro in the imaging analysis program, Optimas.

The results clearly show the water penetration rate of the sleep-aid/analgesic tablets was much faster than that of the analgesic-only tablets. The images in the deuterated medium show that 1) the drug actives in the sleep-aid/analgesic tablet were quickly solubilized; however, the release to the medium was very slow, and 2) the drug active in the analgesic-only tablet was solubilized and then quickly released to the media. A gel-like material appeared in the image of the sleepaid/analgesic tablet, which might be due to the formation of an ion pair complex. The complex was isolated as a precipitate in a mixture of solution with both actives and identified by GC, IR, and solution NMR. The NMR imaging results suggest that water penetration is not the rate-controlling step in the dissolution of the sleep-aid/analgesic tablets. Rather the drug release rate is controlled by the diffusion of drug actives through the gel matrix.

NMR imaging is an ideal tool to study water penetration and active release in general. In our studies of several other systems, we have identified dissolution-controlling processes as water penetration, gel formation, individual particle solubilization, or disintegration, depending upon the nature and composition of the systems.

SATURATION OF POROUS AQUIFERS INVESTIGATION USING SURFACE NMR.

O. A. SHUSHAKOV AND V. M. FOMENKO
Inst. of Chem. Kinet. & Combust.
3, Institutskaya St.
Novosibirsk 630090-RUSSIA.

Macroscopic "samples" of more than 100x100 m porous (or fractured) aquifers can be investigated using surface proton magnetic relaxation measurement in geomagnetic field. An antenna (usually a circular loop) with a diameter of about 100 m is laid out on the ground to excite and receive the NMR signal. An oscillating current with rectangular pulse-shape and the carrier-frequency being equal to the proton-resonance frequency in the Earth's field is passed through the antenna and followed by a nuclear induction emf due to free Larmor precession in the Earth's field. The depth of water-saturated layers can be determined from the NMR signal amplitude dependence on the excitation-current pulse moment and, therefore, this method can be regarded as a surface-NMR tomography of subsurface aquifers.

The technique can be used to register the magnetic-resonance signal of water protons in the Earth's magnetic field, H0, which is of the order of 5*10-5 T. The resonance signal has a frequency of about 2 kHz in field H0, and is excited by a transmission field H1 at the resonance frequency.

This unusual "NMR"-method is peculiar both in experimental and theoretical aspects.

First peculiarity of the surface NMR is that H0 and H1 amplitudes are compatible. Effects of high field H1(so-called Bloch-Siegert shift of resonant frequency) was investigated earlier [1]. Such effects can be described in terms of nonsecular effects of nuclear-magnetic interaction Hamiltonian. The nonsecular effects not being taken into account are able to lead to significant "increase" in the surface NMR-signal amplitude and phase and appearance of virtual "levels" of subsurface "water" whilst solving the surface-NMR tomographic problem.

Another particular quality of the surface-NMR method is that finite ground conductivity can result in induced currents that can screen the NMR signal. High conductivity (low resistivity) is inherent in both saline water-saturated layers and aquatards, for example, clay-rich rocks. The resistivity of clay-rich soil and rock can be as low as 1-10 ohm-m. The resistivity of saline-water saturated rocks can amount the same value. The conductivity can affect both phase and amplitude of the NMR signal at resistivities of a few to a few tens of ohm-m depending on the depth of the water-saturated layers [2]. The effect of electroconductivity on the surface NMR can be applied for groundwater diamagnetic impurities investigation, e.g. to estimate groundwater salinity by integration of an electromagnetic method and surface NMR [3].

The surface nuclear relaxation times measurement allows to investigate some properties of water-bearing soil, such as porosity, or paramagnetic impurities detection. The relaxation times T1,T2, and T2* were measured by the surface NMR both for aquifers as well as for bulk water under ice of frozen lake [4].

1. Bloch F., Siegert A. Phys.Rev., 1940, v. 57, p. 522.
2. Shushakov O. A. Geophysics, 1996, v. 61, p. 998.
3. Trushkin D.V., Shushakov O.A., Legchenko A.V. Geoph. Prospecting, 1995, v. 43 , p. 623.
4. Shushakov O. A. Magnetic Resonance Imaging, 1996, v. 14, p. 959.

NUCLEAR QUADRUPOLE RESONANCE (NQR) FOR DETECTION OF EXPLOSIVES AND LANDMINES

ALLEN N. GARROWAY, MICHAEL L. BUESS+, JOEL B. MILLER, KENNETH J. MCGRATH, JAMES P. YESINOWSKI, BRYAN H. SUITS++, AND GERALD R. MILLER*

Code 6122, Chemistry Division
Naval Research Laboratory
Washington, DC 20375-5342 USA
+SFA, Inc.
Landover MD
++Physics Department
Michigan Technological University
Houghton, MI 49931-1295
***University of Maryland**
College Park, MD

Pure nuclear quadrupole resonance (NQR) of 14N nuclei is quite promising as a method for detecting military explosives such as RDX, TNT and PETN in quantities of interest. Pure NQR is conducted without an external applied magnetic field. Because NQR frequencies of different compounds are quite distinct, we do not encounter false alarms from the NQR signals of other benign materials. We have constructed a proof-of-concept NQR explosives/contraband detector which interrogates a volume of 300 liters. We can detect threat quantities of explosives within the 300-liter inspection volume in 6 seconds.

We first outline the basics of the NQR approach, highlighting strengths and weaknesses, and then present representative results for explosives detection.

We are also examining this technique for detection of landmines, and discuss some of the approaches specific to the detection of TNT and RDX with a surface coil.

NRL has licensed NQR explosives and contraband detection technology to Quantum Magnetics Inc. (San Diego, CA), and QM systems are presently being evaluated at US airports.

This work is sponsored in part by the US Federal Aviation Administration, Office of Special Technologies (Department of Defense) and the Defense Advanced Research Projects Agency.

QUADRUPOLE RESONANCE EXPLOSIVE DETECTION SYSTEMS

T. RAYNER, A.D. HIBBS, B. THORSON, S. BEEVOR AND L.J.BURNETT.
Quantum Magnetics Inc.
7740 Kenamar Court
San Diego, CA 92121

Quadrupole Resonance (QR) has been demonstrated to be an effective technique for detecting the presence of specific chemical compounds. QR is similar to the widely used nuclear magnetic resonance (NMR) and magnetic resonance imaging (MRI) techniques, but has the considerable advantage that the item to be inspected does not need to be immersed in a steady, homogeneous magnetic field. The target compounds arc identified unambiguously by their unique quadrupole resonance frequencies.

Quantum Magnetics is actively developing explosive and narcotic detection devices based upon QR technology. The work presented here describes the development of two systems, a multicompound QR detection system suitable for the scanning of check-in baggage and a dual compound detection system for locating buried landmines and ordnance. The design philosophy is discussed, including test results from both US and UK field trials. The two detection systems represent the current state of QR technology designed for field use in commercial, government and military sectors.

APPLICATIONS OF FLOW IMAGING IN MATERIALS SCIENCE

P. BLÜMLER, K.ROMBACH, S. LAUKEMPER-OSTENDORF, AND B. BLÜMICH

Institut für Makromolekulare Chemie and Zentrum für Magnetische Resonanz
Rheinisch-Westfälische Technische Hochschule Aachen
D-52074 Aachen, Germany

The investigation of mass transport phenomena by NMR imaging has received increasing interest during the last few years. The detection and visualization of flow in NMR imaging can be realized in different ways: 1) Time of flight, 2) tagging and 3) phase methods. The implementation of a simple method for phase encoding of flow in a flow-compensated 3D imaging sequence is described.

Experiments have been carried out to investigate the flow along the longitudinal axis of dialysis modules consisting of single hollow-fiber membranes as well as the counter-flow through the dialysate ompartment. Application of these experiments to different model hemodialyzers provides information about flow distributions within the inner and outer regions of the hemodialyzers.

A standard technique in polymer and food processing is the single-screw extrusion. By means of NMR imaging it is possible to obtain information about flow-velocity distributions, diffusion and shear in a non-invasive fashion. This has been demonstrated by application of the pulse sequence mentioned above to a static mixer and a single-screw extruder. The detection of different chemical phases can be achieved by combining flow imaging with chemical-shift selective excitation.

Another important application is the analysis of waves in liquids. Surface waves of water have been generated in a glass tube by a magnetic paddle. The wave trigger has been used to trigger the imaging sequence as well. In this way the propagation of waves can be monitored. 'Valleys' and 'hills' as well as velocity profiles can be observed.

NON-NEWTONIAN RHEOLOGY AS PROBED BY NMR MICROSCOPY

MELANIE M. BRITTON AND PAUL T. CALLAGHAN
Department of Physics
Massey University
Palmerston North, New Zealand.

Complex fluids exhibit structural properties which encompass the molecular, mesoscopic and macroscopic length scales. Associated with these length scales are dynamical processes whose characteristic times cover a range from picoseconds to hundreds of seconds. It is the intermediate and slow processes that define the mechanical behaviour and hence the non-Newtonian viscosity of a system. These timescales fall into the NMR windows corresponding to pulsed gradient spin echo measurements of velocity and diffusion. With NMR microscopy we are able to follow the shear rate dependent viscosity for a range of complex fluids, and are able to gain insight regarding the molecular dynamics underpinning non-linear rheology.

One very interesting non-linear constitutive property of complex fluids concerns the non-monotonic behaviour in the stress vs shear rate curve (the flow curve), with such behaviour being the subject of considerable theoretical conjecture in recent years. The classes of fluids that exhibit a stress minimum in their flow curve include both high-molecular weight polymer liquids and solutions of wormlike surfactants. Velocity distributions for the wormlike surfactant system cetylpyridinium chloride/sodium salicylate (100 mM/60 mM) will be presented. This system exhibits distinct shear banding when the applied shear rate is set to a value larger than the critical rate of strain. This result also brings into question one of the main assumptions of cone-and-plate rheometry, namely the shear rate is uniform in the gap.

[1] M. M. Britton and P. T. Callaghan, *Phys. Rev. Lett.* 78, 4930-3 (1997)
[2] M. M. Britton and P. T. Callaghan, J. *Rheol.* (submitted)

Simultaneous Measurement of Temperature and Velocity Maps by Inversion Recovery Tagging Method

Kuniyasu OGAWA[1], Makoto TOBO[2], Norio IRIGUCHI[3], Shuichiro HIRAI[1] and Ken OKAZAKI[1]

1 Research Center for Carbon Recycling & Utilization, Tokyo Inst. of Tech.,
2-12-1 Ookayama, Meguro-ku, Tokyo 152 (ogawak@mep.titech.ac.jp)
2 Graduate school, Tokyo Inst. of Tech., 2-12-1 Ookayama, Meguro-ku, Tokyo 152
3 Siemens-Asahi Med. Tech. Ltd., 20-14, Higashi-Gotanda, Shinagawa-ku, Tokyo, 141

INTRODUCTION

Noninvasive measurement of temperature and velocity maps is important to analysis mass and heat transfer phenomena in porous media with single or multi-phase flow and chemical reactions, and in micro-channel type heat exchanger as electric cooler. Magnetic resonance microscopy has advantages over optical methods because it can measure these maps without opaque and scattering effects of porous media and working fluids. Determination of temperature and velocity of phantom using IR tagging method combined with Inversion Recovery and tagging pulse was investigated experimentally.

METHODS

Two experiments have been performed on a Varian UNITY INOVA 300 super wide bore with RF probe of ID 60mm to develop the method of measurement.

In case of non-flowing phantom, temperature map of a phantom (5mmol/l $CuSO_4$ aq.) in cell, which had temperature difference between upper and lower walls, was determined from previously measured relationship between temperature and T_1 relaxation using a conventional spin echo sequence with inversion pulse. In case of flowing phantom, flow image of tags and temperature map of the phantom in a curved tube immersed cooled fluorinert pool was obtained by IR tagging method, which inversion pulse angle was adjusted to 180 degree.

RESULTS

Fig. 1(a) shows the experimental apparatus to measure temperature map of the non-flowing phantom. One dimensional temperature gradient into the phantom was approximately established by upper heated wall and lower cooled wall, and it does not induce flow of phantom due to stable condition. The measured temperature map of the phantom by IR method at relaxation time τ=0.6s is shown in Fig. 1(b). To verify the temperature map, comparison with the results measured by thermocouples at the center axis is shown in Fig. (2). The measured temperature distribution by IR agree with that by thermocouples.

The obtained image and temperature distributions determined at each tag of flowing phantom in the curved tube immersed cooled fluorinert pool was shown in Fig. 3. Although it confirms the temperature decreases with going downward, the accuracy of measurement is not higher due to distorted shape of tags. Improvement of the tagging pulse sequence is necessary to increase the accuracy.

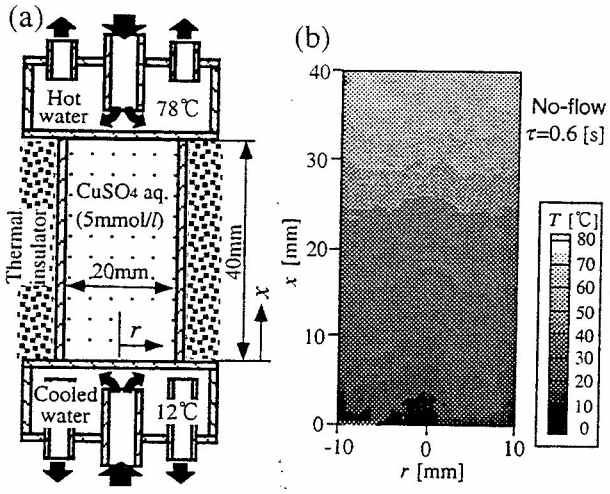

Fig. 1 (a) experimental apparatus
(b)Temperature maps by Inversion Recovery method in case of no-flow phantom

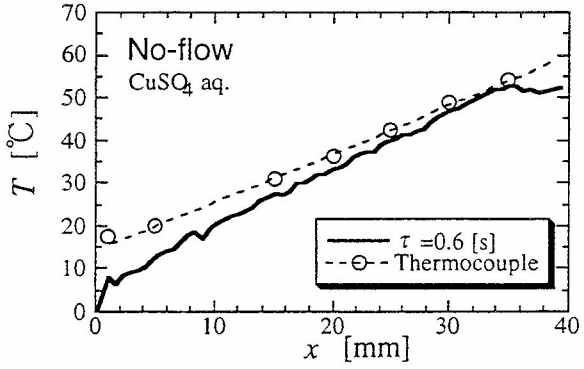

Fig. 2 Comparison with temperature distributions by Inversion Recovery method and thermocouples

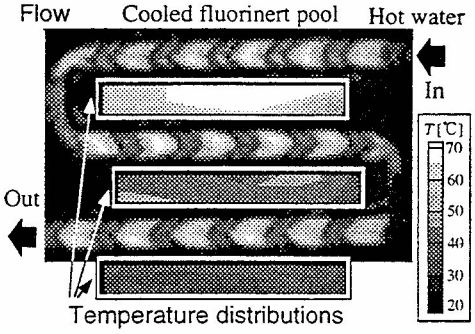

Fig. 3 Image and temperature maps of flowing phantom in curved tube measured by Inversion Recovery tagging method

NMR-IMAGING TECHNIQUES FOR QUANTITATIVE CHARACTERIZATION OF PERIODIC MOTIONS: 'INCOHERENT AVERAGING' AND 'SPECTRAL SIDE BAND ANALYSIS'

UTE GOERKE*, RAINER KIMMICH
Sektion Kernresonzanzspektroskopie
Universitaet Ulm
89069 Ulm, Germany

Conventional motion-sensitive imaging techniques have been frequently used for spatially resolved detection of stationary flow. They have been adapted for the application to time-dependent motions. Eg., fast imaging sequences aim at minimizing total experimental time to reduce temporal velocity fluctuations during imaging. Various types of stroboscopic methods synchronize the acquisition with the pulsating motion to render images of distinct parts of the cycle. In contrast, we present techniques - the method of incoherent averaging and the spectral side band analysis - , which do not require adjusting the timing of the imaging experiment in order to maintain the correlation between the periodicity of the motion and the acquisition governed by the repetition time of the transients.

In these methods, the signal phase is affected by spin displacements in the presence of magnetic field gradients. The incoherent temporal averaging technique implies the accumulation of as many transients as required to obtain a time-independent phase twist owing to motions. Maps of the coherent (stationary) part of the flow are rendered by phase-encoding. Amplitude-weighted images represent the incoherent component referring to temporal fluctuations of the motions. The time-dependence of the spin displacements is investigated by acquiring a series of single transients. These transients, which are recorded in presence of a read gradient, are generated by omitting spatial phase-encoding. Therefore, amplitude-weighting of the signal probes spatially incoherent motion in respect to one of the spatial dimensions. The temporal fluctuations of the spin displacements reveal themselves as modulation of the signal intensity in a series of subsequent transients. In contrast to these methods, a new method - the spectral side band analysis - has been developed to characterize periodic motions without temporal or spatial averaging. This technique is based on the phase modulation in the phase-encoded dimension caused by periodic motions. In the Fourier-transformed data set, this phase modulation generates side bands which are shifted in respect to the original image in the phase-encoded dimensions. To avoid overlapping of the side bands an additional pseudospectral dimension is encoded. Using this method, the pulsation rate and the velocity amplitude can be derived from the offset of the side bands and their intensity, respectively.

Both methods - the technique of incoherent averaging and the spectral side band analysis - were applied to characterize pulsating motion in incubated bird eggs [1, 2]. Consistently, motions above the yolk sac were observed to start on about the fourth day of incubation. These motions are preferentially directed perpendicular to the yolk sac membrane. Quantitative analysis revealed a pulsation frequency of about 0.4 Hz. In conclusion, the incoherent averaging technique and the spectral side band analyis are both suitable methods for the quantitative characterization of periodic motions with a pulsation period less than the total imaging time.

References:
[1] U. Goerke, R. Kimmich, and J. Weis, J. Magn. Res. B 111, 236 (1996)
[2] U. Goerke, R. Kimmich, and J. Weis, Magn. Reson. Imag. 14 (9), 1079 (1996)

INVERSION NULLING IN SLURRY FLOW IMAGING

S. A. ALTOBELLI[1] AND L. MONDY[2]
New Mexico Resonance[1] and Sandia National Laboratory[2]
Albuquerque, NM

Concentrated suspensions are important in manufacturing, but preparing and delivering a uniform mixture of liquid and solids is complicated by the tendency of many suspensions to separate under the influences of shear and buoyancy. Experimenting with these materials is difficult. Direct observation of tracer particles in the interior of concentrated suspensions is possible only with very carefully selected components. Particle beam methods can be used to compute tomograms of particle positions, but velocity measurements have not been possible. Ultrasonic imaging and flowmetry have not been widely applied. Nuclear Magnetic Resonance Imaging has found some use in observing the liquid phase of concentrated suspensions. The volume fraction of the solid phase has been calculated by assuming that together the liquid and solid fill the observed region. The velocity of the solid phase could not be ascertained.

Here, we describe a system which provides volume fraction and velocity measurements of both phases. The liquid phase is a silicone oil, and oil-filled pharmaceutical pills comprise the "solid" phase. The NMR measurements are performed with standard sequences modified by the addition of a simple preamble which selects one of the phases based on the longitudinal relaxation T_1. Three types of flow experiments have been done:

1.Sedimentation
2.Flow in a horizontal, rotating cylinder, and
3.Couette flow,

and examples of each will be presented. This system may be useful to suspension rheologists who study mixing, hydrodynamic particle migration and buoyancy driven flows.

ADVANCES IN STRAY FIELD-GRADIENT TECHNIQUES

EDWARD W. RANDALL

Queen May and Westf ield College,
University of London

Stray field (STRAFI) gradients, which are found near the end of superconducting solenoids, arc typically about 50 T/m. These large gradients are very useful:

1. The echoes produced by the application of multiple pulses are state echoes of the Hahn type, and are independent of spin- spin effects.
2. Only a narrow slice of the sample is excited (the width is determined by the pulse-duration and by the line-width of the sample).
3. Short enough pulses and echo-times, τ , give echoes from both liquids and solids whether diamagnetic or not, and for any type of nucleus: spin-half, quadrupolar half-integral, and quadrupolar integral nucleides.
4. The echo amplitudes are governed by T_1 , T_2 and diffusion, each of which may be determined. The sample can be moved through the sensitive plain to give the spatial variation of these parameters.

New experimental developments which will be presented include the use of

1. Higher fields (magnets with center fields of 14.1 T and 19.6 T).
2. Higher field-gradients (72 T/m).
3. New protocols: the use of very long echo trains.

The last remaining type of nucleide to be studied by STRAFI techniques, namely those with integral spin will be represented by ^{2}H and ^{14}N (I = 1). New results for ^{31}P will also be presented. New calculations of STRAFI echoes made with the Gamma Platform will also be reported.

*Collaborators (and locations):

1. P. R. Bodart and T. Nunes: Deuterium and quadrupolar nucleides with half integral spins. (ICTPOL, Lisbon)
2. R.Fu and A. A. Samoilenko: ^{14}N Hahn echoes at 32 MHz: STRAFI imaging. (NHMFL, Tallahassee and Moscow)
3. A. A. Samoilenko and V. G. Soghomonian: Hahn echoes in high field-gradients: ^{2}H, ^{13}C, and ^{27}Al. (Inst. Chem. Physics, Moscow and NHMF)
4. B. Newling and D. G. Gillies: ^{31}P STRAFI NMR. (Surrey Univ.)
5. S. Smith: Calculations of STRAFI echoes with the GAMMA Platform.(NHMFL., Tallahassee)
6. A. Bohris and D. G. Gillies: Diffusion of the BF_4^- ion: ^{11}B STRAFI echoes.

STRAY FIELD IMAGING OF SOLVENT INGRESS IN POLYMERS.

D. M. LANE AND P. J. MCDONALD

Department of Physics, University of Surrey, GU2 SXH, U.K.

Solvent ingress into polymeric materials is of widespread industrial importance. Although in some applications such as drug release systems, controlled liquid uptake is desirable, more often, solvent absorption is responsible for polymer degradation and for shortening product lifetimes. Experimentally, a rich variety of diffusion dynamics have been observed for liquids ingressing polymers, ranging from Fickian diffusion characterised by uptake varying with time as $t^{0.5}$ through anomalous diffusion to Case II diffusion characterised by uptake varying linearly with time t^1. More recently, it has been realised that the synergetic effects of two or more *mixed* solvents and of residual solvent left over in the polymer as a result of manufacture, can be particularly important when polymer degradation issues are addressed.

The diffusion of solvents into polymethylmethacrylate (PMMA) has been studied by a number of authors. However, for the most part this work has either used liquid state magnetic resonance imaging (MRI) techniques[1,2] or has only studied single component solvents. This paper will concentrate on the results of a *broad line* stray field MRI study of methanol and acetone *mixtures* diffusing into PMMA and of methanol diffusing into PMMA which has been *pre-swollen* with acetone. As well as presenting the results of the PMMA study, mention will also be made of other polymer systems where stray field imaging has been shown to be particularly valuable and more generally of the experimental difficulties which have been encountered and addressed.

In the case of PMMA, broad line experiments have allowed both the polymer *and* solvent concentrations to be measured directly as a function of time and position, something which is difficult to do otherwise. For systems exhibiting Case II diffusion, such as pure methanol into PMMA at room temperature, the concentrations are constant across the swollen region, yet spatial gradients in both the solvent and polymer chain mobilities have been observed[3]. The addition of small fractions of acetone to methanol in a solvent mixture, or directly to the PMMA in advance of exposure to methanol so as to create a pre-swollen polymer dramatically enhances the solvent uptake rate and a transition from Case II to Fickian diffusion is observed. In the case of mixed acetone/methanol solvents, experiments with one or other component deuterated show that within the resolution of the experiment, both solvents ingress together. The Case II to Fickian transition can also be brought about by varying the temperature of the sample; either by raising the temperature of a Case II system, or lowering the temperature of a Fickian system. To that end experiments have been conducted in the temperature range -20 to +60°C. Careful analysis of the absorption profiles for these systems allows testing of theoretical models of solvent uptake in polymers, such as that derived by Thomas and Windle[4] , in the important regime of anomalous diffusion where the uptake varies as t^n, $(0.5<n<1)$.

1. L.A. Weisenberger and J.L. Koenig, *Macromolecules* (1990) 23, 2445.
2. M. Ercken, P. Adriaensens and G. Rogers, *et al, Macromolecules* (1996) 29, 5671.
3. D.M. Lane and P.J. McDonald, *Polymer* (1997) 38, 2329.
4. N.L.Thomas and A.W. Windle, *Polymer* (1982) 23, 529.

Stray-Field Magnetic Resonance Imaging of Hardening Materials

Teresa G. Nunes,[1] Philippe R. Bodart[2] and Edward W. Randall[3]

1 ICTPOL/IST, Departamento de Engenharia de Materiais, Av. Rovisco Pais 1, 1096 Lisboa Codex, Portugal

2 Department of Chemistry, Durham University, South Road, Durham DH1 3LE, UK

3 Chemistry Department, Queen Mary and Westfield College, Mile End Road, London E14NS, UK

The hardening processes of cement pastes and medical polymers were investigated *in-situ*, using the stray-field imaging technique (STRAFI MRI),[1] with a magnetic field gradient of 37.5 T/m, and a ^{1}H frequency of 123.4 MHz. Analysis of one-dimensional projections (profiles) yielded information about the spatial dependence of the hydration rates for the cements, and the free-radical polymerisation kinetics for the polymers.

The use of STRAFI MRI made possible to observe the influence of additives (like gypsum) in the hardening process of *type I Portland cement*[2] and the spatial dependence of the hydration kinetics on the cement/water ratio.[3] Relaxation weighted ^{1}H magnetisation profiles, obtained over 70 h, will be presented and discussed. STRAFI images of quadrupolar nuclei of half integer spin were reported on solids.[4] Single-slice ^{27}Al STRAFI images of dried Portland cement will be shown; two different aluminium sites with tetrahedral symmetry and high quadrupolar coupling constants (8.7 and 9.3 MHz)[5] were reported on $3CaO.Al_2O_3$ (the major cement compound containing aluminium).

The hardening process of *poly n-butylmethacrylate* (PBMA), in a 2:1 blend of polyethylmethacrylate and PBMA used for hip-bone prosthesis, was investigated. The conditions used in orthopaedic practice were employed. The Figure shows the normalised intensities obtained from the indicated slices *versus* time. The curves are the result of fitting the experimental data with the function: $M = 1 - M_0 e^{(t/T)}$. The time-constants deduced are: surface slice 4.16±0.04 min^{-1}, middle slice 3.62±0.02 min^{-1} and bottom slice 3.46± 0.03 min^{-1}. PBMA data will be discussed.

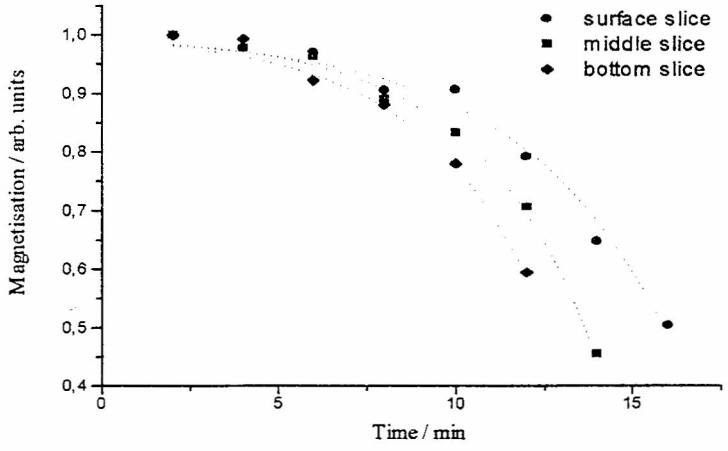

1 Samoilenko A A, Artemov D Yu and Sibeldina L A, *JETP Lett.*, 47, 417 (1988)

2 Nunes T, Bodart P, Randall E W, Samoilenko A A and Feio G, *J. Phys.D: Appl . Phys.*, 29, 805 (1996)

3 Nunes T, Bodart P, Randall E W, *Proceedings of the Second International Conference on NMR Spectroscopy of Cement Based Materials*, P. Colombet, H. Zanni, Eds., Springer Verlag, 1997.

4 Bodart P, Nunes T, Randall E W, *Solid State NMR*, in press.

5 Skibsted J, Bildsoe H and Jakobsen H, *J. Magn. Reson.*, 92, 669 (1991)

Several industrial applications of NMR Microscopy

W. Kuhn

IIC Innovative Imaging Corp., Blieskastel, Germany.

Subject of this lecture will be a wide variety of applications of NMR microscopy in several industrial areas. Results will be shown from investigation of technical rubber products such as car tires, but also recently acquired images of the human skin, using a 3T whole body imager. Although the difficulties of achieving microscopic resolution on alive human skin is not trivial, clear images of the human forearm with 80 microns in plane resolution will be presented. The time course of ingress of different cosmetic creams into human skin has been investigated and will be shown. Furthermore, a detailed discussion of the physico-chemical structure of emulsions, based on NMR diffusion measurements, will be given.

CW MRI OF SHORT T_2 MATERIALS

G.R.DAVIES, S.J. MCCALLUM, I.NICHOLSON, D.J. LURIE AND J.M.S. HUTCHISON

Department of Bio-medical Physics
University of Aberdeen,
Forester Hill
Aberdeen, Scotland. AB25 2ZD

Introduction: Two key problems are encountered in NMR imaging solids. Short T_2s mean signals decay away rapidly in pulsed experiments, a particular problem when one has to switch gradients on and off in the interval between pulse and observation. Broad line widths require the use of large gradients for good spatial resolution. In continuous-wave (CW) magnetic resonance electromagnetic (e.m.) radiation is continuously applied to the sample and the change in the power reflected from the resonator is monitored as the magnetic field is swept through resonance. Such a system requires no rapid switching of e.m. power or magnetic field gradients during the acquisition of each projection. Furthermore, the use of modulation of the swept field, phase-locked detection of the signal and the use of high Q, narrow band, resonators increases the signal-to-noise performance of the system.
Methods: We have constructed a pilot CW NMR system which uses a 7 T, 183 mm horizontal bore, Oxford Instruments magnet together with much of the spectrometer hardware and software from an existing EPR spectrometer along with its own resonator, field-sweep and gradient coils. Samples, up to 50 mm in diameter and length, are mounted on a manipulator, to lie in a birdcage resonator, tuned to 300 MHz. The resonator is co-axial with a split solenoid, a single set of Golay coils, which provide a gradient perpendicular to the magnetic field, and the magnet. Rotating the sample between successive acquisitions, allows multiple projections required to form a two dimensional image to be acquired whilst using a single gradient. Detection of the NMR signal is achieved with a homodyne reflection bridge, its output being fed into a Lock-in-amplifier which supplies the field modulation waveform. On sweeping B_0 the resonance appears at the lock-in-amplifier's output as the first derivative of the line shape. This is collected and processed by a microcomputer which controls the lock-in-amplifier, RF source and field sweep generator and reconstructs the image from a series of spectra using filtered back-projection software.
Results: Figure 1 shows a 2-D image of a "Duplo" brick, side length 3 cm, which is made from ABS plastic with a T_2 less than 500 ?s. A gradient of 70 mT/m and a sweep width of 6.5 mT was used to collect 30 projections of 256 points each. Resolution is of the order of 1 mm and the straight edges demonstrate the uniformity of the gradient field. Figure 2 shows a drawing of a Perspex phantom and the resulting image from 30 projections of 256 points acquired with a gradient of 250 mT/m and a sweep width of 15 mT. The image shows resolution of all the holes down to 5 mm and detection of the 2.5 mm hole in addition to the blind hole which was used to attach it to the manipulator.

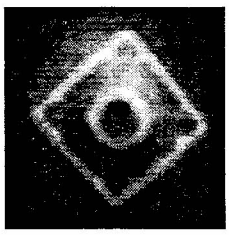

figure 1

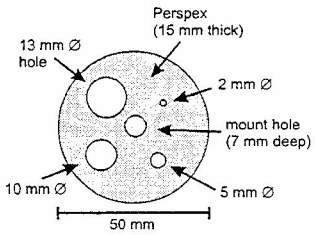

figure 2

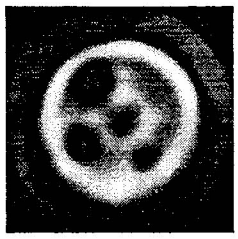

Conclusion: Our pilot experiments indicate that CW-NMR imaging can be used to study materials with very short T_2 values (Perspex has a T_2 of ~ 10 ?s). We are currently investigating methods of obtaining T_1 and T_2 related contrast and have had some success through the use of modulation amplitude and frequency manipulation. In the next phase of this work we will construct a coil assembly with multiple, stronger gradients, which will improve the spatial resolution.

IMAGING THE LUNGS WITH HYPERPOLARIZED HELIUM

L. W. HEDLUND, X. J. CHEN, M. S. CHAWLA, H. E. MÖLLER, G. P. COFER, J. R. MACFALL & G. A. JOHNSON

Center for In Vivo Microscopy, Department of Radiology
Duke University Medical Center, Durham, NC 27710

The availability of biocompatible, signal-rich polarized ^{3}He has made it possible to directly image with MR the airways of lungs of small animals and humans. Using the variety of imaging and gas delivery strategies now available to us, it is possible to image gas flow and distribution in lungs. This presentation will summarize gas polarization and delivery techniques, describe image encoding strategies, and present examples of biological applications.

Hyperpolarized 3He (HP gas) was generated by an optical pumping method described in detail by Middleton et al. (1). A 100-watt diode laser was used to illuminate a cell containing Rb, N2 and 3He mixture. About 600 cc of ^{3}He were polarized to 15 20% in about 8 hours. Anesthetized guinea pigs were intubated by tracheostomy and maintained on isoflurane using a computer controlled ventilator (2). HP gas was delivered to the lungs with the ventilator's two-stage pneumatically controlled valve. Imaging was synchronized to the delivery of HP gas; breaths of air-O2/anesthesia were alternated with HP gas. Typically air/anesthesia tidal volumes were 4-5 cc and HP gas were 2-3 cc and breathing rates were 40-60 per minute. A 2.0 T 30 cm magnet with shielded gradients, controlled by a Signa console (GE Medical Systems) was used for imaging along with a dual frequency (1H & 3He), low pass birdcage coil. Projection encoding sequence acquired radial trajectories of k-space with acquisition synchronized to selected phases of the breathing cycle. Views were acquired at repetition times of 4-20 ms and flip angles of 10-90°.

A broad range of in vivo studies have been done in small animals. By controlling the imaging window in relation to the phase of HP gas breath and the magnitude of the flip angle, we have selectively imaged different levels of the airway structure from the largest conductive airways to the most distal air spaces. By selective airway occlusion, we have also demonstrated the utility of this HP gas technique to reveal airway obstructions (3). Respiratory dynamics can also be seen through the use of time-lapse studies of gas inflow and 3D anisotropic images. Finally, much of the technology developed from these small-animal studies has been successfully translated to the clinical arena where initial human studies are very encouraging.

References

1. Middleton, H et al. Magn. Reson. Med. 33:271-275, 1995.
2. Hedlund, L et al. Proc ISMRM, 327, 1996.
3. Hedlund, L et al. Proc ISMRM, 183, 1997.

Acknowledgments

Research supported by NIH NCRR P41 RR05959, NSF CDR-8622201, and the Whitaker Foundation.

IMAGING OBSTRUCTED VENTILATION IN LUNGS USING INERT FLUORINATED GASES

DEAN O. KUETHE[1], ARVIND CAPRIHAN[1/2], EIICHI FUKUSHIMA[1/2], H. MICHAEL GACH[3], IRVING J. LOWE[3]

[1]Lovelace Respiratory Research Institute

Albuquerque, New Mexico

[2]New Mexico Resonance

Albuquerque, New Mexico

[3]University of Pittsburgh

Pittsburgh, Pennsylvania

Its possible, albeit not easy at present, to image the air spaces in rat lungs by having a rat breathe a mixture of an inert fluorinated gas like SF_6 or C_2F_6 and oxygen whilst making a ^{19}F NMR image. By using a gas with a short T_1 of 5 ms or so, the inherently low signal from the gas can be overcome with frequent and copious signal averaging. A drawback is that the T_2 is also 5 ms or so, leaving insufficient time to pulse magnetic field gradients before the signal disappears. To avoid pulsing gradients we make 3D projection images by collecting free induction decays as soon as possible after hard radio frequency pulses in the presence of steady magnetic field gradients. By repeating data collection with many gradient directions, we build up a 3D data set in "*k*-space", albeit with an annoying hole in the middle. The hole results from the time between the center of the rf pulse and the first data point, the "dead time". To make the individual 1D projections, despite data missing from the dead time, we use the singular value decomposition of a matrix **F** to solve the matrix equation $\mathbf{Fp} = \mathbf{d}$, where **d** is the data vector, **p** is the 1D projection we seek, and **F** is not a discrete inverse Fourier transform, but rather a closely related matrix, taking into account the time coordinates of the elements of **d**.

A disadvantage of imaging lungs this way is that it can not be done on a breath by breath basis, which is possible with NMR imaging of highly polarized noble gases in lungs. Advantages are that the gases are less expensive and no polarization apparatus is required.

The feature which is likely to make our method useful to medicine, is the ability to image where the ratio of ventilation to blood perfusion is low. For example, suppose a region of a lung has obstructed ventilation, but still receives blood flow. When the inhaled mixture is high in oxygen, *e.g.* 70% O_2 : 30% SF_6, the SF_6 concentrates up to 90% in the obstructed region because the O_2 is removed by blood while the SF_6 remains behind. The small amounts of gas entering the obstructed region serve to bring more SF_6 but the O_2 keeps getting removed. In well ventilated regions, the gas remains similar to the inhaled mixture, high in O_2, and low in SF_6. The upshot is that the obstructed region appears bright in an image. We've made such an image of obstructed ventilation in a rat lung and it raised the eyebrows of a pulmonologist, despite the lengthy 2 hours of data collection.

IN SITU IMAGING OF CHARGE CARRIERS IN AN ELECTROCHEMICAL CELL*

Rex E. Gerald II, Robert J. Klingler, Jerome W. Rathke, and †Giselle Sandí
Chemical Technology and †Chemistry Divisions
Argonne National Laboratory, 9700 South Cass Avenue, Argonne, Illinois 60439
Gerald@cmt.anl.gov (630) 252-4214

A toroid cavity NMR detector capable of quantitatively recording radial concentration profiles, diffusion constants, and displacements of charge carriers was employed to investigate the charge/discharge cycle of a solid-state electrochemical cell. One-dimensional radial concentration profiles (1D-images) of the ions solvated in a polyethylene oxide matrix were recorded by ^{19}F and ^{7}Li NMR for several cells. A sequence of such images, recorded at different stages of cell polarization, revealed the evolution of a region of the polymer depleted of charge carriers. From these images it is possible to extract the transference number for each ion. Spatially localized diffusion coefficients and spin-lattice relaxation time constants can be measured simultaneously for the ions in the polymer electrolyte by a spin-labeling method which employs the radial B_1-field gradient of the toroid cavity. A spatial resolution of 3 μm near the working electrode was achieved with a gradient strength of 200 gauss/cm. With this apparatus it is also possible to investigate novel intercalation anode materials for lithium ion storage. These materials are coated onto the working electrode as a thin film. The penetration depth of lithium cations in these films can be imaged at different times in the charge/discharge cycle of the battery.

*Work supported by the U. S. Department of Energy, Division of Chemical Sciences, Office of Basic Energy Sciences, under Contract W-31-109-Eng-38.

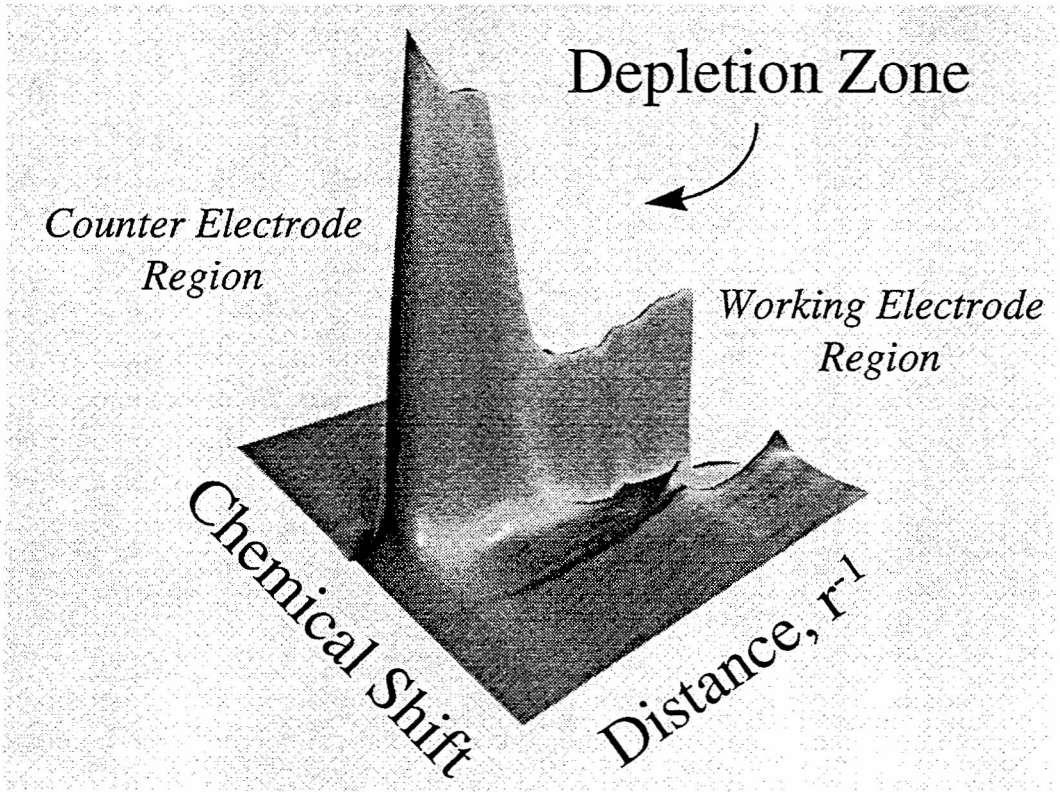

^{129}XE MRM OF GASEOUS PROBES IN SILICA AEROGELS*

D. M. GREGORY, R. E. GERALD II AND R. E. BOTTO
Chemistry Division
Argonne National Laboratory
Argonne, IL 60439

Aerogels represent a new class of open-pore materials with pore dimensions in the nanometer range, thus can be classified as mesoporous materials. In particular, silica aerogels have many unusual properties, including extremely low weight per unit volume, high thermal resistance, low refractive index and sound velocity, and high surface area, which allows for their use in many new applications such as insulated windows for solar applications, catalysts, gas separation media and Cherenkov counters. Numerous techniques have been used to study the pore structure of silica aerogels. These materials have been diffucult to characterize with certainty, largely because available measurement techniques for determining porosity characteristics can give drastically differing results for the same sample. The inherent limitations of the techniques used in the determination of pore structure of aerogels has left several important questions concerning their structure unresolved. It is apparent that BET gas adsorption measurements do not account for the entire pore volume of an aerogel. Does this missing volume result from limitations of the BET method to account for the micro- and macro-pore structure, or rather does it reflect on the "openness" of the aerogel pore network?

In this work, we show that the combination of NMR spectroscopy and chemical-shift selective magnetic resonance microscopy (MRM) can resolve some of the important issues regarding aerogel structure. The use of xenon as a gaseous probe in aerogels is suitable for characterizing the pore structure and the steady-state spatial distributions of xenon atoms in different physicochemical environments. Dynamic NMR and diffusion experiments characterize the mobility of the xenon atoms between the different environments under equilibrium and non-equilibrium conditions. These NMR methods offer unique information and in.sights into the nanoscopic pore structure and microscopic morphology of aerogels and the dynamical behavior of occluded atomic and molecular adsorbates. MRM provides spatially-resolved information on the nature of the flaw regions found in these materials. Pseudo first-order rate constants for magnetization transfer among the bulk and occluded xenon phases in a sample indicate xenon-exchange rate constants of order 1 s^{-1}. Pulsed field gradient (PFG) diffusion measurements show evidence of anisotropic diffusion, with a nominal self-diffusivity constants on the order of $D = 10^{-3}$ cm^2/s for occluded xenon. Complete confinement of the sample tubes in a toroid cavity detector allows for quantitative determination of the partition of the xenon atoms among the different occluded and gas-phase environments by signal integration, and has potential for spatial monitoring of aerogel formation at elevated pressures and temperatures required during supercritical drying.

*Work performed under the auspices of the Office of Basic Energy Sciences, Division of Chemical Sciences, U. S. Department of Energy, under contract no. W-31-109-ENG-38.

LITHIUM VISIBILITY IN RAT BRAIN AND MUSCLE *IN VIVO* BY ^{7}Li NMR IMAGING

RICHARD A. KOMOROSKI,[1-4] JOHN M. PEARCE,[1,2] AND JOSEPH E. O. NEWTON[4,5]

Departments of [1]Radiology, [2]Pathology, [3]Biochemistry, [4]Psychiatry, and [5]Pediatrics, University of Arkansas for Medical Sciences
4301 West Markham St.
Little Rock, AR 72205.

Lithium (Li) is the treatment of choice for manic-depressive illness. The magnitude of the pharmacologic effect of Li depends on the concentration at the receptor sites in the brain, which may not be reflected in the serum concentration. ^{7}Li NMR is potentially a noninvasive, *in vivo* measure of Li concentration, particularly one that can be applied to humans. One advantage of NMR relative to other spectroscopies is that, when properly acquired, the NMR signal usually is proportional to the number of atoms of a given species. However, alkali-metal NMR studies on a wide variety of tissues have shown that the ion concentration determined by NMR is often substantially less than that determined by other analytical methods. The extent to which the ^{7}Li NMR signals from biological tissues, such as brain and muscle, exhibit such reduced visibility *in* vivo has not been determined previously. The apparent concentration of Li *in vivo* was measured for several regions in the brain and muscle of rats by ^{7}Li NMR imaging at 4.7 T with inclusion of an external standard of known concentration and visibility. The average apparent concentrations were 10.1 mM for muscle, and 4.2-5.3 mM for various brain regions under the dosing conditions used. The results were compared to concentrations determined *in vitro* by high resolution ^{7}Li NMR spectroscopy of extracts of brain and muscle tissue from the same rats. The comparison provided estimates of the ^{7}Li NMR visibility of the Li cation in each tissue region. Although there was considerable scatter of the calculated visibilities among the five rats studied, the results suggested essentially full visibility (96%) for Li in muscle, and somewhat reduced visibility (74-93%) in the various brain regions.

A FLEXIBLE PULSE PROGRAMMER FOR MRI USING A COMMERCIAL DIGITAL SIGNAL PROCESSOR BOARD

KATSUMI KOSE AND TOMOYUKI HAISHI
Institute of Applied Physics
University of Tsukuba
Tsukuba-City 305 Japan

Introduction

It is not easy to construct a pulse programmer for MRI because so many parameters including gradient amplitude must be controlled at exact timing and some of them must be changed at every rf excitation. Use of some computer system for the pulse programmer is a good idea, but PC or usual one board computer system cannot generate exact time sequences for NMR because such a system has many D-RAM's and internal system interruptions. Most digital signal processor(DSP) board systems, however, are made to give exact time sequence. We have thus developed a flexible pulse programmer for MRI using a commercial DSP board.

System Description

The DSP board used in this work is DSP6031 (MTT Instruments Corp. Tokyo) which has a 32-bit floating point DSP chip (TMS320C31, Texas Instruments Inc.) running at 40 MHz clock frequency which gives the 50 ns instruction cycle. In addition, this board has four 12-bit ADC, four 12-bit DAC, and 8-bit digital I/O. All of them are assembled on a full PC-AT extension card size. The DSP bus can be extended to give two 32-bit digital outputs using another full PC-AT card size extension board. The DSP board and its extension board are put into a PC running under DOS or Windows95. The pulse sequence program was developed using the internal timer (100 ns clock frequency) of the DSP of which clock is synchronized with the CPU clock. Pulse timing data (event, time, and value) were written with a simple text editor of the PC and transferred to the memory area of the DSP. The sequence program reads the timing data and generates an exact pulse sequence as designed.

Results

The time resolution for the sequence was 100 ns and the minimum time interval between two events was 2.7 micro seconds. This time resolution is enough even for advanced rapid imaging sequences. A flexible and powerful MR pulse programmer has been easily constructed utilizing a commercial DSP board.

NOVEL TRANSVERSE GRADIENT COILS FOR MAGNETIC RESONANCE MICROSCOPY

E. R. ANDREW, M. KEMPKA AND E. SZCZESNIAK
Departments of Physics and Radiology
University of Florida
Gainesville, FL 32611

The paper describes new coil architectures for transverse gradients where the empllasis is on having a compact low inductance structure coupled with extended gradient linearity over a large usable volume with good gradient efficiency. A unit structure has been adopted and the whole coil is assembled from a symmetric coaxial set of such units, whose spacing is carefully computed. Each unit contains a pair of current carrying arcs with return paths in the same plane. Various unit geometries have been devised including coaxial arc configurations and non-concentric circle configurations. A typical gradient set for usc in a 50 mm bore NMR microscope has a linearity within 5% over a diameter 16 mm and length 14 mm and yields a spatial resolution of 30 μ m at 300 MHz. The coils have typically an inductance of 5 ,uH with rise time 3 μ s. By connecting the identical units in parallel the inductance can be still further reduced. These gradient coils may be scaled for use with magnets of any desired bore diameter.

A Compact Superconducting Magnet for MR Microscopy

Stuart Crozier and David M Doddrell

Centre for Magnetic Resonance, The University of Queensland
St. Lucia Qld 4072 Australia
ph +61 7 3365-4100
e-mail Stuart.Crozier@cmr.uq.edu.au

Magnetic Resonance Microscopy (MRM) depends on the use of high field, superconducting magnet systems for its operation. The magnets that are conventionally used are those that were initially designed for chemical structural analysis work. A novel, compact magnet designed specifically for MRM is presented herein that, while preserving high field, high homogeneity conditions, has a length less than one-third that of conventional systems. This enables much better access to samples, an important consideration in many MRM experiments. As the homogeneity of a magnet is strongly dependent on its length, novel geometries and optimization techniques are required to meet the requirements of MRM in a compact system.

The magnets describes in this work were designed by a novel stochastic optimization method. As an example, we present the design of a 7T system, in which the resultant magnet has a peak-to-peak inhomogeneity of < 0.6 ppm over a 40 mm dsv, prior to any superconducting or room temperature shimming, and a total coil length of less than 180 mm (Fig. 1).

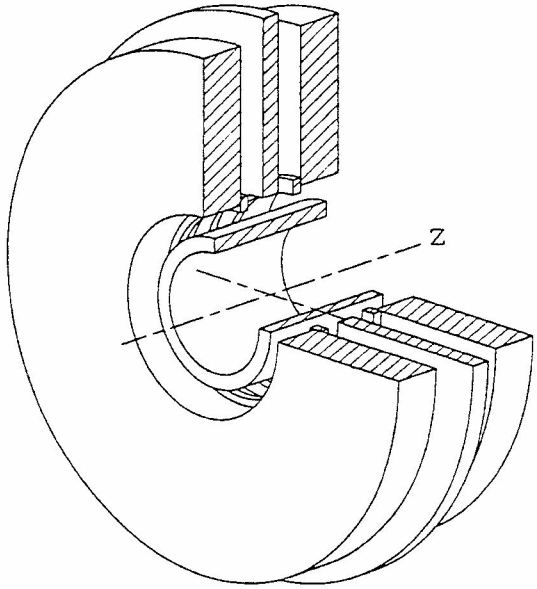

Figure 1 A perspective view of the compact magnet coil layout.

INCREASE IN THE PRECISION OF THE GRADIENT MAGNETIC FIELD MEASUREMENT

KAREL BARTUŠEK, JAROSLAV VOJTA
***Institute of Scientific Instruments**
Královopolská 147
612 64 Brno, Czech Republic

Fast and precise decreasing the gradient magnetic fields to the level of the field homogeneity is an important prerequisite for most NMR spectroscopic, tomographic, and localized spectroscopy experiments which allows the use of a short echo time and generation of a minimum undesirable spin echo. The basis of the eddy current compensation technique [1] in MR tomography magnets is the precise measurement of the time characteristic of the gradient magnetic field. The simple fast method of the gradient magnetic field measurement [4],[5] with a sufficient precision can be used to find out the quality of the gradient fields. The measurement can be performed using the commercial NMR instrument with an adjusted preemphasis compensation. The basic idea is to take off the FID signal after selective excitation of the thin layer and after the end of the gradient pulse. In this case, the time gradient characteristic is proportional to the instantaneous frequency of the complex FID signal. The other method [2], [3] for the measurement of the undesirable gradient fields uses the excitation of the whole sample with a variable time delay after the end of the gradient pulse and the determination of the spectral line amplitude. The gradient magnetic field distorts the spectral line shape. The decrease in the spectral line amplitude is only the integral criterion of the amplitude of the gradient field in the excitation time. By this method, the gradient field can not be measured with a high precision.

The gradient magnetic field is directly proportional to the instan-taneous frequency obtained by taking the derivative of the time-dependent phase of the out-of phase complex component of the recorded Free Induction Decay (FID) [1]. In real experiments, the measured FID signal with a variable instantaneous frequency has a small signal to noise ratio. Owing to the derivation of the instantaneous phase, this ratio increases. That is why the FID signal must be filtered by digital filters defined by numbers of coefficients. These audio-frequency filters cause the error of the instantaneous frequency of the FID signal, owing to their transient response, which results in alteration or amplitude modulation of several early data points of the FID signal and its phase and time shifting. The aim is to choose a filter or some de-noising method that minimally distorts the characteristic of the instantaneous frequency of the measured signal.

For the filtration, some post-acquisition methods can be used for example gliding signal averaging, FIR filtering, and Wavelet de-noising. Error magnitudes for all used techniques are compared in this contribution. The Wave-let technique applied in the time domain causes the least error of the instantaneous frequency in the first part of the FID signal, and the output signal has minimum noise.

This contribution has been supported by the grant No:102/96/1136 of the Grant Agency of the Czech Republic.

References

1, Bartušek K, Jilek B.: Eddy Current Compensation by Adaptive Pre-emphasis Control for NMR Tomography and Spectroscopy. J.Electrical Engineering, 46 (1995), NO.10, 339-344.
2, R.E.Wysong, I.J.Lowe.: A Simple Method of Measuring Gradient Induced Eddy Currents to Set Compensation Networks, Magn.Reson.Med. 29, pp. 119, 1993
3, K.Bartušek, V.Puczok.: An NMR MULTIFID Method for Measurement of Magnetic Field Gradient, Meas.Sci.Technol. 4, pp. 357, 1993
4, K.Bartušek, B.Jílek.: Measurement of the Gradient Magnetic Field Temporal Characteristic, 26. NMR seminarium, Krakow, 1993
5, K.Bartušek, B.Jílek.: Measurement of Gradient Magnetic Field for NMR

SPHERICAL GRADIENT COIL FOR MR MICROSCOPY

HAIYING LIU
University of Minnesota
Box 292, 420 Delaware
Minneapolis, MN 55455

High performance magnetic field gradient coils have always been desirable in today's high resolution magnetic resonance (MR) microscopic imaging applications. For this purpose, we present a Lagrange multiplier technique of a minimum inductance gradient coil with a spherical geometry. Based on this minimization approach, we constructed an energy functional F in terms of the stored magnetic energy, the magnetic field and a set of field constraint points which are chosen over the desired imaging volume. Minimizing F, we obtain the continuous current density distribution for the spherical gradient coil. Applying the stream function technique to the continuous current distribution, the discrete current pattern can then be generated. Employing the Biot-Savart law to the discrete current loops, the gradient magnetic field has been re-evaluated in order to validate the theory. Using this approach, we have been able to design a spherical z-gradient coil which is capable of generating a gradient field of 176 mT/m with slew rate of 3422 T/m/s over a 30 cm diameter spherical volume if driven by a 350V-220A current amplifier. A prototype of the spherical z gradient coil has been built and tested. The agreement between the analytical and experimental results is excellent. Initial imaging experiments have been conducted. The results indicate the potential use of such a coil for in vivo and in vitro fast NMR applications.

SPRITE IMAGING OF SHORT RELAXATION TIME NUCLEI

BRUCE J. BALCOM
MRI Centre, Department of Physics
University of New Brunswick
P.O. Box 4400
Fredericton, N.B. Canada, E3B 5A3

We have recently developed a new MRI pulse sequence which is a time efficient and very flexible version of Single Point or Constant Time Imaging (1). We term this sequence SPRITE (Single Point Ramped Imaging with T_1 Enhancement). The sequence (2) is a pure phase encoding method which relies on broad band RF pulses applied in the presence of a ramped primary phase encode gradient and constant secondary phase encode gradients. The ramped gradient permits repetition of large or small flip angle RF pulses at arbitrarily short repetition times. This permits the introduction of T_1 contrast for samples which may have T_1 relaxation times which range from hundreds of μsec to many seconds. The method is ideally suited to the visualization of nuclei with short T_2*, from tens of μsec to hundreds of μsec which may be difficult to observe by other techniques.

This lecture will outline the basis of the SPRITE method, its hardware and software requirements as well as extension of the method to permit localized T_1,T_2,T_2* mapping of short relaxation time nuclei. The use of the method in polymer and bone imaging (^{1}H and ^{31}P) will be introduced. Application of the technique to heteronuclei and EPR imaging will be discussed as will use of the method in localized calorimetry of water bearing porous media.

1. S. Gravina and D.G. Cory, J. Magn. Reson. B 104, 53 (1994).
2. B. J. Balcom, R. P. MacGregor, S. D. Beyea, D. P. Green, R. L. Armstrong, T. W. Bremner, J. Magn. Reson. A123, 131 (1996).

DRYING OF POROUS CATALYST SUPPORT BODIES: A PENETRATING LOOK

I.V. KOPTYUG[1], R.Z. SAGDEEV[1], V.N. PARMON[2] AND L.YU. KHITRINA[3]

[1]International Tomography Center

[2]Boreskov Institute of Catalysis, and [3]Novosibirsk State University

Novosibirsk 630090, Russia

MRM provides useful means of monitoring directly the distribution of liquid phase inside porous materials in the course of the drying process. This allows one to perform stringent tests of the existing models of drying developed earlier. These models state, inter alia, that the evaporation of a liquid proceeds predominantly from the external surface of the porous solid, and that the resulting losses are replenished by an efficient outward capillary flow caused by capillary suction.

In our experiments presoaked cylindrical samples were positioned inside the rf coil of the NMR probe and were subsequently dried at ambient temperature in a stream of dry nitrogen. One-dimensional two-pulse spin-echo was optimized to yield an acceptable sensitivity for real-time monitoring of the drying process in the samples with very short T2* times (0.5-2.5 ms), and was employed to obtain radial distribution of a liquid in the cylindrical samples. For quantitative analysis the profiles detected have been corrected for the inevitable T2-weighting, employing a calibration curve obtained in a separate experiment. Evaporation of water, acetone, benzene and other solvents from gamma-Al2O3 samples with varying porous structure and from industrial catalyst CRS-31 (TiO2) was studied at various flows of the drying gas.

The results obtained clearly support the hypothesis of surface evaporation and the existence of an efficient outward capillary flow, which compensates for the losses of water at the periphery. The initially rectangular liquid concentration profile (uniform pore filling) transforms later into a round-top shape and thus develops a necessary concentration gradient which drives the outward flow of liquid. The sequence of profile transformations in the course of evaporation is clearly governed by the pore size distribution of the sample under study, being most remarkable for water in bi-porous Al2O3. For these samples a rectangular round-top rectangular round-top sequence of profile transformations is observed, which indicates that capillary suction is efficient enough to maintain a quasi-equilibrium at each instant of the drying process. In the case of acetone evaporation, capillary suction is much less efficient due to much lower surface tension, and concentration gradients gradually increase with time throughout most of the drying process.

To obtain quantitative characteristics of mass transport in the course of drying, the process was modeled as radial diffusion in a quasi-homogeneous medium with appropriate boundary conditions. Evaporation of acetone, benzene, etc. can be modeled reasonably well with liquid content - independent diffusion coefficient. However, our study shows that the effective diffusion coefficient for water decreases substantially with decreasing of water content, and that this dependence is not necessarily monotonous and can show local maxima. Diffusion coefficients extracted are comparable to or even exceed the values of self-diffusion coefficients for bulk liquids. All this indicates that a more appropriate description of the drying process should be sought on the basis of the independently obtained data on pore size distribution and a proper description of capillary suction effects. It is also shown that variation of relaxation times during drying should be a more reliable approach to MR porosimetry than a multiexponential analysis of a single relaxation curve for a liquid-saturated porous sample.

PORE STRUCTURE AND CONNECTIVITY OF POROUS ROCK BY HIGH RESOLUTION NMR MICROSCOPY

DARYL A. DOUGHTY AND LIVIU TOMUTSA
BDM Petroleum Technologies
PO Box 2543
Bartlesville, OK 74005

ABSTRACT

The application of high field magnetic resonance imaging (MRI) microscopy to the study of pore geometry in porous rock must overcome the short T2 relaxation times and broad natural RF line widths which characterize fluids in this environment. These effects are caused by the magnetic susceptibility constrast between the fluid and rock grains and the presence of paramagnetic ions such as iron or manganese on the rock grain surfaces. An imaging protocol based on 3D projection reconstruction using strong imaging gradients has overcome many of these constraints resulting in image resolutions of 23 micrometers per voxel on small core plugs. Magnetic field gradient strengths used in the imaging process for these small core plugs were about 80 gauss/cm. MRI experiments were per-formed on brine saturated core plugs from several sandstones including Bentheim, Fontainebleau, and Almond. A novel method was developed using this higher resolution data to independently determine the porosity from histograms of image voxel intensity which estimates the contribution from fractionally filled voxels. Semilog plots of the histograms versus intensity bin number reveal a linear region. The weighted sum of the voxel counts under the linear fit, where the weight factor accounts for the bin width and the fractional filling of the voxels, represents the actual volume of the fluid-filled porosity. Results in excellent agreement with traditional porosity determi-nations were obtained for the natural sandstone samples. Using software developed in our laboratory 3D pore size calculations on binarized MRI data using a process of successive erosion/dilations showed signficant differences in the pore connectivity in the different samples. The results reveal that the pore throats in the Fontainebleau sandstone are significantly smaller than the 23 micrometer resolution in the image data while the more porous Bentheim and Almond sandstones have larger average pore throats approximating the image resolution. Comparison with measurements using petrographic image analysis (PIA) and mecury injection porosimetry for these rock types show excellent agreement with the MRI microcsopy data.

KEYWORDS

NMR, MRI microscopy, projection reconstruction, porosity, pore size, pore connectivity, pore structure.

THE TRANSLATIONAL SELF-DIFFUSION OF 1,3-PROPYLENE GLYCOL IN TRACK ETCHED MEMBRANE PORES

E. VASINA[*], V. SKIRDA[*], V. VOLKOV[**], A. NECHAEV[**], B. MCHEDLISHVILI[**]

[*]Dept. Molecular Physics, Kazan State University, Kremlevskaya str.181 Kazan 420008, Russia

[**]Shubnikov Institute of Crystallography, RAS Moscow, Russia

The translational diffusion of 1,3-propylene glycol in pores of polyethyleneterephthalate track membranes (1) was studied by PFG (pulsed field gradient) NMR method (maximum pulse gradient magnitude 200T/m, ^{1}H frequency - 60 MHz, the technique of stimulated spin echo). The thickness of the membrane films is about 10 um, the pore's diameter is about 0.2 - 0.25 μ m (by data of electron microscopy). The angular distribution of the channel orientation towards the normal drew to film's surface is in limits from 0° to 30°. It gives the opportunity of channels to cross in the membrane. The pack of film's sheets was saturated with 1,3-propylene glycol. The sample tube was put in sensor of spectrometer so that the gradient vector was directed along the film's surfaces. The registration of echo attenuations was made under $\delta^2 g^2$ = const condition (δ - duration of gradient pulse, g - amplitude of gradient pulse) which allows to identify a presence of "fully restricted" diffusion $D \propto t^{-1}$ (D - self-diffusion coefficient, t - diffusion time). It was shown that for the component of diffusive attenuation with the least self-diffusion coefficient - D_a the $D_a = t^{-1}$ regime exists. Sizes of restrictions (about 0.26 μ m) were calculated by using of the Einstain's relation. These sizes are in good accordance with pore diameters, obtained by electron microscopy measurements (0.2 - 0.25 μ m). The population of the component characterized by the self-diffusion coefficient Da decreases while the diffusion time increases. Under these conditions, the values of average self-diffusion coefficients are constant. It shows that molecular diffusion exchange of diffusate in pore and bulk propylene glycol is taken place (2). The experimental lifetime distribution function in pores was obtained according to the procedure proposed in (3). This function F(t) was also calculated by using of the solution of the First Passage Problem (4). These functions are similar but some distinctions maybe explained by that the First Passage Problem don't consider the cross pore size.

$$F(t) = \frac{1}{\sqrt{2\pi D t^3}}\left(2DtA^{-1}\left[1-\exp(-\frac{A^2}{2Dt})\right] - A\exp(-\frac{A^2}{2Dt})\right)$$

where A - length of channels, D=6x10^{-11} m2/s of free 1,3-propylene glycol.
Thus, we have registered the liquid diffusion into pores of track etched membranes and molecular diffusion exchange between liquids living into and beyond pores, and obtained the experimental lifetime disribution function in pores.

References

1. Mchedlishvili BV, Beriozkin W and AN Other, J Memb Sci,79,285 (1993)
2. Valiullin RR, Skirda VD, Stapf S, Kimmich R, Phys Review E, 55,2664 (1997).
3. Maklakov Al, Skirda VD, Fatkullin NF, Encycl of Fluid Mechanics, Chap.22,705 (1990).
4. Darling DA, Siegert AJ, The first Passage Problem for a Continuous Markov Process, Ann.Math. Statist.24, n.4,624 (1953).

DIFFUSION, RESTRICTED DIFFUSION AND MOTION CORRELATION BY MICROIMAGING

JANEZ STEPISNIK
Physics Department, FMF, UL
Jadranska 19
Ljubljana, Slovenia

Subjected to perpetually changing interaction with surrounded particles and boundaries, the spin-bearing molecule of the fluid is induced to carry out an irregular movement. Its macroscopic manifestation is diffusion and in a porous structure, it is a restricted self-diffusion. Spin echo with two gradient pulses separated by a well-defined time interval is very useful method for its exploration.

With the presumption of Gaussian randomness either for the spin frequency fluctuations or for the spin phase shifts within sub-ensemble, the expression for diffusive attenuation follows right from spin phase average, without any direct reliance to the Fick's diffusion law. It provides very general relationship between spin attenuation and the microscopic particle motion i.e. its single-particle velocity correlation. It shows that instead of the two-pulse gradient modulation the other gradient modulations are possible in which the molecular motion is detected in a different manner. With them, one treats the effect of the gradient via the time dependence of the accumulated spin phase. The spectral density of the transitional velocity auto-correlation is "probed" by a sampling function given by the frequency spectrum of the time-integral of the effective gradient waveform. It distinguishes the molecular motion over differing time-scales, provides the information about the translation dynamics of macromolecules, and gives a fresh insight regarding the problem of turbulent flow and perfusion.

We can extend this theory to the problem of diffusion in porous structure and show that it is not the sole application of modulated gradient method. It also can resolve the microscopic structure that limits the migration of molecules. In this case, the spin echo attenuation is considered as a discord of spin phase structure created by gradient within the pore. A new approach surpasses a drawback of the propagator method being amenable only with the short gradient pulses and to the Markoff processes. Using the propagator formalism, a relationship between the parameters of structure that restricts the migration of particles and the spin echo can be determined, when a complete knowledge of diffusion propagator is available. However, usually people rely on the propagators derived from the Fick's equation that are amenable only for the Markovian diffusion. The bounded diffusion certainly has non-Markovian character that can be treated by a new approach.

The limit facing the Pulsed Gradient Spin Echo method concerns the spatial resolution. It depends both on the maximum available magnetic field gradient and the degree to which the gradient pulse amplitudes can be accurately matched. Most methods for producing large pulsed magnetic field gradients rely on the use of a specialized wire array, which surrounds the RF coil. Rather than surrounding our sample with an external gradient coil, we have inserted a current carrying wire in the sample itself and utilize the divergence in gradient strength, which occurs in the vicinity of a current-carrying wire. Thus, we can generate very large amplitude gradient pulses, indeed larger than can be achieved in the stray field method and with greater intrinsic signal sensitivity, rapid switching capability, high dynamic range and remarkable ease of use. At the heart of the method is the capacity to spatially resolve the sample and depends on the use of NMR micro-imaging technique now routine in a large number laboratories.

The potential applications of the gradient in single-wire proximity are numerous. With the gradients on the order of 100 T m^{-1} it should be possible to measure molecular displacements on the order of 10 nm. The gradient with two-dimensional spatially distributed vector field is able to reveal diffusion anisotropy and provides information about the structure in the case of the diffusion within porous material.

IMAGING DIFFUSION IN GELS, POLYMERS, AND SOLIDS

KLAUS WOELK
Inst. Phys. Chem., University of Bonn
Wegelerstr. 12
D-53115 Bonn, Germany

Magnetization-grid rotating-frame imaging (MAGROFI) [1] describes a robust two-pulse imaging sequence to measure diffusion, coherent flow, and T1 relaxation. Applied with the B1 gradients of surface coils or toroid cavity detectors, the first pulse generates a z-magnetization grating that, subsequently, decays because of diffusion and T1-relaxation. The second pulse is part of a rotating-frame imaging [2] procedure that samples the remaining z-magnetization with incrementally increasing pulse widths. With the remaining magnetization grating imaged, it is possible to obtain simultaneously diffusion coefficients, T1 relaxation times, and, if present, coherent-flow velocities from one set of experiments. From Fick's laws, mathematical equations and approximations are derived to determine diffusion coefficients from surface-coil and toroid-cavity NMR images, respectively. However, these equations only apply for homogeneous samples without further boundary conditions and, therefore, cannot be used for phase-transitions or heterogeneous materials. A finite-difference numerical approach is introduced to describe more generally the decay of magnetization gratings, e.g., for diffusion between phases.

Examples are presented of gases diffusing into solids, or supercritical CO2 swelling fluorinated polymers. Moreover, diffusion and self-diffusion in gels are evaluated as part of investigating modern methods of medical drug delivery, such as phonophoresis or iontophoresis [3].

[1] R. Kimmich, B. Simon, and H. Köstler, J. Magn. Reson. A 112, 7 (1995);
K. Woelk, R. E. Gerald II, R. J. Klingler, and J. W. Rathke,
J. Magn. Reson. A 121, 74 (1996).

[2] D.I. Hoult, J. Magn. Reson. 33, 183-197 (1979).

[3] N. N. Byl, Phys Ther. 75, 539 (1995);
C. T. Costello and A. H. Jeske, Phys. Ther. 75, 554 (1995).

NEW NMR AND NQR TECHNIQUES FOR STUDYING ULTRASLOW MODULATION WAVE MOTIONS IN INCOMMENSURATE SOLIDS*

DAVID C. AILION
Department of Physics, University of Utah, Salt Lake City, Utah 84112, USA

NMR has traditionally been used to study slow atomic diffusion in solids, either by direct measurement of the relaxation times [1] or by observation of a spin echo of reduced amplitude for spins diffusing in an inhomogeneous magnetic field [2]. For nonrestricted diffusion in a magnetic field gradient, the amplitude of the echo following a Hahn 90 °-180° sequence decays more rapidly than that following a CPMG sequence and decays like
$M=M_0 \exp(-Kt^3)$, where K depends on the product of the diffusion constant D and the square of the field gradient.

Recently, similar effects (i.e., a rapid Hahn decay $\propto t^3$) have been discovered in incommensurate (I) insulators in pure NQR [3] and in quadrupole-perturbed NMR [4] for spins in which there is no magnetic field gradient present. Unlike the usual magnetic field gradient experiments in which the moving nucleus is observed, these observations detect electric field gradient (EFG) variations seen by a stationary nucleus arising from slow modulation wave motions. (An incommensurate system is characterized by 2 or more competing periodicities - that of the modulation wave(s and that of the underlying crystal lattice [5].) Due to the fact that the EFG in an I system varies enormously over small distances, this technique has detected diffusion constants that are several orders of magnitude smaller than those observed even by the largest available magnetic gradients.

Low field and rotating-frame spin-lattice relaxation times have also been widely used for detecting ultraslow atomic and molecular motions that cause dipolar fluctuations [1]. However, they have not been extensively applied in NQR to detect ultraslow motions of quadrupolar nuclei.

We report NMR studies of the spin 1/2 nucleus ^{109}Ag in the I system proustite (Ag_3AsS_3) in which we observed an exponential dependence of the Hahn decay on the cube of the diffusion time. This is the first case in which the above technique has been applied to a nonquadrupolar nucleus. We also report the results of pure NQR ^{35}Cl $T_{1\rho}$ measurements in the I system, Rb_2ZnCl_4.

References

* This research was supported by the US NSF under Grant DMR-9624962.

1. **D.C. Ailion,** *Adv. Magn. Reson,* [Academic Press, NY 1971], Vol. 5, Chapter 4.
2. **C.P. Slichter,** *Princ. of Magn. Reson.,* 3d ed. [Springer-Verlag, NY 1990],App. G.
3. **G. Papavassiliou et al.,** *Phys. Rev. Lett.* **74**, 2387 (1995).
4. **D.C. Ailion and J.A. Norcross,** *Phys. Rev. Lett.* **74**, 2383 (1995).
5. **R. Blinc,A.P. Levanyuk,** "Incommensurate Phases in Dielectrics", Vol. I [Elsevier, Amsterdam 1986].

A SIMPLE MATRIX FORMALISM FOR SPIN ECHO ANALYSIS OF RESTRICTED DIFFUSION UNDER GENERALISED GRADIENT WAVEFORMS

PAUL T. CALLAGHAN
Department of Physics
Massey University
Palmerston North, New Zealand.

The problem of restricted diffusion in Pulsed Gradient Spin Echo NMR has been solved exactly (in the case of regular geometries) by assuming infinitesimally narrow gradient pulses and using the method of eigenfunction expansion[1]. Until recently the problem of how to deal with finite gradient pulses has remained intractable. Interest in solving this problem has received an impetus because of the development of generalised gradient methods, and especially those which probe frequency domain behaviour[2]. Recently Caprihan, Wang and Fukushima[3] proposed a means of dealing with generalised gradient waveforms by using a succession of sharp gradient impulses. Building on that approach a simplified mathematical treatment has been developed which allows closed form expressions for the echo attenuation, *E(q),* in spin echo diffusion experiments, for practically all gradient waveforms and for the case of restricted diffusion in enclosing pores, with or without wall relaxation[4]. This method leads to *E(q)* being expressed as a product of matrix operators corresponding quite naturally to the successive sandwich of phase evolution and Brownian migration events. Such a product can be easily evaluated using computational tools such as Matlab. Simple expressions are given for the case of the finite width gradient pulse PGSE experiment, the CPMG pulse train used in Frequency-Domain Modulated Gradient Spin Echo NMR, and the case of a sinusoidal waveform. The finite width gradient pulse PGSE and CPMG pulse trains are evaluated for the case of restricted diffusion between parallel reflecting planes. The former results agree precisely with published computer simulations while the latter calculation provides useful insight regarding the spectral density approach to impeded Brownian motion.

1. P.T. Callaghan, *Journal of Magnetic Resonance,* A113, 53(1995)
2. P.T. Callaghan and J. Stepisnik, *J. Magn. Reson.,* A117, 118 (1995)
3 A. Caprihan, L.Z. Wang and E. Fukushima, J. *Magn. Reson,* A118, 94(1996)
4. P.T. Callaghan, *J. Magn. Reson.* (submitted)

POSTERS

MRM IN THE MODELLING OF THE OSSICULAR CHAIN

E.W. ABEL*, J.A. CHUDEK, G. HUNTER, R.M. LORD*, R.L. MACKAY, AND R.P. MILLS+.

Department of Chemistry
University of Dundee
Dundee. DD1 4HN, UK.
***Dept. of Biomedical Engineering**
University of Dundee
Dundee. DD1 4HN, UK.
+ENT Department
Ninewells Hospital
Dundee. DD1 9SY, UK.

Chronic suppurative otitis media is an important cause of conductive hearing loss. While the disease can be alleviated surgically, the significant failure rate of this operation has led to some sufferers being treated unsuccessfully. The methods used in this treatment were first performed three decades ago and while they have been improved over the intervening period, developments still involve the creation of a link between the ear drum and the stapes head based loosely on the structure of the columella ears found in birds and reptiles rather than on the mammalian three-ossicle ear. A more promising approach is to reconstruct the chain along more physiologically relevant lines and initial attempts have led to very encouraging results.

In a project to develop a more successful treatment for this complaint, finite element analysis is being used to conduct vibrational studies on different configurations of physiological ossicular chain reconstruction, for experimental evaluation. However such analysis requires an accurate representation of the geometry of both the ossicular chain and the surrounding tissues to which it is attached. Conventional methods of measurement have proved inadequate. In contrast we have successfully used MRM in this work. By immersing the bones in a variety of different media types 3D spin-echo images have been acquired which have accurately shown both the chain geometry and the anchor points.

This presentation demonstrates the use of MRM in this work and the preliminary results from the finite element analysis.

DIFFUSION WEIGHTED MR MICROSCOPY OF ISOLATED BRAIN SLICES

STEPHEN J BLACKBAND
University of Florida
PO Box 100245
Gainesville, FL 32610

Introduction: The brain slice is an established model for investigations into neural structure, metabolism and function, providing an accessible layer of tissue similar to in situ brain tissue. The model has been examined using a variety of methods, including optical, radiological, electrochemical and histological techniques. Recently we performed the first MR microimaging studies of isolated perfused brain slices and demonstrated signal changes as a function of gross osmotic perturbations. In the present work we investigate the stability of the brain slice model and demonstrate that signal changes can also be observed following physiologically relevant perturbations (20% tonicity changes) representative of in vivo perturbations. Preliminary experiments of the effects of blocking sodium channels with ouabain will also be described. We aim to use this model in conjunction with similar data obtained on single neurons to construct a working model of brain tissue.

Methods: Rat hippocampal slices (500 um thick) were isolated using standard methods and placed in a home built perfusion chamber constructed from Delrin and consisting of a hollow cylindrical support arrangement in three parts, with the central chamber holding the brain slice between gauze sections. Slices were imaged using a Doty probe in a Varian 600 MHz instrument. In baseline studies the slice was maintained in the same perfusate over 8 hours, and in seperate experiments the perfusate was exchanged every 1.5 hours to determine slice stability as assessed by the MR signal. In other studies slices were initially perfused with oxygenated isotonic CSF at room temperature, which was then exchanged for a 20% hypotonic solution followed by a 20% hypertonic solution. A standard diffusion weighted spin echo imaging sequence (TR=2 s, TE= 22 ms, 2 averages,)was utilized. Images were collected at a resolution of 40 x40 or 80 x 80 (x 300) um.

Results: In experiments on 6 slices monitored over an 8 hour period significant signal changes were observed ($p<0.001$). When the slice perfusate was exchanged every 1.5 hours, there was no significant signal change in 4 slices. In the tonicity experiments a mean signal increase of 16(sn-1 = 11)% was measured for the hypotonic perturbation and a 26(sn-1 = 10)% decrease for the hypertonic perturbation ($p<0.0005$). In preliminary experiments introducing ouabain to the perfusate a signal increase is observed in the diffusion weighted images, indicating an overall decrease in the diffusion coefficient.

Conclusions: The results demonstrate qualitatively that brain slices can be maintained in a stable condition for at least 8 hours with short perfusate exchanges. It is convenient that the slices need not be continuously perfused, since this results in flow artefacts on the images. The tonicity experiments demonstrate that the MR signal from the slices is significantly altered by physiologically relevant hypertonic and hypotonic perturbations in a fashion consistent with previous observations on humans and single cells. Preliminary experiments using ouabain as a sodium channel blocker also cause signal changes. These data may be used to aid the development of realistic models of tissues in conjunction with data obtained on single cells and intact animals using MR and other modalities. We believe that the brain slice will be an important model for MR microimaging for the examination of a variety of neurological conditions.

Acknowledgements: Supported by the University of Florida's Brain Institute and Center for Structural Biology, and the National High Magnetic Field Laboratory, Tallahassee and an AHA fellowship award.

MRM, AN ALTERNATIVE APPROACH TO THE STUDY OF HOST/PARASITOID RELATIONSHIPS IN INSECTS.

J.A. CHUDEK, I.E. GEOGHEGAN#, G.HUNTER, R.L. MACKAY, M.E.N. MAJERUS+, S. MORITZ, R.J. MCNICOLL#, AND A.N.E. BIRCH#

Department of Chemistry
University of Dundee
Dundee. DD1 4HN, UK.
#Scottish Crop Research Institute
Invergowrie, Dundee. DD2 5DA, UK.
+Dept. of Genetics
University of Cambridge
Cambridge. CB2 3EH, UK.

Predatory coccinellids are among the most important of the natural biological controls of aphids, which damage crops and plants either by direct feeding or by transmitting viral diseases. A single seven-spot ladybird (Coccinella septempunctata), the commonest British species, consumes circa 5,500 aphids in its life-time. However, this ladybird is under threat from a small parasitic wasp, Dinocampus coccinellae, and levels of infestation, in some populations in Scotland, reached more than 50% in 1996. This has an adverse effect on the reproduction capabilities of the ladybird and on their efficiency as biological control agents. It is therefore necessary to develop policies to reduce the impact of this wasp. A necessary precursor to this exercise is to develop a method whereby the wasp larva development inside the ladybird can be studied and the effect of this larva on the internal organs of the ladybird can be monitored. Conventional dissection studies followed by light microscopy are difficult because of the number of individual specimens needed to follow the developmental sequence.

NMR microimaging provides an important tool in the pursuance of studies into the ladybird/wasp, host/parasitoid relationship. As well as avoiding sacrifice of the sample, 3D spin-echo studies of infected hosts show that the presence of the parasitoid wasp larva can be detected at a very early stage in its development. This is not always possible using conventional methods, which at this point in the growth cycle usually requires a detailed and highly destructive search to be performed on the host. The nature of the chemistry of the host/parasitoid pair provides MRM sufficient contrast for either to be identified at all stages of development. It further allows both lipid and water images to be acquired.

The non-destructive approach of NMR microimaging is therefore an important tool for early detection and gives a better insight into the developmental stages and behaviour of the parasitoid. At a time of increasing concern over the use of chemical insecticides, this research is providing important information about the interaction between a highly beneficial group of insects, the ladybirds, and one of their most dangerous enemies.

DOES HYPOXIA PRODUCE ALTERATIONS IN CORTICAL AND MEDULLARY OSMOLYTE CONCENTRATIONS? AN ASSESSMENT BY VOLUME LOCALISED ^{1}H MAGNETIC RESONANCE MICROSPECTROSCOPY (MRS)

G.J. Cowin, I.A. Leditschke, * S.Crozier and Z.H. Endre

University of Queensland, Dept. of Medicine and *Centre for Magnetic Resonance, St. Lucia, Brisbane, Australia

Intracellular osmolyte accumulation enables renal medullary cells to remain functional, despite high and variable extracellular osmolality. The regulation of intracellular osmolyte levels is poorly understood. We used volume localised ^{1}H MRS to assess the regional disposition of renal osmolytes and the response to hypoxia in isolated perfused rat kidney. The RARE sequence used for scout imaging provided excellent cortico-medullary resolution and enabled selection of voxels of ~24 μl for ^{1}H spectroscopy, using the VOSY sequence, within the cortex or medulla. Acquisition of 10 min cortical and medullary spectra were alternated during each experiment.

To induce hypoxia, the circuit gas mixture was changed from 95%O_2/5%CO_2 to 95%N_2/5%CO_2 after the initial spectra. Changes in the regional concentration of betaine and GPC were estimated from the betaine-GPC peak at 3.2 ppm (fig1). Renal function changed as expected following hypoxia with increases in renal vascular resistance, fractional excretion of Na and K and an initial increase in urine flow and decreases in U/P and GFR. The intensity of the Betaine-GPC peak from cortex and medulla decreased at similar rates in control experiments and after hypoxia.

In summary, the rapid decrease in kidney function, including loss of urinary concentration, caused by hypoxia, is not due to increased loss of the osmolytes, betaine and GPC.

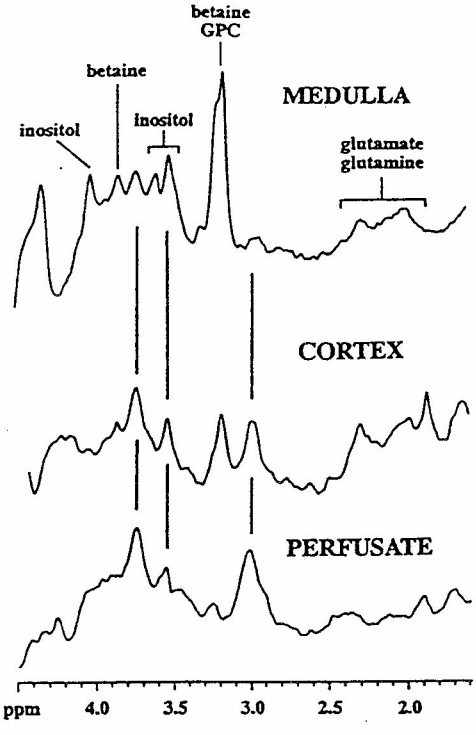

Figure 1. regional spectra (24 µl)

^{19}F Chemical Shift Imaging of F-nuc Formed from 5-FU in Mouse Tumor. Fast Spin Echo vs. Spin Echo for a Short T_2 Signal

Yoshihiro Doi and Yoko Kanazawa

Faculty of Pharmaceutical Sciences, Kyushu University, Fukuoka 812-82, Japan

Metabolite mapping by NMR imaging is a promising method for the monitor of drug dynamics. After the first ^{19}F imaging of 5-FU, an established anticancer drug, and its catabolite F-β-alanine (FBAL) in rat by Brix et al. where these 2 signals have been acquired subsequently [1], we have shown a simultaneous imaging of 5-FU and FBAL+F-ureido-propionic acid(FUPA) in mice [2]. However, these methods give only a part of drug information, side effects. For the evaluation of 5-FU and its prodrugs, it is important to monitor F-nuc, the effective metabolites of 5-FU consisting of nucleoside and nucleotide forms of 5-FU giving a signal in the close vicinity of 5-FU on the ^{19}F spectrum. So far, F-nuc has not been imaged largely because of short T_2. Here, the first ^{19}F image of F-nuc in mouse tumor is reported.

[Methods] The female C3H mice were transplanted with MH134 cells as subcutaneous tumor 1-2 weeks prior to the NMR experiments. After 3 - 4 hours fasting, 1 or 2 mmol/kg of 5-FU was administrated orally as the CMC suspension. NMR imaging was performed under halothane anesthesia on the Varian Unity-INOVA with a 9.4 T vertical magnet and $^{19}F/^{1}H$ tunable 40 mm rf coil tuned to 376 MHz for ^{19}F. After ^{1}H scout image and ^{19}F spectrum, ^{19}F images were obtained by either spin echo or fast spin echo with FOV of 8 x 4 cm^2 without slice selection and 64 x 16 data points, Tr = 1.0 - 1.2 s and Te or echo-spacing of 3 - 6 ms. Simultaneous acquisition of 2 or more signals were achieved by the alternate sampling using both chemical shift selective 90 and 180 pulses (Te = 6 ms) [3]. In order to obtain the image of F-nuc, the refocussing pulse was changed to non selective (hard) for shorter Te or echo-spacing (3 ms) abandoning the information of the other signals.

[Results and Discussion] The 2D imaging of F-nuc were successful by spin echo and also by fast spin echo. In fast spin echo, T_2 decay during 8 or 16 echo trains had an considerable effect on the signal strength distribution in k space as anticipated from the *in vivo* T_2 value of F-nuc of 12 - 20 ms. In the images, however, the quality of fast spin echo was comparable to that of spin echo obtained under the same scan numbers if the initial point of phase encoding was set at the k-space center. Considerable time reduction was attained by this exponentially weighted image. The application of fast spin echo will be appropriate for the weak and short T_2 signals of drugs.

[1] Brix,G. Bellmann,M.E. et al. Magn.Reson.Med. 34, 302 (1995). [2] Doi,Y. Kanazawa,Y. et al. Proc. 5th ISMRM (1997) Vancouver. [3] Narazaki,M Kanazawa, Y. 25th JMRM Meeting (1997) Omiya, Japan.

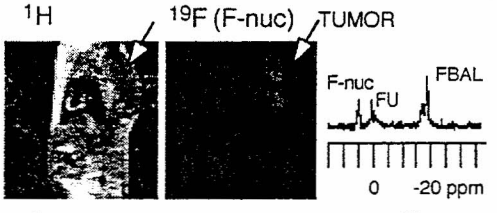

Fig.1. ^{1}H Scout Image, F-nuc Selected ^{19}F Image & Spectrum of FU Administrated Tumor Mouse.

APPLICATION OF PFG NMR TO BIOLOGICAL AND POROUS MATERIALS

ROLAND GIESEN
Inst. für Makromol. Chemie, RWTH Aachen
Worringer Weg 1
D 52074 Aachen, Germany

Pulsed field gradient studies have proven to be a versatile method in the field of structured matter [1]. They can be used to give contrast in imaging and to investigate molecular movements of both random (diffusion) [2] and coherent (flow) type [3]. We present diffusion weighted images of biological samples and pulsed field gradient measurements in one and two dimensions on static and flowing systems. Systems of special interest for PFG measurements are those showing anisotropic diffusional behavior. We have investigated anisotropically restricted diffusion in an arrangement of capillaries or the flow and dispersion properties of liquids flowing in a porous medium. Such experiments provide an insight to flow on a molecular level which can not be resolved by NMR imaging [4]. In another experiment diffusion weighted imaging was used to examine the intervertebral discs of rabbits with and without applying strain. It is shown that the nucleus pulposus and annulus fibrosus of the discs exhibit different properties of diffusion constants when applying strain.

References

[1] P.T. Callaghan, Principles of Nuclear Magnetic Resonance Microscopy, New York 1991
[2] A. Coy, P.T. Callaghan, J. Chem. Phys., 101 (1995) 4599
[3] J.D. Seymour, P.T. Callaghan, J. Magn. Reson., A 122 (1996) 90
[4] D.N. Guilfoyle, P. Mansfield, J. Magn. Reson., 97 (1992) 342

APPLICATION OF NMR MICROIMAGING TO THE STUDY OF WATER TRANSPORT IN EYE LENSES

B A MOFFAT[#], R J W TRUSCOTT* , M H J SWEENEY*, AND J M POPE[#]

[#]Centre for Medical and Health Physics, Q.U.T.
Queensland, Australia, 4000.
***Australian Cataract Research Foundation**
Department of Chemistry
University of Wollongong
NSW, Australia, 2522.

Purpose: The cause of presbyopia and cataract formation that occurs with ageing is still unclear. In this project magnetic resonance microscopy (MRM) has been used to study the kinetics of water transport, which are believed to play an important role in the onset of presbyopia and senile cataract in human lenses. Transport of water containing nutrients and anti-oxidant species from the cortex to the nucleus is vital for maintaining the structures of the proteins (crystallins) in the lens nucleus because the nucleus (being metabolically inactive) is unable to produce them. A deficiency in this transport may be responsible for the onset of presbyopia and cataract.

Method: Human lenses were obtained and stored at 34.5° C in artificial aqueous humour (AAH) containing nutrients and metabolites similar to those in vivo. MR images were acquired over approximately a twenty hour period following replacement of H_2O based AAH with D_2O based AAH to measure the rate at which H_2O diffuses out of the lenses. Signal intensities from regions of interest in the cortex and nucleus were plotted against time, and fitted to a decaying exponential curve using a Levenberg-Marquardt method of non-linear regression.

Results: NMR signal intensity from the lenses decreased with time corresponding to a decrease in concentration of H_2O within the lenses. It was observed however, that in lenses from older individuals (over 65 years) there appeared to be a barrier that restricted the diffusion of water out of the nucleus of the lenses. This was not observed in younger lenses (less than 65). The rate of NMR signal loss from nuclei was measured and it was found that this reduced with increased age of the lenses confirming the observation of a barrier to diffusion in older human lenses.

Conclusions: These results show that as lenses age there is reduction in the rate at which water and water soluble low molecular weight metabolites can enter the cells of the lens nucleus via the epithelium and cortex. Since this is the only mechanism by which nuclear cells can obtain nutrients and anti-oxidants to protect the crystallins from degradation, the decrease in transport rates would lead to increased damage to lenses with age, and ultimately a potential cause of presbyopia and senile cataract.

IN VIVO HISTOLOGY: MRI IN THE STUDY OF KIDNEY TOXINS.

PAUL MULLINS, STEVE POLLEY, DANIEL BRADELY, PAUL HOCKINGS, ANIL DHIRI, DAVID MIDDLETON, DAVID REID, JOHN CONNELLY

University of Queensland
Analytical Sciences, SmithKline Beecham
The Frythe , Herts. U.K. AL6 9AR

In the pharmaceutical industry it is as important to determine if a compound has any toxic effects as it is to determine benifical ones. Magnetic Resonance Imaging (MRI) can provide a non-invasive method to monitor the chemical and anatomical changes that may occour as a response to these toxic effects. This study was performed to see if MRI could detect kidney damage caused by two well known nephrotoxins and formed part of a larger study to develop a database of nephrotoxic effects and characterise changes detectable with a variety of magnetic resonance imaging techniques.

Bromoethanamine (150 mg/kg/day) a papillary toxin, and Hexachlorobutadiene (200 mg/kg/day) were independently administered by single interperitoneal injection to two groups of rats (n=6 per group). Six rats where administered saline to act as controls. Images where acquired on a Bruker AMX 300 spectrometer interfaced to an 18cm 7T horizontal magnet system. A 3D RARE sequence with the following Parameters was used: FOV (5x5x5) cm3, matrix (256x128x128) read extension factor =2, TE=6.5ms, with a rare factor=32 (giving effective T2 weighting), effective TR +1 sec. Animals were sacrificed after imaging and the kidneys removed for histology.

The control images showed good contrast allowing the three areas of the kidney - cortex, medulla and Papilla- to be easily defined. In the treated animals damage was easily discernable and the location of the abnormalities correlated well with histology and the area of known effect for these two toxins.

CHARACTERIZATION OF MALIGNANCY IN TUMORS OF THE CENTRAL NERVOUS SYSTEM THROUGH FRACTAL ANALYSIS

DEMIAN PEREIRA*, CIRA ZAMBRANO AND MIGUEL MARTIN-LANDROVE

Departamento de Fisica and Centro de Resonancia Magnetica
Facultad de Ciencias
Universidad Central de Venezuela
A.P. 47586, Caracas 1041-A, Venezuela and
***Departamento de Fisica Aplicada**
Facultad de Ingenieria
Universidad Central de Venezuela
Caracas, Venezuela.

In this work, we propose a method based on the analysis of NMR images (Proton Density and T_2) in brain axial cuts, to detect and characterize the irregularity of the external edge which belongs to malignant tumors (particularly, gliomas) compared with the relatively smooth edge observed in benign lesions like the cystic ones. The first stage in this process is the detection of the edge using techniques of Digital Image Processing employing a Laplacian Edge Detector, followed by the closing of the contour. The second stage is the codification of the tumor's contour using the technique of the Fourier Descriptors, to represent the perimeter of the structure as a time series. The third an final stage of the process, is to analyze this time series to calculate the possibly fractal dimension that could represent the irregularities present. We performed this analysis on cystic benign lesions and malignant ones, specifically astrocytomas, and multiform glioblastomas, both with different grades of malignancy. The main result of all this study, is that we found a consistent difference between the degree of the irregularities belonging to benign and malignant lesions, and also that the degree of irregularity varies with the grade of malignancy in the tumor.

MORPHOMETRIC ANALYSIS OF CARTILAGE GROWN IN A HFBR USING NMR MICROSCOPY

K. POTTER[*], E. PETERSEN[*], J. BUTLER[†], R. BALAKIR[†], P. PRECHT[†], K.W. FISHBEIN[*],W.E. HORTON[†], AND R.G.S. SPENCER[*]

NMR Unit[*] and Cartilage Biology Unit[†],National Institute on Aging, National Institutes of Health,4940 Eastern Ave,Baltimore, MD 21224

The development of three-dimensional cartilage tissue from isolated chondrocytes is a critical process underlying the success of autologous cell transplantation as a treatment for articular cartilage disease. To study this process, we have developed an NMR compatible hollow fiber bioreactor (HFBR) system in which the production of cartilage by chick sternal chondrocytes can be studied using non-invasive NMR microscopy. By comparing quantitative NMR images with histologic sections of cartilage tissue generated four weeks postinoculation we were able to correlate NMR measurable parameters with tissue cellularity. NMR microscopy was also used to interrogate the morphology of chick growth plate cartilage (GPC). This tissue was selected because the size of the resident chondrocytes increases with distance from the articular surface and the spatial variation of extracellular matrix (ECM) composition has been well documented.

Experimental: For bioreactor studies, chondrocytes were isolated by enzymatic digestion of embryonic chick sterna. The cells were injected into the extra-capillary space of a HFBR designed in our laboratory. Cartilage produced four weeks post-inoculation was analysed with NMR microscopy. For GPC studies, coronal NMR images of an embryonic chick femur, dissected free of muscle tissue and immersed in media, were acquired at 37°C. All NMR experiments were conducted on a Bruker AMX spectrometer operating at 9.4 T (400.1 MHz for 1H). Bioreactors were maintained under incubator-like conditions (95% CO2 / 5% air, 37°C) during data acquisition. Images of the following NMR parameters were acquired for HFBR tissue and GPC: water proton longitudinal (T1), and transverse (T2) relaxation times, the magnetization transfer (MT) ratio, the magnetization transfer rate (km), and the water diffusion coefficient (D). Here, MT = [1 - Mso/Mo], where Mso/Mo gives the ratio of image intensities acquired with and without the application of an off-resonance saturation pulse. After NMR analysis, HFBR tissue and GPC were fixed in formalin, sectioned, and stained with Alcian blue.

Summary of results: Cartilage tissue completely filled the extra-capillary space of the bioreactor by four weeks post-inoculation. The cartilage produced was histologically similar to immature hyaline cartilage. Histologic sections of the tissue confirmed that there were regional variations in tissue morphology. There was a definite gradation of tissue properties with increasing diffusion distance from the fibers: near the fibers the cartilage appeared more cellular with less territorial matrix while further away cells appeared enlarged with increased matrix deposition. The NMR properties of neo-cartilage tissue were dependent on tissue cellularity. Regions with high cell densities had the lowest relaxation times (T1 and T2) and the highest MT values. However, NMR studies of femoral growth plate from a chick embryo revealed that the composition of the ECM impacts on measured NMR parameters. The following observations were made for GPC: (1) the longitudianl relaxation time (T1) increased with increasing cell volume fraction, (2) the transverse relaxation time (T2) was dependent on the volume fraction and composition of the extracellular matrix, (3) the MT ratio increased with in-creasing cell numbers, (4) the magnetization transfer rate (km) increased as the ECM collagen content increased, and (5) the measured diffusion coefficient of water along the growth axis increased as the cell size increased.

Conclusions: Quantitative NMR images of neo-cartilage tissue correlated with tissue cellularity. NMR images of GPC have revealed that the NMR properties of the different zones were dependent on the volume fraction and composition of the ECM. Since chondrocytes at different stages of growth reside in a unique macro-molecular environment, NMR imaging is capable of characterizing developmental changes that occur during cartilage formation in a HFBR. Future studies will focus on using NMR imaging to study the impact of different growth factors and cytokines on cell proliferation and matrix deposition in a HFBR.

NMR MICROIMAGING OF CELL SORTING PROCESS IN THREE DIMENSIONAL DISSOCIATED CELL AGGREGATES

KOJI SAITO[1,3], NAOKI KATAOKA[2], PETER BLUEMLER[3], BERNHARD BLUEMICH[3], AND YASUJI SAWADA[2]

[1]Advanced Technology Research Laboratories
Nippon Steel Corporation
3-35-1 Ida Nakahara-ku, Kawasaki City 211, Japan
[2]Research Institute of Electrical Communication
Tohoku University, Sendai, Japan
[3]Magnetic Resonance Center MARC
RWTH-Aachcn
D-52056 Aachen, Germany

1. Introduction

Hydra is an highly regenerative animal[1], in that regeneration into a whole animal occurs from a tissue as small as one fiftieth of the whole tissue volume or even from a random aggregate of dissociated cells. Many stages are involved in the regeneration process from a random cell aggregate to a whole animal. The first stage from 0 to 6 hours is the cell sorting process. The second stage from 6 to 24 hours is the cavity formation process. The third stage from one day to 2 days is the tentacle formation process. The final stage from 2 days to a few days is the body axis formation process. In all the proceeding experimental observations, the measurement of cell sorting were either on the surface of aggregates or in the artificial two dimensional system. Internal images of cell arrangement in the cell sorting process of a .single three dimensional aggregate have been looked for. NMR microimaging may be the only experimental method for this purpose available at present without invasiveness[2]. We present first the results of NMR microimaging and the analysis of cell sorting in an aggregate of dissociated hydra cells.

2. Materials and Experimental

Hydra Viridissima which contained symbiotic Chlorella in the endodermal epitherial cells was used for this experiment. Eight animals were dissociated and centrifuged into a 800 mm diameter cell aggregate, which was cut into 6 pieces. One piece of cell was introduced into a NMR microimaging sample tube filled with culture solution. Temperature scheduling was used for the present experiments, with alteration of the measuring phase (3 °C; lS0 min.) and the regenerating phase (18 °C; 15, 30, 60, 120 min.). The NMR microimaging system used in this study consisted of a JEOL α 400 NMR spectrometer fitted with microimaging units and a 89 mm bore magnet. A gradient strength of about 60 G/cm and a spectral width of 200 KHz were used. In the 3D NMR imaging experiments, the experimental conditions were 5 ms echotime, 10 s repetition time, 150 ms diffusion observation time, 1024(X)*1024(Y)*16(Z) digital complex data points. Data acquisition required 2.5 hours. The measurements were performed with stimulated echo sequence.

3. Results

1) The raw data present the first observation of cell sorting process inside a three dimensional cell aggregate. By transforming the intensity profile to cell density profile, the analysis of the raw data show the progress of thc cell sorting more clearly and quantitatively.

2) The sorting mechanism is now discussed among the differential adhesion aided by random fluctuation and differential adhesion with hydrodynamic coherent motion.

References
1) Technau, U. and Holstein, T(1992). Cell Sorting during the Regeneration of
Hydra from Reaggregated Cells, Dev. Biol., 151, 117 - 127; Yasuji Sawada, Physica A 204, 543,(1994)
2) Magnetic Resonance Microscopy, Edited by B.Bluemich and W.Kuhn, 1992, VCH

MAGNETIC RESONANCE MICROIMAGING (MRM) OF TEETH

S. N. SCRIMGEOUR*, C. H. LLOYD*, G. HUNTER+, J. A. CHUDEK+ AND R. L. MACKAY+

Dental School* and Chemistry Department+
University of Dundee
Dundee DD1 4HN, Scotland, UK

Introduction. Arguably, dental caries is the most widespread endemic disease which requires the intervention of health professionals. Though preventive policies are in place in many countries the incidence of caries remains high and the resources required for it's treatment consume a significant proportion of healthcare budgets. Continued research on the aetiology and effect of the disease is justified.

Imaging. In a pilot project, reported upon at The Third International Conference on Magnetic Resonance Microimaging[1], images of affected dentine around large cavities (advanced to the extent that the pulp was involved) were produced. This work has continued using a Bruker microimaging attachment mounted in a 7.1T AM300WB spectrometer with data processed by an X32 workstation. Spin-echo pulse sequencing produced the best quality images. Full data sets of medium resolution (90 μ m voxel size) were acquired. The result for one tooth in particular has given information to modify the protocol used when imaging teeth. A posterior tooth had been extracted from a patient attending Dundee Dental Hospital. It was nonfunctional and periodontally involved. When it was examined using MRM high intensity full surface reconstruction images for the pulp chamber and a region adjacent to the occlusal surface were seen. They were separated by apparently healthy dentine. Visual examination of this surface showed it to be discoloured but hard (to probing) and intact with the exception of a small hole (ca. 0.25mm) in a fissure. The high intensity region near the surface is the result of caries. Given the discolouration and the small hole a dentist might suspect that the tooth is unsound, but without destructive intervention the extent of the lesion would not be known. Even with intervention it is not possible to be sure that all the diseased tissue has been cut away. MRM reveals the full extent of the affected tissue. However, the pulp cavity structure appeared exceptional and would require an unusual pathogenesis to account for the morphology - a large pulp chamber and closed root canals. The tooth was (physically) cut into 0.25mm serial slices along an axial line and compared with the respective MRM slices. Root canals, albeit narrow and of low intensity in the rnr image, existed in both with an excellent correlation for morphology. It is reasonable to conclude that the intensity produced by the material in the canals must be below that required to register in the full surface reconstruction. The use of artificial colour and the range selected for displaying the images was not a factor in the presence / absence of features.

Conclusions. A full surface reconstruction cannot be used in isolation. Full data sets must be acquired and all slices should be examined. From these particular slices can be selected either as representing healthy structure or because they contain disease affected tissue or an abnormality.

1. J.A. Chudek, G. Hunter, C.H. Lloyd, R.L. MacKay, S. N. Scrimgeour. 3rd International Conference on Magnetic Resonance Microscopy, Wurtzburg (1995) 113

ANALYSIS OF ESOPHAGEAL MOTILITY BY FAST MR IMAGING

Y. SEKI, S. NARUSE[1], Y. SEO[2], M. MURAKAMI[3], T. OZAKI[3], M. KITAGAWA, H. ISHIGURO, Y. NAKAE, AND T. HAYAKAWA[1]

[1]Internal Medicine II
Nagoya University
Tsurumai 65, Showa-ku, Nagoya 466;
[2]Physiology I
Kyoto Prefectural University of Medicine
Kawaramachi-Hirokoji
Kamigyo-ku, Kyoto 602; and
[3]National Institute for Physiological Sciences,
Myoudaiji, Okazaki 444, Japan

Advances in fast MR imaging techniques enable us to visualize the dynamic movements of organs in living animals and humans. Esophageal contraction following the act of swallowing is one of the fastest movement in the gastrointestinal tract. In the present study we have tried to record the swallowing of a balloon by esophageal peristalsis of conscious rabbits.

1H imaging of the esophagus was performed with a 4.7T magnetic resonance spectrometer for animal studies (Biospec ABX 47/40, Bruker, Germany) with a bird-cage RF-coil (inner diameter of 20 cm). Japanese white rabbits (3.0-3.7 kg) were fixed firmly on an animal support in the prone position without anesthesia, and a pair of earplugs was applied to keep out noise from gradient coils. Median sagittal images were taken by a fast gradient-echo imaging (Snapshot) at 3 images/sec. Typical values used were as follows: field-of-view 22.5 cm, datamatrix 96x96, spectral width 72 kHz, relaxation delay 3.4 msec,echo-time 1.9 msec, slice-thickness 6 mm, number of accumulation 1. A 6 Fr. silastic tube with a balloon at the tip was inserted nasally into the upper esophagus,¡¡ and was placed just distal to the upper esophageal sphincter. The balloon was then inflated to 1 cm diameter by infusion of 0.6 ml of 0.3 % (w/v) ferric ammonium citrate.

The esophagus was clearly visualized from the pharynx to the esophago-cardia junction in the median sagittal image of rabbits. One to 10 sec after inflation the balloon moved from the upper esophagus to the lower esophagus. The balloon often staged just proximal to the lower esophageal sphincter for two to five sec and then moved into the stomach by the next peristaltic movement started from the upper esophagus. The calculated maximal velocity of the balloon was 8.3 cm/sec.

Fast MR imaging allows us to observe clearly a rapid movement of a bolus along the entire length of esophagus during swallowing.

MR IMAGE OF CORTICAL BONE USING CONSTANT-TIME-IMAGING METHOD

H. TAKAMIYA*, Y. KUSAKA*, Y. SEO, T. MORIMOTO**, Y. HIRASAWA***

***Dept. of Orthop. Surg. & **Dept. of Physiol.**
Kyoto Pref. Univ. of Med.
Kyoto 602 Japan

INTRODUCTION:

Acquisition of NMR information from the cortical bone with conventional MR imaging method is very difficult because of its very short T2 relaxation time. This is the reason why the cortical bone is always imaged negatively against the adjacent soft tissues, i.e. bone marrow, periosteum, muscles etc.. Constant-time-imaging (CTI) or Single-point-imaging (SPI) is a new imaging modality which allows to get images with the echo time less than 100 _(I5_(Js. In the present study, we imaged the cortical bone and the cancellous bone using the 3D-CTI method and compared the image obtained by the 3D-gradient-echo (GE) method.

MATERIAL AND METHODS:

Imaging was performed using AMX-300 spectrometer (Bruker, Germany) and a micro5 micro-imaging probe (12mm diameter). Materials were the proximal femur of a rat, bovine vertebral body, 5th toe of a rabbit and the diaphysis of a rabbit femur. Typical parameters used were as follows; FOV was 0.8x0.8x1.6cm, matrix was 64x64x128, phase encoding time was 0.1ms, maximum gradient strength was _(I1_(J92.5G/cm, ramp time was 0.3ms, stabilization time was 0.3ms, spectral width was 125kHz, RF pulse width was 1.5 _(I5_(Js (flip angle 8_(I!_(J), pulse repetition time was 25ms and number of averages was 3. Because the data was acquired point by point, the total image acquisition required 11 hours.

RESULTS:

The 3D-CTI method clearly visualized the structures of the cortical as well as trabecular bones within the femoral head with positive contrast. Similarly we could get the positive NMR signal from the cortical bone of the bovine vertebral body, 5th toe of a rabbit and the diaphysis of a rabbit femur. In contrast, the 3D-GE method did not acquire any signal from bony trabeculae or cortical bone as evidenced by negative contrast of these tissues on the images.

DISCUSSION:

The morphological observation of the bone with 3D-GE method is hindered by magnetic susceptibility as well as chemical shift artifacts. Furthermore, the 3D-GE method gives us no NMR information of the bone, some of which may have a diagnostic value for the bone pathology. The 3D-CTI method which was first introduced for bone tissue examination in this study is not influenced by the above described artifact. We believe, using this method in combination with some other NMR techniques such as presaturation pulses or relaxation analysis, it is possible to analyze pathological conditions of the bone tissues.

In conclusion, the 3D-CTI method is a quite useful technique for imaging of bony tissue because it allows not only morphological examination but also quantitative analysis of the bone tissue.

REFERENCE:

1. D. G. Cory. Ann Reports of NMR spectr 24, 114, 1992

DETECTION OF EXPERIMENTAL ALLERGIC ENCEPHALOMYELITIS MOUSE MODEL USING IN VIVO MR MICROSCOPY

SU XU[1], E. KAY JORDAN[1], WEN LI[2], STEFAN BROCKE[3], JEFF W. M. BULTE[1], LAURA QUIGLEY[3], NANCY TRESSER[3], YIHONG YANG[1], JOHN L. OSTUNI[1], SCOTT A. CHESNICK[4], HENRY DEF. WEBSTER[2], HENRY F. MCFARLAND[3], JOSEPH A. FRANK[1]

Laboratory of Diagnostic Radiology Research[1], OD, OIR
Laboratory of Experimental Neuropathology[2], NINDS
Neuroimmunology Branch[3], NINDS
Laboratory of Cardiac Energetics[4]
NHLBI, National Institutes of Health
Bethesda,MD 20892, USA
Bldg.10, Room B1N-256, LDRR
National Institutes of Health
Bethsda, MD 20892

Abstract:

In vivo MR microscopy with or without the use of contrast enhancement with MION-46L, a superparamagnetic iron oxide contrast agent, was investigated for its ability to increase the sensitivity of in vivo 3D MR microscopy in the detection of brain lesions and treatment effects of insulin-like growth factor-I (IGF-I) in chronic relapsing experimental autoimmune encephalomyelitis (crEAE) mouse model. Lesion conspicuity on postcontrast 3D MR microscopy was dramatically enhanced as compared to precontrast images and corresponded to those demyelinating lesions staining positive for Prussian blue iron stain. In the crEAE mice treated with placebo, precontrast MRI demonstrated areas of abnormal signal throughout the cerebrum, brainstem and cerebellum. Similar areas were not detected in IGF-I-treated brains and their signal intensities did not differ significantly from those observed in brains of normal mice. These tissue alterations did not have a corresponding histopathological finding. The technique would be useful in differentiating the various stages of pathology and demonstrating the efficiency of novel therapeutic approaches for crEAE.

High resolution in vivo magnetic resonance microscopy of the rat heart at 4.7 T using a local RF transceiver coil

Sudeep Chandra, Konstantin Gurbanov, Robert Strittmatter, Eliot H. Ohlstein, Giora Z. Feuerstein and Susanta K. Sarkar

SmithKline Beecham Pharmaceuticals, 709 Swedeland Road, King of Prussia, PA-19406.

High resolution non-invasive magnetic resonance cardiac microscopy of animal models (rat, rabbits etc,) has enormous potential to help the process of evaluating novel therapeutics in vivo and to follow their chronic effects serially in each animal. Cardiac gated (~60msec from the QRS complex) MR imaging was used to generate images of the rat heart using a 4.7 T BRUKER imaging spectrometer with insertable gradient coils. A spin echo pulse sequence (TR/TE = 5000/13 msec; FOV= 4 x 4 cm; 256 x 256; Navg= 2) was used to acquire high resolution MR k-space data. Simultaneous respiratory gating was not required since motion artifacts from chest movements did not adversely affect the cardiac gated images. To optimize the echo time (TE), a read-gradient of 3.7 G/cm was used to generate an acquisition bandwidth of 62.5 kHz over the field of view. The in-plane spatial resolution was sufficient to measure left ventricular wall thicknesses (~2.5-3.0 mm) with good reproducibility. The gain in resolution was principally achieved using a local half-birdcage radiofrequency coil, which provided adequate signal-to-noise ratio for appropriate optimization of resolution and imaging time. The radio frequency (RF) power levels for the excitation pulses were adjusted in real time to provide a fairly uniform RF profile over the rat heart. The non-uniformity in RF intensity, if any, across the imaging plane did not affect anatomical quantitation since relative intensities were not used for any calculations. The RF profile was uniform over the entire ventricular region (the slice dimension) of the rat heart and provided the option to acquire contiguous slices and subsequently generate volumetric estimates of structural parameters. To illustrate the feasibility of using MR microscopy for non-invasive volumetric measurements of serial changes in cardiac wall thicknesses/ventricular dimensions and hemodynamic parameters, quantitative serial data will be presented from a chronic volume overload model of cardiac dysfuntion.

CONCENTRATION POLARISATION: AN *IN SITU* STUDY.

D. AIREY, V. CHEN*, J. WU* AND J. M. POPE

Centre for Medical and Health Physics
Queensland University of Technology
GPO Box
2434 Brisbane
Australia 4001 and
***UNESCO Centre for Membrane Science and Technology**
University of New South
Wales, Sydney, Australia 2052

Crossflow microfiltration is an important separation process based on the use of porous membranes and driven by a trans-membrane pressure difference. It has wide industrial applications. The dynamics of the process, however, are not well understood, with traditional models under-predicting filtration rates by up to two orders of magnitude. It is known that concentration polarisation (CP), the process by which a layer of solute builds up at the membrane wall, is a determining feature of microfilter operation with a significant influence on the filtration efficiency, but the relative contributions of mechanisms which limit the build up of the CP layer are not fully understood, in part because of a lack of non-invasive methods for studying their formation and development.

Magnetic resonance imaging (MRI) has been used to produce images of the concentration polarisation layer *in situ* in a crossflow microfiltration system under a variety of conditions. The system is based on an Enka 'Accurel' tubular polypropylene membrane with an average pore size of 0.2 - 0.4 ~m, inner diameter 5.2 mm and a wall thickness of 1.65 mm and uses colloidal silica (particle size 12 nm) as a test feedstock. The silica particles to not directly produce any signal but may be detected through their effects on the water content, and the transverse and longitudinal relaxation times (T1 and T2) of the solution. Because the silica is not neutrally buoyant, the CP layer flows under the action of gravity and is not symmetric in the steady-state - being up to 3mm thick and the thickest part and less than 201lm at the thinnest.

Spin-echo images (12mm FOV with 128x128 resolution) with short TR (0.5s) were taken at 6 minute intervals to record growth of the CP layer with time at different positions and under different crossflow regimes. Quantitative measurements have also been made on the steady-state thickness of the CP layer as function of position. The effects of crossflow rate on this distribution were also examined. Long TR (8.0s) images at 512x512 resolution were used to construct approximate concentration profiles revealing a gradual transition between the bulk concentration of the feedstock and the maximal concentration at the wall.

CAPILLARY PRESSURE CURVES FROM MRI IMAGES OF CENTRIFUGED RESERVOIR ROCK

BERNARD BALDWN
Phillips Petroleum Co.
103 GB
Bartlesville, OK 74004

Capillary pressure curves for porous rocks describe the ability of that rock to retain fluids. Oil companies are primarily interested in the maximum amount of hydrocarbon which can be produced from a reservoir. That amount is determined by the interaction of the hydrocarbon with the surface of the reservoir rock and the pressure differential across the production volume. This information can be obtained from a capillary pressure curve. In the past capillary pressure curves have been determined by three techniques: A) the porous membrane/plate method, B) mercury intrusion as a function of pressure and C) centifuging the core at several increasing speeds. The porous plate method takes weeks to months per pressure and thus takes several months to produce a limited number of points on the capillary pressure curve. The mercury method is fast, but there is concern about translating information about a non-wetting fluid to represent oil and water. The centrifuge method is rapid, but requires assumptions or modeling to estimate the saturation distribution of fluids in the core since it only measures the amount of fluid produced as a function of centrifuge speed.

The method described in this paper uses MRI to determine the fluid saturation inside the porous rock after centrifuging. Since the pressure can be calculated at any point in the rock from the density difference of the fluids, the height of the point above the free water level and the centrifuge speed, the saturation distribution can be directly converted to a capillary pressure curve. Expermentally determined calibration curves were used to produce the saturation distribution from the MRI intensity. The oil phase was frozen while the rock was being centrifuged to prevent redistribution of fluids. Preliminary tests on two diverse types of reservoir rock, sandstone and chalk, show that the technique is applicable to a variety of reservoirs.

SIMULATED RELAXATION RATE AND LOCAL MAGNETIC FIELD DISTRIBUTIONS IN POROUS SYSTEMS

ALFONSO BENAVIDES*, SIGIFREDO GONZALEZ, DAMARIS BARRANTES AND MIGUEL MARTIN-LANDROVE

Departamento de Fisica and Centro de Resonancia Magnetica
Facultad de Ciencias, Universidad Central de Venezuela
A.P. 47586, Caracas 1041-A, Venezuela and
***Instituto de Ciencias de la Tierra**
Facultad de Ciencias, Universidad Central de Venezuela
A.P. 47586, Caracas 1041-A, Venezuela

The relaxation process in a porous material is not a well understood problem due to the disordered geometrical and physicochemical properties of the pore space. No matter this fact, the relaxation in a porous material is usually assumed to be multiexponential or stretched exponential, with the inclusion of some phenomenological parameters, i.e., mean relaxation rates or stretched exponents, a description which is rather simple and avoids the possibility to establish a relationship between the measured relaxation and the microscopic properties of the porous material. In the present work, we have performed numerical simulations to evaluate the relaxation rate distributions for different model pore spaces and compare them to predictions obtained by analytical models. The algorithm used for the simulations evaluates directly the spectral density associated to the magnetic field fluctuations inside the porous material taking into account its disordered nature and the dynamics of the molecules in the fluid. Besides the relaxation rate distributions, the local magnetic field distributions are also calculated. the evolution of the distributions functions as the time interval for the simulation is changed is compatible with the observed experimental behavior in consolidated rocks.

MOISTURE PROFILES OF DRYING CONCRETE USING SINGLE-POINT IMAGING (SPI)

S.D. BEYEA, B.J. BALCOM, P.J. PRADO, R.L. ARMSTRONG, T.W. BREMNER[1]

Magnetic Resonance Imaging Centre and [1]Department of Civil Engineering, University of New Brunswick Fredericton, NB, E3B 5A3, Canada

Moisture content and spatial distribution affect cement and concrete materials in many ways. Knowledge of spatial variations of moisture to submillimetric resolution under the action of drying, freeze-thaw, and salt water ingress are fundamental to the understanding of the long term behaviour of concrete structures. Recently we have demonstrated the use of the SPI sequence (1,2), based on the constant-time technique of Emid and Creyghton (3), for imaging concrete. This sequence is ideally suited to this study given the characteristically short relaxation times of water in concrete ($T_2^* < 200$,us). Using this technique we have studied the effect of mixing and curing parameters on the drying of concrete cylinders with submillimetric resolution (50 mm X 70 mm, white Portland cement, 14 mm maximum aggregate) (4).

1. B.J. Balcom, R.P. MacGregor, S.D. Beyea, D.P. Green, R.L. Armstrong and T.W. Bremner, J. Magn. Res. A, 123, pp. 131 (1996).
2. M. Bogdan, B.J. Balcom, T.W. Bremner and R.L. Armstrong, J. Magn. Res. A, 116, pp. 266 (1995).
3. S. Emid, J.H.N Creyghton, Physica 128B, pp. 81 (1985)
4. S.D. Beyea, B.J. Balcom, T.W. Bremner, R.L. Armstrong, D.P. Green and P.J. Prado, Cem. Conc. Res., submitted.

3D Microscopy of Moisture at the Paste/Aggregate Transition Zone in Hardened Concrete using SPRITE

S.D. Beyea[1], B.J. Balcom[1], P.J. Prado[1], R.L. Armstrong[1], T.W. Bremner[2]
P.E. Grattan-Bellew[3]

[1] Magnetic Resonance Imaging Centre and [2] Department of Civil Engineering, University of New Brunswick, Fredericton, NB, E3B 5A3, Canada
[3] Institute for Research in Construction, National Research Council, Ottawa, ON, K1A 0R6, Canada

The transition zone between hydrated cement paste and aggregate particles directly effects the structural characteristics of concrete, through such fundamental properties as tensile strength, permeability, modulus of elasticity and overall deterioration resistance. Indeed, although composed of the same elements as the bulk hydrated cement paste, the properties of the transition zone are so different that they are often treated as a separate phase of the concrete structure. The understanding of the properties of this zone are crucial, as it is considered to be the strength limiting phase of concrete. Many of these properties are due to variations in the local water-cement ratio in the transition zone, as compared to the bulk paste. This three-dimensional variation in moisture content makes this a natural candidate for studies by MRI, however the short relaxation times of water in concrete ($T_2^* < 200$ μs and $T_1 < 4$ ms) make it impossible to observe by traditional MRI sequences. The use of SPRITE (*S*ingle *P*oint *R*amped *I*maging with T_1 *E*nhancement) (1) however, allows us to obtain three dimensional images of concrete cylinders at high resolution with excellent S/N. Using this technique we have obtained images of moisture variation surrounding both porous and non-porous aggregates in hardened concrete cylinders.

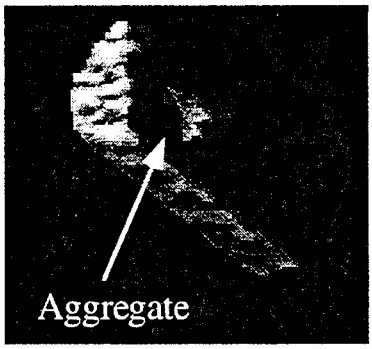

Figure 1. 3D surface rendered Image of a hardened mortar containing a single non-porous coarse aggregate (≈14 mm). Data is viewed in cross section to reveal aggregate.

1. B.J. Balcom, R.P. MacGregor, S.D. Beyea, D.P. Green, R.L. Armstrong and T.W. Bremner, J. Magn. Res. A, **123**, pp. 131 (1996).

A BROAD LINE MAGNETIC RESONANCE IMAGING STUDY OF WATER TRANSPORT IN CEMENTITIOUS BUILDING MATERIALS

A.J. Bohris[+], P.J. McDonald[+], M. Mulheron[*], B. Newling[+] and B. LePage[*].
Departments of Physics[+] and Civil Engineering[*]
University of Surrey, Guildford, Surrey, GU2 5XH, UK

Water transport within cementitious materials depends critically on the pore structure morphology and hence on the mix proportions and cure conditions of the cement. For instance, samples prepared with a water to cement ratio of 0.3 generally have a closed pore structure, while those prepared with a water to cement ratio of 0.5 have a much more connected pore structure. Moreover, closed pore structure cements cured under sealed conditions or underwater generally exhibit considerably more water locked up in the structure than those cured in open conditions. The motivation to understand water transport in these systems stems from the fact that water transport underlies all the primary causes of degradation of cementitious building materials. Degradation is now to the fore of economic and scientific concern. Indeed, in Europe, the commercial turnover associated with the repair and replacement of existing buildings which have become degraded now exceeds the turnover for new construction.

MRI offers an excellent means of monitoring the spatial distribution of water in curing, wetting and drying cement samples. This paper reports the principal results of an MRI study to profile changing water content within a large (>150) number of Portland cement paste samples. These samples reflect a wide range of water-cement ratios, hydration and cure regimes (open, sealed, water saturated) and age. Since conventional MRI techniques are severely limited for the study of cements due to considerable NMR line broadening, resulting from susceptibility gradients and impurities in the samples, broad line stray field and gradient echo magnetic resonance imaging techniques have been used.

The study has led to a picture of the way in which the water transport depends on the cement paste pore morphology; a picture which will be described in the paper. The study has also generated a large volume of baseline data which can be used to test theoretical models of the diffusion process and as a standard by which to measure the effectiveness of different technologies designed to control water transport and hence degradation.

The application of hydrophobic surface treatments is an important method of protecting exis~ing buildings as well as some new ones. In a complementary study to that described above, the effects of an industry standard surface treatment on both the ingress and, importantly, the egress of water in green building sandstone has been studied as a function of the treatment cure conditions. Interestingly, it has been shown that the treatment is considerably more effective after periods of water saturationl.

l. A.J. Bohris, P.J. McDonald and M. Mulheron, J. *Mat. Sci.* 31, (1996) 5859.

NMR IMAGING IN THE DEVELOPMENT OF FORMULATIONS FOR THE CONTROLLED RELEASE OF DRUGS

COLIN A. FYFE, ALMIRA I. BLAZEK, HILTRUD GRONDEY
Department of Chemistry
University of British Columbia
2036 Main Mall
Vancouver, B.C., Canada V6T 1Z1 and
BRIAN J. FAHIE, AVINASH NAGIA AND SHAM K. CHOPRA
Pharmaceutical Sciences Division
Glaxo Wellcome Inc.
7333 Mississauga Road
Mississauga, Ontario, Canada L5N 6L4

Important current developments in the pharmaceutical industry involve the design of delivery devices for the predictable controlled release of drugs. Some of these devices have utilized unique geometrical arrangements. These devices rely on the different chemical and physical properties of separate components to achieve the desired release profile. Current methods of analysis, such as tablet dissection and drug release profiles, provide some indication about the behavior of the delivery device during dissolution. However, these techniques do not provide direct, real-time details regarding the microscopic changes to the delivery device which, ultimately, control the release of the drug. NMR imaging is an ideal tool in the development of these controlled release devices as it allows the formulations scientist to visualize the change in the device during dissolution and provides the necessary information to correct or enhance device performance.

In the present work, NMR imaging was used to investigate the *in-vitro* dissolution behavior for a variety of controlled release devices, specifically, for the optimization of a modified compression coated tablet developed by Glaxo Wellcome Inc. and, generally, to determine the important properties for successful performance of these devices. The compression coated tablet is comprised of a soluble core containing the drug and a coat that surrounds all of the core except for the cylindrical face. The theoretical dissolution rate of the tablet core is proportional to the surface area of the core exposed to the dissolution media. Initial formulations for this tablet gave faster than predicted dissolution rates. Dissection of the tablet showed that water was penetrating the interior of the core but the route of the penetration was not easily discernible. Two dimensional, cross-sectional images of the tablet dissolving *in-vitro* clearly indicated that the dissolution media was rapidly passing through the coat at its thinnest point and was dissolving the core material, thereby increasing the exposed surface area. When the formulation of the coat was altered to reduce its permeability to the dissolution media, the images of the final tablet formulation showed that the tablet was dissolving as designed producing the predicted dissolution behavior. NMR imaging investigations of osmotic pump delivery devices and gelatin coated capsules will also be presented and discussed in relation to the mechanism that controls the release rate of the contained drug.

NMR CHARACTERISATION OF PAN SOLUTIONS AND THEIR NON-SOLVENT INDUCED PHASE SEPARATION

JOHN A. GOLIGHTLY, KEN J. PACKER, ROGER N. IBBETT
Department of Chemistry, University of Nottingham
Nottingham, UK, NG7 2RD
Courtaulds, Lockhurst Lane
Coventry, UK

Polyacrylonitrile dopes are the starting materials in the production of acrylic fibres. NMR has been used to characterise a series of polyacrylonitrile ternary solutions of differing polymer concentrations. Variable temperature studies of transverse and longitudinal relaxation, and self diffusion measurements have provided information about the mobilities and interactions of the various species present.

Phase separation is brought about by introducing a non-solvent to the polymer solution. This process has been studied using 1D proton NMR imaging techniques. The proton concentration profiles have been produced as a function ofcoagulation time and have been fitted to diffusion models in order to produce diffusion coefficients relating to the onset of coagulation.

Polyacrylonitrile films have been cast under various coagulation conditions and the relaxation behaviour of the water trapped in the polymer network gives information about the porosity of the film. The nature of this porous network has been confirmed by SEM.

Due to the nature of the solvent it has been possible to use sodium 23 NMR to aid in the characterisation of the polymer solutions. This has complemented the proton studies.

MAGNETIC RESONANCE IMAGING OF THE FLOW BEHAVIOR OF HIGHLY FILLED MATERIALS.

J. H. IWAMIYA, S. W. SINTON, AND A. W. CHOW,
Advanced Technology Center, Lockheed Martin Missiles & Space
Mail Stop O/H1-32, B/204
3251 Hanover Street
Palo Alto, CA 94304.

There is a constant push to produce higher quality products at a lower cost. Irrespective of the product, there is a need to understand: a) how new materials behave when standard processing approaches are utilized during processing; b) the behavior of well known materials in new processing approaches or; c) when new materials are subjected to new processing approaches. In the area of energetic materials processing, there is a demand to reduce the life cycle waste. To achieve this objective, we have been applying a number of techniques to understand what phenomena are occurring during processing of highly filled materials. In this paper, we will discuss the application of mri, rheological, and other technques to examine the flow behavior of highly filled materials in simple geometries. We will present results which validate theoretical particle migration models for simple flow geometries as well as experimental results on more complex industrial geometries.

NMR EVIDENCE FOR REPTATION DYNAMICS IN SEMI-DILUTE POLYMERS?

M.E. KOMLOSH AND P.T. CALLAGHAN
Department of Physics
Massey University
Palmerston North, New Zealand.

The dynamics of entangled high molecular weight polymers is a controversial subject in which there are a number of competing models. The reptation theory (1-3) is one approach to describe such polymer motion. In the reptation model the polymer entanglements play the key role in determining the polymer Brownian motion. According to this theory the topological constraints due to these entanglements define a "tube" (1-3) in which the polymer is not free to diffuse in any direction in space but it confined to "reptate" along the tube's curvilinear axis. This motion has a characteristic time-dependence (3), depending on the distance over which the polymer segments move. The smallest scale motion which we consider is that of the free Brownian displacements in which the polymer segments are free to diffuse up to the dimension of the tube diameter *(a)*. At a higher distance scale is the reptation along the tube, motion which persists up to the scale of the polymer dimensions, and which is ultimately terminated by tube disengagement.

One means of describing the polymer motion is via the rms laboratory frame displacement of the polymer segments, $\varphi(t) = < (R_n(t) - R_n(0))^2 >$. This is precisely the parameter measured in the initial Echo decay in a Pulsed Gradient Spin Echo NMR experiment (4). The characteristic behaviour of over the various time regimes represent a signature for reptative motion, namely,

(I) free Rouse motion

$$t \le \tau_e,\ \varphi(t) \le a^2,\ \varphi(t) \approx t^{\frac{1}{2}}\ ; \tag{1}$$

(II) Rouse motion constrained to the tube

$$\tau_e \le t \le \tau_R,\ a^2 \le \varphi(t) \le \overline{R}a,\ \varphi(t) \approx t^{\frac{1}{4}} \tag{2}$$

(III) curvilinear diffusion in the tube

$$\tau_R \le t \le \tau_d,\ \overline{R}a \le \varphi(t) \le \overline{R}^2,\ \varphi(t) \approx t^{\frac{1}{2}} \tag{3}$$

(IV) long-range centre-of mass motion

$$\tau_d \le t,\ \overline{R}^2 \le \varphi(t),\ \varphi(t) \approx t. \tag{4}$$

τ_e, is the equilibrium time, τ_r is the Rouse time and τ_d is the tube disengagement time.

Very high magnetic field gradient coils enable us to measure the motion on a time scale between a few seconds to a few millisecond and on a distance scale smaller than the polymer dimensions. The ability to detect motion in this range has made it possible to detect the t, $t^{1/2}$ and $t^{1/4}$ regimes (3) in semi-dilute polymer solutions. Preliminary results, using high molecular weight samples, shows an evidence of spin diffusion.

[1] S. F. Edwards *Proc. Phys. Soc.* 92,9(1967)
[2] P.G. de Gennes, J. Chem. Phys. 55, 572 (1971)
[3] M. Doi and S.F. Edwards *The Theory of Polymer Dynamics* (Oxford Univ. Press, Oxford, 1987)

OBSERVATION OF WATER DISTRIBUTION AND DIFFUSION DURING THE DRYING PROCESS IN TEXTILES

JOHANNES LEISEN, HASKELL W. BECKHAM, W. W. CARR
Georgia Institute of Technology
School of Textile & Fiber Engineering
Atlanta, GA 30332-0295

Most textile production processes include a drying step for fibrous substrates that are wet as a result of the application of dyes and finishing chemicals via aqueous solutions. This study focuses on industrially produced carpets. Here, the drying process is achieved by an air flow through large carpet sheets. Since about 30% of the thermal energy needed for the manufacturing process is used for the drying step, a thorough understanding of the drying mechanism will allow process optimization, leading to energy conservation. In order to achieve this understanding it is important to know the spatial distribution of water within samples and observe how this distribution will change as a function of different drying conditions (i.e., rates and direction of air-flow, temperature).

Simple NMR spin-echo images of wet carpet samples reveal already important information for textile engineers. Short echo times were selected to reflect the distribution of water within the carpet. In a carpet sample consisting of a primary backing and cut pile nylon fibers moisture was found to exist primarily in the nylon tufts. No significant water concentration is found for the region between individual tufts, especially in the void spaces, formed near the backing as the tufts are constricted to pass through the backing.

A special setup was developed to simulate the industrial drying of carpet samples inside a microimaging probe allowing the observation of drying processes of sample with a diameter of 20 mm. During the industrial drying process using air with a temperature of approximately 100 oC, carpet samples will lose moisture within one minute. The recording of standard spin echo images during the drying process is therefore not possible. However, when air is blown along the direction of the tufts, a thorough understanding of the drying mechanism due to water diffusion and evaporation can already be achieved from the analysis of moisture profiles along this direction. Therefore, the drying process can be followed accurately by recording moisture profiles measured by using a spin-echo sequence. Effects such as changes in relaxation times due to heating and interactions of water with the carpet fibers via hydrogen bonding have to be considered.

In a first series of experiments the effect of an air flow penetrating carpet samples from the upper side was investigated. In this case the air stream has to migrate through the tufts before leaving the sample through the backing. It is observed clearly that the carpet yarn near the backing dries out much slower than the rest of the carpet. Either the moisture located in this region is simply more difficult to dry or the incident air stream is transporting water to this region from the underlying pile region.

The potential of MR microimaging for the investigation of engineered fibrous substrates is very great. Due to their structural anisotropy, small-molecule penetrants are expected to exhibit anisotropic molecular diffusivity within these substrates. In addition to drying studies, MRM techniques should prove valuable in characterizing novel textile structures for fluid absorption and management.

NOBLE GAS NMR OF MODEL POROUS MEDIA

R. MAIR*+, C.H. TSENG*+, G.P. WONG*, R.L. WALSWORTH*, M. HURLIMANN#, L. SCHWARTZ# AND S. PATZ+

Harvard-Smithsonian Center for Astrophysics
Cambridge, MA
 # Schlumberger-Doll Research
Ridgefield, CT
+ Brigham and Womens Hospital and Harvard Medical School
Boston, MA.

Gas-phase NMR has recieved considerable recent attention with the use of optical pumping techniques to produce noble gas samples with nuclear spin polarizations up to 5 orders of magnitude greater than those in thermal equilibrium (1,2). In addition to increasingly well-known biomedical applications (3,4), NMR of laser-polarized 3He and 129Xe (the two spin 1/2 noble gas nuclei) may advance the study of porous materials such as sandstone rock, matrix polymers, and granular media. Gases have much larger diffusion coefficients than liquids, and thus may sample a greater number of pores during an experimental observation time. Laser-polarized addition, the large magnetization of laser-polarized noble gas may enable high-resolution imaging in porous media (as has already been achieved in human lungs (4).

In our present study we are applying known methods (5) to noble gas NMR to determine the tortuosity of model porous media: packed beads. We are measuring the time dependent diffusion coefficient (i.e. restricted diffusion) using the PGSE method modified for applications in porous systems to account for background gradients (6). This technique has been used previously with water proton NMR to characterize the tortuosity of packed glass beads, but was found to be inappropriate for studying natural rocks, because surface relaxation attenuates the signal before the spins diffuse through a large number of pores (7).

The application of traditional NMR techniques to laser-polarized noble gases is non-trivial, for two reasons: (i) the laser-polarized magnetization is finite and not rapidly renewable, so one must design sequences that conserve this magnetization, or else implement technically-involved methods to remove the "spent" (de-polarized) gas and replace it with freshly polarized gas; and (ii) the application of PGSE techniques to rapidly diffusing gas samples; not been previously attempted; may test some of the underlying assumptions of this technique, potentially requiring extremely short gradient pulses which could task conventional hardware.

We are currently developing NMR techniques for laser-polarized noble gases to allow rapid measurement of restricted diffusion in porous media. In parallel, we are investigating the applicability, for thermally polarized gas, of using traditional NMR techniques to measure restricted diffusion. We are using thermally polarized 3He and 129Xe gas infused in various packed bead samples. Each sample contains beads of uniform size, with different samples covering a range of bead sizes from 100 microns to 5 mm. We are also investigating potential systematic dependences of measured restricted diffusion parameters (such as tortuosity) on bead material, noble gas and oxygen partial pressure, noble gas polarization, etc. Finally, we are relating our restricted diffusion data to geometrical parameters of the porous system. The latest results from this ongoing study will be presented.

1) W. Happer, et. al., Phys. Rev. A, 29, p. 3092 (1984).
2) M. Albert, et. al., Nature, 370, p. 199 (1994).
3) K. Sakai, et al., J. Magn. Reson., B111, p. 300 (1996).
4) J. Mugler, et al., Magn. Reson. Med., 37, p. 809 (1997).
5) M. Hurlimann, et. al., J. Magn. Reson., A111, p. 169 (1994).
6) L. Latour, et al., J. Magn. Reson., B101, p. 72 (1993).
7) R. Kleinberg, et. al., 36th ENC proceedings, Boston (1995).

INITIATION OF CHEMICAL REACTIONS IN LIQUID BY WEAK SHOCK WAVES

I.V. MASTIKHIN, V.S. TESLENKO, V.A. MOROSOV, G.S. ANANCHENKO, S.I. DIKALOV

International Tomography Center, SB RAS

International Tomography Center

Institutskaya 3a st.

Novosibirsk, 630090, Russia

Application of weak shock waves (SW) for localized initiation of chemical reactions in liquid has been studied. To this end, home-made generator of focused SW was used, parameters of SW are: pulse length is 0.5 mks, acoustic pressure in focus is 450 Bar, the focal zone dimensions are 1*1*5 mm. Samples were treated inside plastic 1ml cuvette. Generation of OH-radicals in distilled water by SW-pulses has been determined by ESR with spin traps; concentration of OH-radical was 0.1 mkM/l after 30 SW-pulses. Also decomposition of hydrogen peroxide by SW has been found. Initial acoustic energy of the weak SW even in the focus is at least 1000 times lower than it is necessary to break chemical bonds of compounds studied. The most probable mechanism of accumulation of SW-energy is "cavitation", that is, processes of appearance, pulsation and collapse of microbubbles of gas and vapour of the liquid. To investigate possible correlation of cavitation processes with peculiarities of spatial and temporal kinetics of chemical reactions initiated by SW, Bruker NMR microimaging unit (MSL-300) was used. Aqueous solution of hydrogen peroxide (1mM/l) and spin trap TEMPONE-H (2mM/l) was treated by SW-pulses. After decomposition of hydrogen peroxide (H2O2-->2OH) TEMPONE-H + OH --> TEMPONE - stable free radicals, i.e. paramagnetic centres, decreasing T1 of water protons. It let us study spatial dependence of free radical generation inside the SW focal zone. As another model reaction sensitive to SW, polymerization of acrylamide with ammonium dipersulfate as radical activator was studied. Changes of relaxation properties of water protons during polymerization were used. Single SW-pulse was applied to the aqueous solution of monomer to decompose the activator. After that, 8 CPMG 8-echo image sets were acquired, time delay between sets was 2 minutes, time of magnetization recovery was 0.5 s to enhance T1-contrast, spatial resolution - 100*100*600 mkm. "Proton density" maps were calculated. It was shown that polymerization after SW-pulse proceeds granularly and SW-initiation is the most effective near free surface of the solution. It can be explained by well-known fact of inversion of pressure wave into rarefaction wave on the free surface, that amplifies cavitation processes near boundaries. This assumption is confirmed by the optical map of cavitation dynamics acquired by super-fast photo shooting of SW.

NMR RELAXIVITY AND DIFFUSIONAL STUDIES OF WATER IN CONTACT LENS HYDROGELS

PATRICK McCONVILLE[#], JAMES M. POPE[#] AND JOSEPH W. HUFF*

[#]Centre for Medical and Health Physics, School of Physical Sciences
Queensland University of Technology
GPO Box 2434
Brisbane, Australia 4001
***Cornea and Contact Lens Research Unit**
School of Optometry and Cooperative Research
Centre for Eye Research and Technology
University of New South Wales
Sydney, Australia.

Purpose: Hydrogels, which are hydrated polymers, are used extensively today for soft contact lens manufacture, but have a tendency to dehydrate when placed on the eye, resulting in changes in fit, impaired oxygen transport and associated discomfort and damage to the corneal epithelium. The purpose of this study was to use NMR relaxivity and diffusional measurements to characterise the behaviour of water for a series of contact lens materials.

Methods: A range of commercially available contact lens hydrogels of known composition were cut and hydrated to equilibrium water content, at constant temperature. T_1 was measured as a function of water content at the on-eye temperature of 34.5°C and for temperatures in the range -30°C to 80°C, using the inversion-recovery technique. Similar measurements of T_2 were made using the Carr-Purcell Meiboom-Gill method.

Diffusion coefficient was also measured in this temperature range, and as a function of the diffusion measuring time, Δ, using both the Stejskal-Tanner spin echo technique and the stimulated echo (STE) technique.

Results: In general the relaxation times were found to be longer for higher water content materials. A plot of T_1 vs T_2 was found to separate different hydrogel materials, including those of similar water content. The temperature dependent relaxation behaviour of water was also observed to be highly material dependent, in the case of T_2 exhibiting both local maxima and minima over the temperature range studied. Relaxation measurements were also made as a function of water content during drying of the materials at 34.5°C. The data was not consistent with a simple 2-site chemical exchange model, incorporating 'bound' and 'free' water.

Diffusion coefficient (D) was found to be highly material dependent. Again a correlation with water content was observed for different materials. At long Δ the STE diffusion coefficient was effectively reduced, which was interpreted as evidence for cross-relaxation.

Discussion: The NMR data provided evidence that water proton relaxation and diffusion in contact lens hydrogels must be interpreted in terms of a model that incorporates chemical exchange and cross relaxation as well as a range of binding environments which themselves are hydration dependent. On the NMR timescale, these different states of water were not distinguishable, and $T_1/T_2/D$ are weighted averages over all binding states.

The NMR relaxation and diffusion behaviour was highly material dependent, with significant differences observed for *different* materials of the *same* water content. This is consistent with data in the literature for on-eye dehydration of contact lenses. Further NMR studies of this type should lead to a better understanding of hydrogel hydration, and ultimately a better means of predicting and controlling contact lens dehydration on the eye.

Natural convection and self-diffusion measurements by NMR

Ales Mohoric, Janez Stepisnik, Miha Kos, Gorazd Planinsic, Jadranska 19, 1000 Ljubljana, tel.: +386 61 1766591, fax.: +386 61 217 281, e-mail: ales@fiz.uni-lj.si, Department of Physics, University of Ljubljana

NMR has been widely used for the self-diffusion measurements [1]. In combinaton with NMR imaging, we can obtain the information on the self-diffusion coefficient space distribution [2]. However, when we measure slow processes, we need to use large gradient fields and the usual expressions, that take into account only one component of the magnetic field, have to be altered [3].

We have noticed that natural convection causes additional attenuation of the signal. This is clearly seen on the images taken. The first image shows spin density image and the second one shows an image taken with the double gradient pulse technique. On the image there are clearly visible shadows that grow as the gradient duration is increased. We think this is due to the convection effects in the liquid. We have made an image where the natural convection was suppressed with wadding. There are no shadows visible. Although the theory does not predict that stationary non-random velocity would have an effect on the amplitude of the signal but rather only on the phase of it, the summation of many, slightly phase shifted echoes, needed for noise reduction, would have the same effect. In addition the convection is not stationary and the summation of the amplitudes has the same effect as if the liquid would have different diffusion properties that we could describe with some effective diffusion constant D_{eff}.

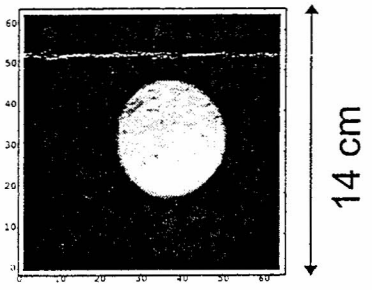

Fig.1: Image of a cylindrical phantom filled with ethanol

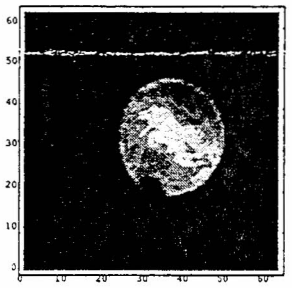

Fig.2: Image obtained after double gradient pulse preparation (200 ms, 1.2 10^{-4} T/cm)

Literature:

[1] N. Blombergen, E.M. Purcell and R.V. Pound, *Phys. Rev.*, **73** (1948) 679;
E.L. Hahn, Phys. Rev., **80** (1950) 580;
E.O. Steyskal, J.E. Tanner, *J. Chem. Phys.*, **42** (1965) 288;
H.C. Torrey, *Phys. Rev.*, **76** (1946) 1095; **104** (1956) 563;

[2] A. Mohoric, J. Stepisnik, 13. EENC, Paris, 1996;
J. Stepisnik, A. Mohoric, 12. EENC, Oulu, 1994;

[3] P.T. Callaghan, J. Stepisnik, *Phys. Rev. Lett.*, **75** (1995) 4532-4535;
J. Stepisnik, *J. Mag. Res.*, **107** A (1994) 167-172;
J. Stepisnik, *Z. Phys. Chem*, **190** (1995) 51-62;

PARTICLE COMPACTION AS OBSERVED BY MRI

R. A. WAGGONER,* M. NAKAGAWA,† J. GLASS,†† M. REECE,†* AND E. FUKUSHIMA**

***The Institute of Physical and Chemical Research(RIKEN), Saitama, Japan.**

†Colorado School of Mines
Golden, CO.

††, †*Sandia National Laboratories
Albuquerque, NM 87185.

****The Lovelace Institutes**
Albuquerque, NM 87108

The behavior of particles undergoing compaction is of interest in a variety of areas such as, ceramic engineering, civil engineering, and food processing. Ceramic components are often formed by compressing a ceramic powder in a die and then sintering. A non-uniform packing density of the green powder will result in differential densification during sintering. The resulting ceramic component will have less than optimum mechanical properties and it may require an additional processing step of machining to be usable. To better understand and control the compaction to produce more uniform packing densities, particle compaction has been studied by a variety of techniques such as mercury porisometry, ultrasound, x-ray radiography and microscopy. MRI offers the ability to image a sample at successive stages of compaction and, in particular, in model systems, it can resolve each individual particles. When individual particles are located, orientation of contacts can also be determined. The figure below shows 3D images of 3mm pharmaceutical pills in a cylinder at various stages of compaction as well as a plane out of the center of each image.

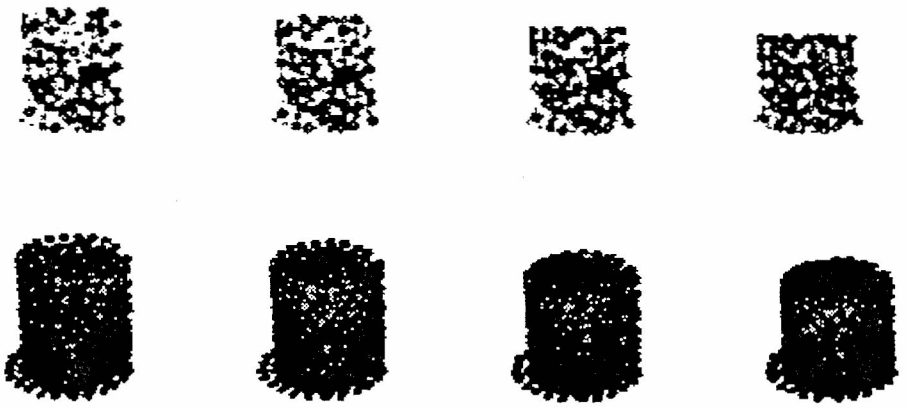

3D rendering and single planes from 3D images of compacted pharmaceutical pills.

EVALUATION OF MIXING PROFILES OF POWER LAW FLUIDS IN SCRAPED SURFACE HEAT EXCHANGER GEOMETRY USING MRI

W. WANG[†], J.H. WALTON[§], M.J. MCCARTHY[†] & K.L. MCCARTHY[†]
[†]Dept. of Food Science and Technology and [§]NMR Facility
University of California
Davis, CA 95616

The application of scraped surface heat exchangers in the food industry is varied, applications include continuous cooking of starch jellies, production of shortening, cooling of aerated marshmallow, and pasteurization of tomato paste. Mixing induced by the scraped surface heat exchanger promotes heat transfer and thus uniform cooking.

In this study we imaged the mixing of a fluid stream injected through the wall of a scraped surface heat exchanger. The apparatus consisted of coaxial cylinders in which a straight flight rotates with the inner cylinder and spans the annulus between the surfaces. Fluid doped with $MnCl_2$ to provide T_2 contrast was introduced upstream of the NMR coil while fluid was flowing in the axial direction through the rotating scraped surface heat exchanger. T_2 weighted images were used as a noninvasive method to evaluate mixing profiles in the angular directions down stream for the injection point.

The degree of mixing obtained at a fixed distance from the injection point increased with rotational speed and decreased with axial velocity. The power law fluid (CMC) had better mixing than did the newtonian fluid (corn syrup). Numerical simulations performed agree with our data.

STRAY FIELD IMAGING (STRAFI) AND MAGNETIC RESONANCE MICROIMAGING (MRM) STUDIES OF THE ANISTROPIC ABSORPTION OF SOLVENTS BY EXTRUDED POLYPROPYLENE

R.J. ABBOTT, J.A. CHUDEK, G. HUNTER, R.L. MACKAY, L. SQUIRES*, P.J. MCDONALD§

Department of Chemistry
University of Dundee
Dundee DD1 4HN, Scotland, UK
***Non-wovens Division**
Don and Low plc., Glamis Road, Forfar
Angus DD8 1EY, Scotland, UK
§Department of Physics
University of Surrey
Guildford GU2 5XH, England, UK

Introduction:

Isotactic polypropylene is a semi-crystalline thermoplastic whose worldwide production approached 22 million tonnes in 1995. It finds many uses and most of these involve either moulding or extrusion. Very rapid freezing occurs where a melt is in contact with a cooled mould or die, causing the polymer to retain a high degree of molecular orientation along the direction of flow. The core of the sample undergoes a much slower cooling, allowing randomisation of the polymer chains and the degree of orientation is therefore very much less. Between the two extremes of the well oriented skin layer and the randomly oriented core there exists a subsurface transition zone that has a high shear orientation and is often the site of mechanical failure [1]. In contrast to the core region, the undamaged skin layer is remarkably resistant to the absorption of normally good organic solvents and we have described a preliminary MRM study of polypropylene swollen by the anisotropic absorption of carbon tetrachloride into the extruded thermoplastic [2]. Solvent absorption occurred almost exclusively via the cut ends of the sample or where the surface had been deliberately damaged. STRAFI is a more general technique as it is able to image polymer components with both long and very short T2's [3] and it is therefore possible to observe both swollen polypropylene and those regions with low polymer backbone mobility.

Imaging Studies.

The samples studied were long cylinders of isotactic polypropylene (Shell grade KY 6100) which were the sprue associated with injection moulded blanks. As the mould is injected via such a sprue the samples can be anticipated to have a skin layer with a high degree of molecular orientation along the flow direction. One-dimensional STRAFI images (superconducting magnet nominal field 9.4T; fringe field accessed 5.6T; fringe field gradient 58Tm-1; solid echo pulse sequence; 250 micron slice thickness) were obtained for samples immersed in carbon tetrachloride, toluene. and cyclohexane. In the case of carbon tetrachloride the skin layer appeared to be almost totally resistant to solvent penetration, whereas for the others the skin proved to be only a temporary barrier, absorption occurring after a substantial initiation period. Nevertheless, even subsequent to the intiation period, the rate of solvent diffusion parallel to the melt flow was more than an order of magnitude greater than that normal to the flow direction.

[1] L.C. Sowyer and D.T. Grubb, "Polymer Microscopy", Chapman and Hall, London, 1987
[2] R.J. Abbott, J.A. Chudek, G. Hunter, and L. Squires, J. Mater. Sci. Lett., 15 (1996) 1108
[3] P.J. McDonald, Prog. NMR. Spectr., 30 (1997) 69

STRAY FIELD IMAGING (STRAFI) AND MAGNETIC RESONANCE MICROIMAGING (MRM) STUDIES OF HIGH IMPACT POLYSTYRENE, AN ELASTOMER-TOUGHENED MATERIAL

J.A. CHUDEK, G. HUNTER, F. MOHD. SOM, P.J. MCDONALD*, B. NEWLING*

Department of Chemistry
University of Dundee
Dundee DD1 4HN, Scotland, UK
***Department of Physics**
University of Surrey
Guildford GU2 5XH, England, UK

Introduction: High Impact Polystyrene (HIPS) is an example of an industrially-important thermoplastic composite material with much improved impact properties compared with brittle polystyrene[1]. It is produced by the polymerisation of bulk styrene monomer in the presence of about 8% by weight of dissolved polybutadiene (PB)[2] and consists of a polystyrene (PS) matrix in which are dispersed PB droplets which themselves include grafted and ungrafted PS domains1. The graft copolymer tends to accumulate at the interfaces, stabilising the heterogeneous mixture[3]. When HIPS is deformed, crazing is the dominant energy absorbing mechanism, usually beginning at the crack tip. However, the extent of stress-whitening does not give a satisfactory indication of the distribution of stress in this material as the craze bands are very diffused[3]. Stray Field Imaging (STRAFI) is able to image polymer components with both reasonably long (PB) and very short (PS) T2's[4] and by utilising the sensitive dependence of T2 on changes in the polymer chain mobilities it is possible to monitor reliably the distribution of induced stress within HIPS.

Imaging Studies: Samples of commercial HIPS, initially 3mm thick, were pressed in a hydraulic press. One-dimensional STRAFI images (superconducting magnet nominal field 9.4T; fringe field accessed 5.6T; fringe field gradient 58 Tm-1; solid echo pulse sequence ; 250 mm slice thickness) were obtained for an assembly of an unstressed piece and one pressed at 10 tonnes. T2 values were extracted from the biexponentially decaying echo trains and used to construct one-dimensional profiles. The boundary between the adjacent pieces was clearly delineated in the profile given by the longer T2 component (decreasing on compression from ~8 ms to ~5ms) but not in the profile given by the very short T2 component (constant at ~50 us), atttributed to the PS matrix. "Liquid" MRM images of the longer T2 component of a stack of 11 pieces of material (unstressed at the top, pressed at 10 tonnes pressure at the bottom) showed a sharp decrease in image intensity on moving from a compression of 1 to 2 tonnes, thereafter remaining constant on greater compression, despite a continuing decrease in sample thickness.

Conclusions: Deformation of HIPS clearly affects the molecular motions of the PB domain(s). However, it is also clear that at compressions of greater than about 2 tons either there is no remaining free volume in the PB domain(s) or that the physically entangled chains have been stretched to their maximum limits. In contrast, the molecular mobility of the PS region is unaffected by such deformation and remains very restricted at ambient temperature

1 C.B. Bucknall, "Toughened Plastics", Applied Science, London (1977)
2 J.L. Amos, Polym. Eng. Sci., 14 (1984) 1
3 I.S. Miles and S. Rostami, "Multicomponent Polymer Systems", Polymer Science and Technology Series, Longman Scientific and Technical (1992) Chp. 5
4 P.J. McDonald, Prog. NMR Spectr., 30 (1997) 69

INVESTIGATION OF BLOWING AGENTS IN INSULATING POLYMER FOAMS BY 19F MICROSCOPIC NMR IMAGING

C. A. FYFE, Z. MEI AND H. GRONDEY
Chemistry Department, University of British Columbia
Vancouver, B.C., Canada, V6T IZl

Currently, there is no reliable and readily accessible technique with which the distribution and diffusion of blowing agents in rigid insulating foams can be detected and monitored. In this paper, we demonstrate that ^{19}F NMR microscopic imaging together with ^{19}F solid state MAS NMR spectroscopy is ideally suited for such measurements and yield quantitatively reliable information which will be critical to the development and fabrication of optimized insulating materials with alternative blowing agents.

Polystyrene (PS) and polyurethane (PU) foam samples were investigated with the objective of determining quantitatively the amount of blowing agents in the gaseous phase and dissolved in the polymer phase, and to determine and monitor the distribution of the blowing agents in aged foams as a function of time and temperature. The concentrations of the gaseous blowing agents in the cells and dissolved in the solid were simultaneously and quantitatively measured by ^{19}F MAS NMR spectroscopy. An unfaced oneyear old PS foam filled with CH_3CF_2Cl has about 13% of total HCFC's dissolvcd in the solid; while there is about 24% of HCFC's in the solid of a faced 3-months-old PU foam filled with CH_3CCl_2F. The data from ^{19}F NMR imaging demonstrate that the distributions of the blowing agenls in an aged foam are quite uniform around the center part (2 cm away from any edge) of a foam board; however, a gradient in blowing agent concentration was found as a function of distance from the initial factory cut edge. The effective diffusion coefficients of the blowing agents can be directly calculated from the imaging data. Quantitative diffusion constants and activation barriers were determined.

Additionally, a foam treated with a second blowing agent was monitored with chemical shift selective imaging and the diffusion of the second gas into the foam and the outdiffusion of the original gas were determined.

NMR RELAXATION MEASUREMENTS ON SOFT MATTER BY THE NMR MOUSE

A. GUTHAUSEN
Institut fur Makromol. Chemie
RWTH Aachen, Worringer Weg 1
52054 Aachen, Germany

The NMR MOUSE (MObile Universal Surface Explorer) is a novel NMR device designed for relaxation measurements on surfaces of arbitrarily shaped samples. Both the B0 and the B1 magnetic fields are strongly inhomogeneous which can be used for measurements of self diffusion coefficients and also for obtaining spatially resolved images. The order of magnitude of the B0 gradients amounts to 10 T/m. Reexamination of pulse sequences known from conventional NMR is necessary because of the large field inhomogeneities. Favorable measurement schemes are steady-state sequences which use a dynamic magnetization equilibrium and multi echo sequences. Potential applications of the MOUSE are in the field of material science as well as in medicine. Elastomers are investigated representing the general class of soft-matter materials. The measurements reveal differences in cross-link density, local stress, and temperature. They also demonstrate the sensitivity of transverse relaxation to aging processes.

COMPARISION OF DIFFERENT NMR IMAGING SEQUENCES TO MAP MATERIAL PROPERTIES BY USING THE TRANSVERSAL RELAXATION IN POLYMER NETWORKS

UWE HEUERT, MANFRED KNÖRGEN, HORST SCHNEIDER
University Halle, dep. of physics
Friedemann-Bach-Platz 6
D-06108 Halle, Germany

"Material Properties Imaging" is often used to describe spatial resolved the properties of polymer networks. Such material properties are for instance lokal inhomogeneities produced by aging and swelling. One can get parameter images showing contrast in crosslink density and correlation times by fitting a set of images. But it is difficult to measure exactly the relaxation decay of each imaging pixel (voxel). In dependence on the applied model the function to fit the non-exponential decay can have up to 4 or 5 parameters. A good signal to noice and especially the accurate measuring of short echo time delays (less than 500 us) in combination with imaging is nessesary. The directly application of simple Fourier imaging is not possible because of switching and stabilization of gradients. Some pulse sequences without these problems are applicable. We will compare the results of the following experiments:

- T2-filter in combination with Fourier imaging and filtered backprojection,
- variation of the echo time with applied gradients in combination with filtered backprojection,
- combination of phase corrected profiles (short echo times) after the time-correct acquisition with magnitude profiles (longer echo times) in combination with backprojection.

All experiments were carried out on a self-made NMR microscope with active shielded gradient system (up to 50 G/cm) as an additional device of a Unity 400 from VARIAN.

THE INFLUENCE OF THERMAL AGING ON DIFFERENT FILLED ELASTOMERS SHOWN BY NMR MICROSCOPY

MANFRED KNÖRGEN, UWE HEUERT, HORST SCHNEIDER
University Halle, Dept. of Physics
Friedemann-Bach-Platz 6
D-06108 Halle, Germany

We investigated the aging course of a three dimensional sample space (filler, filler content and polymerisation of the basic polymer e- or s-SBR). The samples are placed at our disposal by Conti (Hannover). The thermal aging was done at a temperature of 150 °C in normal atmosphere and for a duration up to 1070 min. Besides the overall changing of the parameters releated to the elastomeric net- work (T2, anisotropy parameter q and other) we focus our attention on the occurence of local inhomogeneities, mainly the growth of surface layers. The experiments were carried out on a self-made nmr-microscope as an additional device of an unity 400 from VARIAN. The active shielded probe was able to produce a gradient up to 50 G/cm, which yields together with a line width of about 2kHz a limitation of the resolution of about 100um pixel size. The sample was cut in small pieces of about 5mm*3mm and a thickness of 0.5mm. All images were made without slice selection. It was secured, that one edge was an originally aged surface layer. The measurements were carried out at 60 and 20°C. Images for different echo times were aquired and backprojection was used. It was possible to fit for each image-point the relaxation decay in terms of a relaxation model based on a simple spin-pair-approximation and a gaussian-like distribution of the residual dipolar interaction. As a qualitative trend the growth of the surface layer during the aging course is observable in the parameter images. A histogram representation was choosen to realize a quantification of network changes besides the images. The result could be described with up to 4 fit-parameters:

- T2 (or a fast correlation time, which preaverages the dipolar interaction)
- q*M2 (q = anisotropy parameter, M2 = second moment of dipolar interaction).
- A (the part of the intercrosslink chains)
- B (the part of the dangling ends)

Among others one result of the investigations concerns a different aging course 0between the silica and carbon black filled sbr-samples:

- The second shows a distinct surface layer, growing with aging time.
- In opposite to this, silica filled rubber shows a more overall but even stronger changing of the network.

THE APPLICATION OF STRAY FIELD IMAGING (STRAFI) TO DENTAL MATERIALS SCIENCE

D. LANE*, S.N. SCRIMGEOUR[+], C.H. LLOYD[+], G. HUNTER[+], P.J. MCDONALD*

[+]Dentistry and Chemistry Depts
University of Dundee
Dundee DD1 4HN, Scotland.
***Department of Physics**
University of Surrey
Guildford GU2 5XH, Surrey, England.

Introduction. Dental materials science is a potential beneficiary from the development of stray field magnetic resonance imaging (STRAFI). Results from preliminary investigations are presented covering three areas of interest for restorative dental materials.

1. Visible light initiated polymerisation. Most dental restorative materials introduced in recent years rely upon visible light initiated polymerisation to convert a mouldable plastic putty into a rigid hard solid. A selection of differently shaded uncured composite pastes were packed into openended PTFE cylinders 6mm long and 5mm intemal diameter. The curing light was applied to one end for times ranging from 20 to 60 seconds. Specimens were stepped through the $58Tm^{-1}$ fringe field gradient, using a quadrature echo sequence to acquire ^1H signal in consecutive 100 μ m slices as described in previous STRAFI experiments[1]. Signal contrast was achieved between polymerised composite on the exposed surface and the remaining uncured composite at the other end of the cylinder. The cure front was found to extend over a small but finite distance. The "depth-of-cure" can be defined as the distance from the fully cured end to the half-maximum signal signal intensity difference at the cured / uncured interface. The depthof-cure was seen to increase with exposure time and with lighter shades. The change in relative polymer chain mobilities across the cure front has been determined by ^1H spin-spin T_2 relaxation analysis.

2. Absorption of liquid mixtures in cured materials. The polymer matrix in composite restorative materials may absorb liquids from saliva, drink and food. Some liquids have the potential to soften the polymer and thereby increase the wear rate of the filling to reduce its effective lifetime. A diacrylate resin used in some dental composite products was light cured under glass to form thin sheets 300 to 500 μ m in thickness. One surface on these sheets was exposed to ethanol: water mixtures. The solvent ingress was profiled using the frequency sweep surface coil STRAFI technique[2] in 24 μ m slices across the affected region. Solvent front displacement followed Fickian dynamics (i.e. varying as $t^{0.5}$) and increases with ethanol fraction in the mixture.

3. *Release of fluoride.* The application of fluoride to tooth surfaces is the comerstone of dental caries prevention policy. Tt is delivered as an addition to drinking water, in toothpaste and in restorative materials. Consequently, the ability to image fluoride is considered important in dental research. A feasibility study has been undertaken using STRAFI to determine the fluoride concentration in some glass polyalkenoate and related dental restorative materials. These materials were packed in glass cylinders then fully cured throughout the specimen. Relative fluoride concentrations as well as a measure of fluoride mobilities have been determined.

Conclusions. These preliminary results show the ability of STRAFI to provide non-destructive evaluation of curing and diffusion mechanisms in dental restorative materials as well as a method for determining the fluoride concentrations and release mechanisms. STRAFI offers a significant improvement in signal-to-noise ratio and spacial resolution on conventional magnetic resonance microimaging of dental materials[3].

1. D. M. Lane, P. J. McDonald Polymer 38 (1997) 2329.
2. P. M. Glover, P. J. McDonald, B. Newling *accepted* J Mag Res.
3. C. H. Lloyd, S. N. Scrimgeour, J. A. Chudek, *et al* Dent Mater 10 (1994) 128.

J-CROSS POLARIZATION ^{13}C EDITED IMAGING OF ELASTOMERS

A. SPYROS[1], N. CHANDRAKUMAR, R. KIMMICH
Sektion Kernresonanzspektroskopie
Universitat Ulm
Albert Einstein Allee 11,
89069 Ulm, Germany.

During the last few years NMR imaging has become an indispensable tool in polymer materials research. Elastomers are especially attractive, due to their intermediate behaviour, from an NMR point of view, in-between solids and liquids. The present report explores the use of J-cyclic cross polarization (CYCLCROP) for the acquisition of ^{13}C-edited ^{1}H images of elastomers in the solid state. This technique uses the ^{1}H - ^{13}C J-coupling to effect a cyclic ^{1}H -> ^{13}C -> ^{1}H transfer of magnetization through which all ^{1}H coherences of no interest are edited out. Its main advantages include the use of the large carbon chemical shift range that facilitates editing, and the increase in the signal to noise that stems from the cross-polarization magnetization transfer and the final acquisition of 'H images.

Imaging experiments were performed on a Bruker DSX-400 spectrometer using a double resonance microimaging probe (2.5 cm diameter), equipped with actively-shielded gradient coils. CYCLCROP was used to record 'H images of specifically the PI component in bulk samples consisting of PI and a second polymer. Natural abundance polyisoprene, PI, and ^{13}C enriched polyisoprene (54% enrichment at the C-δ position) were used for the imaging. ^{13}C enriched PI was intermixed with various types of polymers in the preparation of samples typically weighing 30-50 mg. ^{13}C-edited ^{1}H images of the PI component were recorded in this case that effectively map the distribution of PI in each sample. For reference, pure ^{1}H and ^{13}C images were also recorded. The calculation of difference images from ^{1}H and ^{13}C-edited ones provided images that map indirectly the distribution of the second component in the polymer mixture. The factors that affect the efficiency of cross polarization in elastomeric polymers were also investigated.

[1]A. S. is indebted to the Alexander von Humboldt Foundation for providing financial support through a research fellowship (ref. no: IV-1-7108-1027150)

APPLICATION OF IMAGING TO THE STUDY OF ENZYMATIC DEGRADATION OF POLY(β-HYDROXYBUTYRATE), A BIODEGRADABLE POLYMER.

A. SPYROS[1], R. KIMMICH
Sektion Kernresonanzspektroskopie
Universitat Ulm, Albert Einstein Allee 11,
89069 Ulm, Germany

NMR imaging is a powerful tool for material science research, especially in the field of polymers and polymer composites. The main advantages of NMR imaging are its inherent noninvasive character, and the variety of contrast mechanisms available to the NMR spectroscopist. In this report we present an application of ^{1}H spin echo NMR Imaging for the monitoring of enzymatic degradation of thin films of a biodegradable polymer, poly(β--hydroxybutyrate), PHB. The degrading enzyme was depolymerase B isolated from the bacterial species *Pseudomonas Lemognei* The sample was a PHB film (15 x 5 x 0.2 rnm) casted from the melt, and subjected to enzymatic degradation for various time intervals. Imaging experiments were performed on a Bruker DSX-400 spectrometer using a microimaging probe equipped with actively-shielded gradient coils. A standard ^{1}H spin echo imaging sequence utilizing a hard 180° refocusing pulse was used, without slice selection.

The polymer film was ~65% crystalline by DSC, so the ^{1}H images of the film, recorded at 20h degradation time intervals, are in effect maps of amorphous polymer distribution as a function of degradation time. The crystalline part of the film does not contribute to the image signal under the high resolution experimental conditions used in the present study. After 220h of degradation the film weight loss was 50%, while ^{1}H image loss was 70%. The ^{1}H imaging experiments showed that the depolymerase has a strong preference towards amorphous material at the beginning of the degradation process, which starts at the surface of the film. After about 120h of degradation amorphous and crystalline material is consumed at the same rate. Further studies using a variety of biodegradable polymers and enzymes are in progress. In conclusion this report describes the first and successful application of ^{1}H NMR imaging to the study of enzymatic degradation of biodegradable polymers.

[1]A. S. is indebted to the Alexander von Humboldt Foundation for providing financial support through a research fellowship (ref. no: IV-1-7108-1027150), and to Dr. Jendrossek, Institut fur Mikrobiologie, Georg-August Universitat Gottingen for providing the enzyme.

MONITOR DEGREE OF CURE OF CARBON/EPOXY COMPOSITES WITH THE NMR RELAXATION TIME T_2.

RONALD DEAN STODDARD
Washington University
Department of Physics - 1105
1 Brookings Dr.
St. Louis, MO 63130

New techniques for manufacturing carbon/epoxy aircraft components are under development which eliminate the need for curing in an autoclave. These techniques require partial pre-curing of the carbon/epoxy material before lay-up and it is critical to the mechanical properties of the manufactured component that the material is cured to the correct level. Presently, no effective method of in-situ (on-line) monitoring of cure exists. We demonstrate here that nuclear magnetic resonance (NMR) is a promising method for in-situ monitoring of cure. We show that the NMR transverse relaxation time T2 is very sensitive to changes in molecular motion induced by curing in the Hexcel 8552 and ICI/Fiberite 977-3 carbon/epoxy systems. We have also determined the relationship between T_2 measured at a known temperature and the degree of cure (DOC) for 977-3. This allows quantitative determination of DOC from T_2 measurements. We have also shown that changing the NMR measurement temperature changes the range of DOC values to which we are maximally sensitive. The thrust of this project is to develop a practical method for monitoring DOC of carbon/epoxy systems on-line, as they are cured.

NMR IMAGING OF MECHANICALLY TREATED POLYMERS

B. TRAUB, D. MARING, S. HAFNER, H. W. SPIESS
Max-Planck-Institut für Polymerforschung
Ackermannweg 10
55128 Mainz, Germany

Mechanical deformation of polymers leads to structural changes on the macroscopic as well as on the microscopic length scale. Parameter-selective NMR microscopy allows the investigation of both: the macroscopic changes can be visualized by imaging, whereas the microscopic material properties are mapped via spectroscopic or relaxometric parameters.

In this contribution the applicability of NMR microscopy to the investigation of mechanically affected polymers is demonstrated and the resulting images are compared with polarisation microscopy and Small Angle X-ray scattering (SAXS). Standard Fourier imaging methods and the more sophisticated magic-echo multipulse imaging methods were applied to different polymer materials.

The first investigated system is a PS-PI-Blockcopolymer with lamellar orientation. The local orientation of the lamellas can be changed by periodically shearing the sample. The different orientation-angles of the lamellas relative to the static B0-field result in typical frequency shifts in the 1H-spectrum. This can be exploited by mapping the orientation distribution using 2D chemical shift imaging. Comparison with 2D SAXS measurements shows a good correspondence between both techniques.

The second part of this contribution concentrates on rigid polymers. As previously shown, the mechanical stress distribution in polycarbonate can be mapped as T2e-relaxation time contrast. In order to overcome the broad lines magic-echo imaging sequences are applied. Phase- and frequency encoding techniques are combined to generate 2D parameter images. This technique is applied on a series of samples which have been prepared under different drawing conditions. Polarisation microscopy images are presented for comparison.

References:

(1) F. Weigand, S. Hafner, H. W. Spiess, J. Magn. Reson. A 120, 201-205 (1996)
(2) S. Hafner, B. Traub, F. Weigand, H. W. Spiess, Extended Abstracts - 28th Congress Ampere, 1.-6.9. 1996, Canterbury, p. 390-391

SINGLE POINT MR MEASUREMENTS OF GRADIENT WAVEFORM

B.J. BALCOM, M. SHEA, S. D. BEYEA
MRI Centre, Department of Physics
University of New Brunswick
Fredericton, NB, E3B 5A3, Canada

Modern high speed imaging methods and in vivo spectroscopy methods demand high speed precision gradient switching. The time varying magnetic fields of the gradient pulse induce eddy currents in surrounding conductive materials and thereby create transient secondary magnetic fields. Time varying gradient fields may be present during data sampling leading to loss of signal, imperfect rephasing of echoes and distorted images or spectra. It is important to have control over, or precise knowledge of, the gradient waveform so that undesired artifacts can be minimized. Despite the advent of active gradient shielding it appears that gradient preemphasis is usually required to improve gradient performance. We have developed a simple single point MR method of determining the complete gradient waveform. This method provides a simple means of checking gradient performance. It will permit rapid interactive or automatic adjustment of gradient preemphasis. It should permit precise determination of gradient waveforms employed in spiral scan and EPI imaging to facilitate retrospective k space data regridding to improve image quality.

We have previously employed a Single Point Imaging method of determining the gradient waveform (1) . This method is slow (several minutes) and assumes that the time constant of the switched gradient does not vary with the gradient amplitude. Our new method suffers from neither of these limitations. The method relies on broadband RF excitation of a simple linear gel phantom offset from the gradient origin in the magnet. The phase of the MR signal acquired 30 - 50 usec after the RF pulse must depend on the gradient time history during the short phase encoding interval. The signal phase, in fact, is directly proportional to the average gradient during the 30-50 usec encoding interval. The RF pulse, phase encode, single point acquisition triplet is repeated throughout the gradient pulse. The gel phantom is heavily doped to permit multiple acquisition points during each gradient pulse. Repetitive gradient pulses with offset, interleaved acquisitions permit high temporal resolution of the gradient waveform.

1. B. J. Balcom, M. Bogdan, and R. L. Armstrong J. Mag. Reson. A 118, 122 (1996).

THE ANALYSIS AND DEVELOPMENT OF PULSE SEQUENCES FOR SELF DIFFUSION WEIGHTED STRAY FIELD IMAGING

A.J. BOHRIS*, D.A. FAUX*, D.G. GILLIES+ AND P.J. MCDONALD*

Departments of *Physics and +Chemistry
University of Surrey
GU2 5XH, UK

Stray field magnetic resonance imaging[1] and self diffusion analysis[2] techniques are increasingly used to image broad line systems such as cementitious materials and polymers and to measure small diffusion coefficients in systems such as polymer melts respectively. Both the imaging and diffusion applications exploit the extremely strong and stable magnetic field gradients found around high field superconducting magnets. One drawback of these methods is that the gradient cannot be switched off during the radio frequency pulses. Consequently, all the applied pulses are spatially selective. In multiple pulse sequences a large number of coherence pathways are excited and complex phase cycling is required to eliminate signals from unwanted pathways. Another drawback is that the gradient strength cannot be varied so that in diffusion sequences the pulse gaps are the only available means to vary the scattenng vector, **q**. Moreover, unless a second magnet operating with a centre frequency equivalent to the stray field frequency of the first is available, comparative measurements cannot be made in the absence of the gradient. This means that spin relaxation must be carefully and fully accounted for in the diffusion analysis. Careful pulse sequence analysis is therefore required before any new sequences can be used with confidence.

This paper presents a Fourier method of solving the Bloch equations for nuclear magnetisation precession in a strong magnetic field gradient which has been developed for the purpose of simulating the increasing number of pulse sequences now used in stray field experiments. The simulation explicitly includes the action of the gradient during the pulses and the effects of spin relaxation and diffusion.

We show here the application of the simulation to the analysis of a multiple echo diffusion sequence which is designed to offer a spatially resolved one shot (multiple **q**; near constant diffusion time, Δ measurement of self diffusion in the stray field. A rapid one shot method is required because stray field imaging is inherently slow since the measurement must be repeated at each spatial location.

The developed sequence is $(\alpha_x \tau_1)$ - 90_y - (n direct echoes, τ_2) - 90_y - (n stimulated echoes) where α is a low flip angle pulse. The sequence is an adaptation of standard simulated echo[3] and DANTE[4] type sequences. Following Kimmich and Fischer[5], the diffusion coefficient is evaluated from the ratios of the direct and stimulated echo intensities so that the measurement is independent of T2 relaxation. Moreover, so long as $\tau_2 >> n\tau_1$, T_1 relaxation enters only as a constant factor which need not be known. The analysis will be compared with experimental measurements of model systems.

1. A.A. Samoilenko, D.Yu. Artemov and A.L. Sibel'dina, *JETP Lett.* (1988) 47, 348.
2. R. Kimmich, W. Unrath, G. Schnur and E. Rommel, J. *Magn. Reson.* (1991) 91, 136.
3. J.E. Tanner, J. Chem. Phys. (1970) 52, 2523.
4. G.A. Morris and R. Freeman, J. *Magn. Reson.,* (1978) 29, 433.
5. R. Kimmich and E. Fischer, J. *Magn. Reson. A,* (1994) 106, 229.

GENERALISED TREATMENT OF MODULATED GRADIENT SPIN ECHO ATTENUATION FOR RESTRICTED DIFFUSION IN SPHERICAL PORES

SARAH L. CODD AND PAUL T. CALLAGHAN
Department of Physics
Massey University
Palmerston North, New Zealand

A simple matrix formalism presented by Callaghan(1), and based on the multiple propagator approach of Caprihan et al (2), allows for the calculation of the echo attenuation, *E(q),* in spin echo diffusion experiments, for practically all gradient waveforms and for the case of restricted diffusion in enclosing pores, with or without wall relaxation. The generalised gradient waveform is dealt with by breaking it into discrete time intervals and the narrow pulse approximation of the PGSE q-space diffraction is retained for each time interval. This leads to the gradient waveform being represented by a series of sharp equally spaced gradient impulses with appropriate amplitudes. *E(q)* is then expressed as a product of matrix operators corresponding to the spin phase evolution and Brownian diffusion in each time interval. Previously Callaghan used this method to evaluate the finite width gradient pulse PGSE and CPMG pulse trains for the case of restricted diffusion between parallel reflecting plates. The method has now been applied to the more useful case of restricted diffusion in spherical geometries. Using the known eigen-expansions, the three matrices,

$$A_{kk'}(q) = \int dr\, u_k^*(r) u_{k'}(r) \exp(i2\pi q \cdot r)$$

$$S_k(q) = V^{-1/2} \int dr\, u_k(r) \exp(i2\pi q \cdot r)$$

and $$R_{kk} = \exp(-\lambda_k \tau)$$

have been calculated. The finite width gradient pulse PGSE experiment has been evaluated and compared with published simulations (3). However these three matrices are all that is required to evaluate any generalised gradient waveform. Another application which requires generalised formalism is that of multiple gradient pulse CPMG trains. These provide access to the frequency domain of molecular translational motion. The echo attenuation for such experiments have been calculated. Many systems can be modelled using restricted diffusion in spherical pore geometries. Experiments on model glass bead systems have begun.

[I] P.T. Callaghan J. *Magn. Reson.* (submitted)
[2] A. Caprihan, L.Z. Wang and E. Fukushima, J. *Magn. Reson,* A118, 94(1996)
[3] P. Linse and 0. Soderman, J. *Magn. Reson.,* A116, 77(1995)

Novel, Asymmetric Gradient Coil Sets for MRM

Stuart Crozier, Wolfgang U. Roffmann and David M Doddrell

Centre for Magnetic Resonance,The University of Queensland
St. Lucia Qld 4072 Australia
ph +61 7 3365-4100
e-mail stuart.crozier@cmr.uq.edu.au

In the vertical bore magnets typically used for MRM, space is at a premium. Usually gradient sets are quite long in these systems. For rat and mouse neural imaging, however, it is often preferable to use as large an animal as possible, and though the brain is the organ for imaging, it is the thorax that delimits the space. We have, therefore, developed an asymmetric gradient set that does not restrict the thorax of the subject. Asymmetric transverse gradient designs have been presented for MRI neural imaging applications (1-3) and are quite well understood, their major design challenge being to balance the torque inherent in their design. This proves to be more difficult in MRM as the torque is heavily dependent on the magnet in which the gradients reside and the dsv's of MRM magnets are typically quite small. Results are presented for torque balanced MRM transverse gradients.

The more novel aspect of this work is the design of asymmetric Gz gradients. In MRI head gradients symmetric G_z coils are typically used. We present designs for G_z coils where the linear region is very close to one end of the coil, importantly B_0 components must be minimized in such designs. Figure 1 shows the experimental results from a prototype coil measured using a pick-up coil. We will show that these results match theory very well.

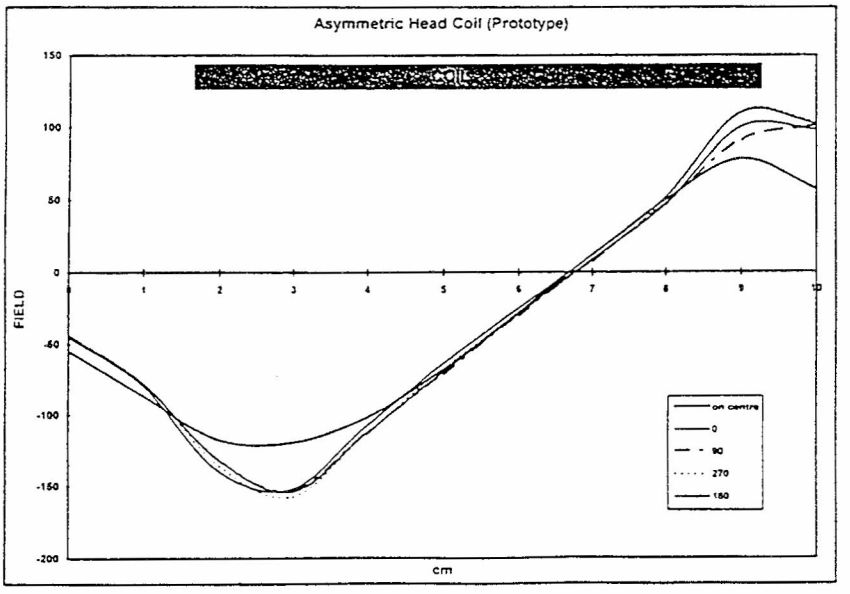

Figure 1. Measured field pick-up from an asymmetric Gz coil. The coil radius was 31mm.

Diffusive Edge Enhancement in NMR Microscopy

Andrej Duh[(#)], Janez Stepišnik[(*, +)], Aleš Mohorič[(*)], Igor Serša[(+)]

Institute of Mathematics and Physics, University of Maribor, Faculty of Electrical Engineering and Computer Science, Smetanova 17, 2000 Maribor, Slovenia, Phone: +386 62 221 112, e-mail: andrej@fiz.uni-lj.si
* Physics Department, University of Ljubljana, Jadranska 19, 1000 Ljubljana, Slovenia
+J.Stefan Institute, Jamova 39, 1000 Ljubljana, Slovenia

The molecular restricted self-diffusion that tends to attenuate the NMR signal at PGSE is responsible for the effect of edge enhancement in NMR imaging. At the boundaries there is less attenuation due to the spin motion and in certain circumstances could cause an enhancement of boundaries in NMR images. The idea was proposed and demonstrated theoretically by Putz *et al.*[(1)]. It was first experimentally confirmed by Callaghan *et al.*[(2)] and de Swiet[(3)] has provided an extensive quantitative theory of the effect solving the Torrey equation. We have derived[(4, 5, 6)] a precise explanation of the spatial distribution of the attenuation for motion restricted by boundaries. We have expanded a non-uniform spin phase distribution into series of waves that characterize geometry and boundary conditions of confinement. Random motion disrupts the initial phase structure and discords the waves. In the slab geometry the echo signal has the following spatial distribution:

$$E(x,\tau) = \exp[-iFx]\sum_{n=0}^{\infty} a_n(F)\exp\left[-\frac{1}{2}\left(\frac{n\pi}{l}\right)^2 R_F^2(\tau,x)\right]\cos\left[\frac{n\pi}{l}x\right],$$

where $a_n(F)$ is the q-space domain Fourier transform of spin phase distribution and $R_F(\tau,x)$ is an average diffusion length along gradient in time τ at site x.

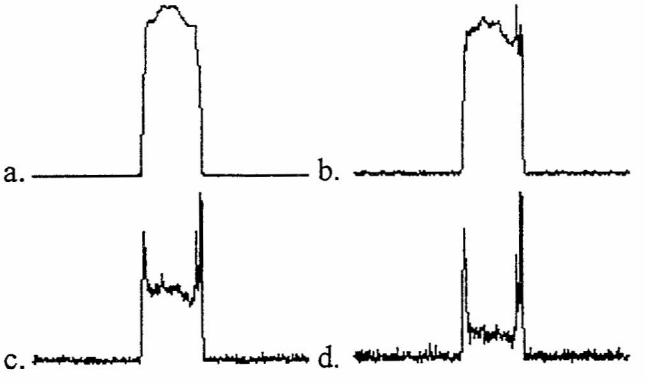

On the images above we draw measured cross-sectional NMR images of water slab with wall-to-wall dimension l = 2.8mm (a. τ = 35ms, magnification = 1, b. τ = 70ms, magnification = 36, c. τ = 78ms, magnification = 87, d. τ = 85ms, magnification = 186).

References:

1. B. Putz D. Barsky, and K.Shulten, J. Mag. Reson. **97**, 27 (1992)
2. P. T. Callaghan, A. Coy, L.C. Forde and C.J. Roffe, J. of Mag. Res. A101, 347, (1993).
3. T.M. de Swiet, J. of Mag. Res. B109, 12, (1995).
4. J. Stepišnik, 28th Congress Ampere, Canterbury, 1996, Book of extended abstracts, p. 91-92
5. J. Stepišnik and A. Duh, EENC 96, Paris 1996, Book of Abstracts p. 361.
6. J. Stepišnik, J. of Mag. Res. (to be published)

NONGRADIENT NMR IMAGING OF SOLID POLYMERS

K.V. ERMOLAEV, N.N. VOLKOVA, V.A. DUBOVITSKIJ AND L.N.EROFEEV

Dimensional effect in polymer films that involves the dependence of chemical properties vs thickness of the film is of great importance for polymer and material sciences. Local NMR study of the dimensional effect in epoxy films requires spatial resolution of 100 - 200 mm for samples whose T2 does not exceed 30-50 ms. To produce magnetic field gradients needed for such measurements is a complex technical problem. Moreover, spatially resolved spectra provided by conventional NMR imaging techniques are typically obtained by decoding procedures that can distort fine features of the spectrum. The application of non-gradient NMR imaging i.e., imaging that does not require external field gradients makes it possible to perform experiments on any NMR spectrometer and provides accurate spectral information. We report an ingenious technique of NMR imaging in stray RF field that provided resolution of 200mm in epoxy samples with linewidth of 20 - 30 kHz without any spectral distortion. The spatial distribution of residual mobile polymer phase whose concentration does not exceed 3% has been studied. Another approach to local NMR study of polymer layers in the vicinity of surface is application of surface coils. The resolution provided by such a coil is defined by the coil size and can hardly be better then a few millimeters. Reconstruction of a low resolved pattern by a 2D version of histogram procedure [1,2] based on the optimal integral representation method has been simulated. Nearly 10-fold improvement in resolution has been achieved for the signal-to-noise ratio of 5%.

References

1. K.Ermolaev, V.Dubovitskij, and L.Erofeev, Extended Abstracts of the XXVII Congress AMPERE, Kazan, August 1994, p.703.
2. V.A.Dubovitskij and K.V.Ermolaev, Zh.Fiz.Khim, 1996, v.70, N7, pp.1233-1238.

A REAL TIME NMR IMAGE RECONSTRUCTION-DISPLAY SYSTEM USING A HIGH-SPEED PERSONAL COMPUTER

TOMOYUKI HAISHI, KATSUMI KOSE

Institute of Applied Physics, University of Tsukuba

Tsukuba, Ibaraki 305, JAPAN

We describe a real-time NMR image processing device which can be easily added on to an existing NMR imaging system. It is based on the Intel family of personal computers and the Windows 95 operating system. The system is flexible, can be easily programmed by users, and is of low cost. In comparison to our previous work, this work achieves faster processing times by using a 32-bit C++ compiler, it improves on the image display technique and uses the multi-tasking capabilities of the Windows 95 operating system to let the users perform other tasks during a real-time imaging experiment. The system was evaluated on three typical high-speed NMR imaging techniques - FLASH, single-shot EPI, and multi-shot EPI. For a 128x128 FLASH image acquired on a 200 MHz Pentium computer with an ISA bus based A/D board, the data transfer time to the PC memory was 66 ms, the image reconstruction time was 48 ms, image display time after expansion to a 256x256 matrix was 8 ms, and the mean transfer time to the hard disk was 3 ms. System performance was compared with the Pentium processor operating at different speeds from 75 MHz to 200 MHz and between the Pentium and the Pentium-pro family of micro-processors.

THE NMR-ENDOSCOPE

R. HAKEN, P. BLÜMLER, B. BLÜMICH
MARC, Magnetic Resonance Center
Worringerweg 1
D-52056 Aachen, Germany
BIOMAT, Interdisciplinary Centre for Clinical Research
RWTH Aachen, Germany

Minimal invasive surgery guided by NMR techniques are receiving increasing attention in medical applications. It can be realized in standard and preferably „open" magnets. NMR im-ages, which are displayed on-line on a screen, are used to follow the process. The NMR endo-scope is an diagnosis instrument, which allows the surgeon to gain specific local information about tissues, body liquids, implants, etc.

The NMR probe consists of a flexible shaft with a micro coil at the tip. The coil is part of an rf resonant circuit and is used as a surface coil for NMR experiments. By relaxation and spec-troscopy experiments one can get additional information during minimal invasive surgery. Analogous to NMR imaging in a medical tomograph the endoscope can be employed to obtain images close to the micro coil by the application of appropriate pulse sequences. High sensitiv-ity and good spatial resolution due to an excellent filling factor are further advantages of such micro coils in comparison with standard surface and whole body-coils.

Instruments used in NMR-guided surgery have to ensure reliable positioning, which means, that they need to be detected in an NMR image without serious disturbance of the imaging process. To facilitate the visualization the endoscope is equipped with a switchable marker.

For use independent from a tomograph in medical offices the endoscope will be provided with permanent magnets. With its own static magnetic field the probe becomes a transportable NMR instrument for medical diagnosis. A first prototype of the NMR endoscope has been realized and tested. Exploration of clinical application is in progress.

Analytical gradient coil design: A practical approach towards optimized construction of NMR microscopy systems

R. Kimmlingen, H. Adolf and A. Haase

Physikalisches Institut, Universität Würzburg, 97074 Würzburg

Introduction

In order to take advantage of fast NMR imaging methods optimized gradient coil systems are required. For this purpose a versatile analytical design method [1] has been developed in our group. The design is verified with numerical computations and the construction of a prototype for microscopy applications.

Methods and materials

It has been shown that the current density on a cylinder surface can be expressed in terms of *Bessel Functions* [2]. An optimization formalism is applied introducing Langrange Multipliers for inductivity and homogeneity. As a result, simple analytic expressions describing gradient coil characteristics can be derived. The prototype parameters were chosen such that comparison with the *Bruker BG-60* microscopy system is possible.

Theoretical values for gradient strength and homogeneity were verified using MAFIA, a program package for finite elements computation.

Fig. 1 shows a contourplot of the new systems X-Gradient ($\partial B/\partial x$). Deviations from reference gradient strength are less than 10% within the area enclosed by the innermost contours.

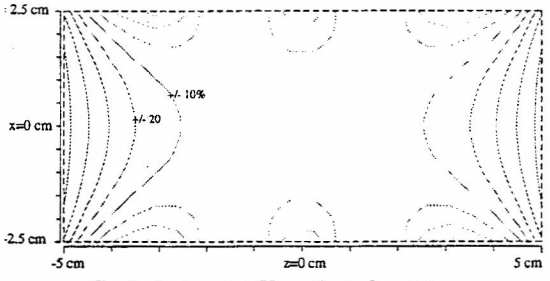

Fig. 1: Contourplot: X-gradient of prototype

Wire patterns and positions were generated from contourlines of the *Stream Function*, which is the integral of the current density. One quadrant of a cylinder surface pattern can be seen in fig. 2.

Fig. 2a: Etching pattern

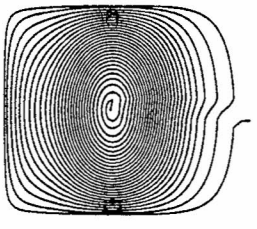

Fig. 2b: Milling map

The Z-coil of the new system was fabricated using copper wire glued to suitably milled grooves on a tube of epoxy-glass resin (GFK). Wire patterns for transversal gradients were etched on double sided copper foil, which was glued to the coil body afterwards. The new coil geometry is identical to the *Bruker BG-60*, which has an inner diameter of 60 mm. Both coils are used inside the 190 mm bore of a 7 T *Bruker* BIOSPEC magnet.

Results

The properties of the new gradient were compared to the *BG-60* using a cylinder phantom filled with water. A gradient echo image of the phantom (Fig. 3) shows the improved homogeneity of the new coil. In order to achieve an equal FOV, the amplifier current for the prototype had to be 12% higher. Experimental results for gradient efficiency are 7.01 ± 0.04 (theory: 7.55) mT/Am in comparison to (8.00 ± 0.04) mT/Am for *Bruker BG-60*.

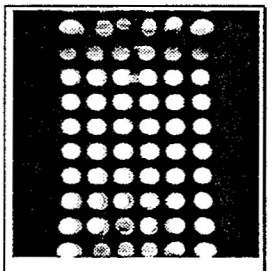

Fig.3a: Bruker BG-60

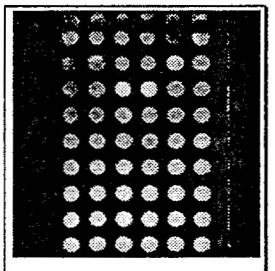

Fig.3b: Prototype

Discussion

It is shown that the presented design technique delivers results which allows construction of a coil for imaging applications. Measured and simulated properties (gradient strength, homogeneity, inductivity) correspond well with theoretical predictions. Deviations caused by approximation of the continous current density and fabrication errors are less than 10%.

Due to the applied foil technique, the new system resistance is four times higher than the *Bruker BG-60*, which limits (uncooled) operation to low gradient strengths ($I < 50$ A). A second prototype solving this problem is under construction. It contains wire patterns milled on the surface of Cu/GFK tubing using a CNC-machine.

References

[1] H. Adolf: *Dissertation*, Würzburg, 1996

[2] R.Turner, *J.Phys. E:Sci.Instrum.* **21**, 948-952, 1986

PHYSICAL AND COMPUTATIONAL MODELS FOR MAGNETIC RESONANCE IMAGING BY POPULATIONS

JOHN J. LEE[1], DAVID J. SCHNEIDER[2], JACK H. FREED[3], PAUL C. LAUTERBUR[1]

[1]Biomedical Magnetic Resonance Laboratory,
University of Illinois at Urbana
Champaign, Urbana, IL 61801
[2]Cornell Theory Center,
Cornell University
Ithaca, NY 14853
[3]Baker Laboratory of Chemistry,
Cornell University
Ithaca, NY 14853

Keywords: MRI, Relaxation, Self diffusion, Stochastic liouville forms, Operator splitting, Krylov-space methods.

Conventional methods of MRI suffer significant losses in sensitivity and resolution with the presence of sharply varying magnetic fields and rapid self diffusion. Encoding and decoding spatial information normally depends largely upon the persistence of spin coherences in the presence of controlled field gradients, but diffusion-induced dephasing destroys this information content. The physical basis for diffusive dephasing has b~en known since Hahn's discovery of its effect upon spin echoes. It is noteworthy that the underlying physics allows for much longer lifetimes for spin populations. As we shall suggest below, this may be put to good use for enhancing imaging. We re-examine conventional methods of magnetic resonance imaging (MRI) and take care to evaluate the dynamics of spin populations as compared to spin coherences. We briefly sketch a generic, physically motivated model of MRT which employs populations to encode and decode spatial information. We also present a corresponding computational model which treats in detail the salient spatio-temporal dynamics. We comment on issues of stability, accuracy and efficiency.

Acknowledgements: This work received financial support from the NIH, Biornedical Research Technology Grant PHS 5 P41 RR05964, the Illinois Department of Commerce and Community Affairs, No. 92-82144, and the Servants United Foundation. JJL also acknowledges support as a GAANN Fellow in Com.plltational Biology through the U. S. Department of Education and as a Hazel I. Craig Fellow at the University of Illinois at Urbana-Champaign. This work made use of computing resources at the Cornell Theory Center, which is one of four high performance computing and communications centers supported by the National Science Foundation. Activities of the center are also funded by New York State, the Advanced Research Projects Agency, the National Center for Research Resources at the National Institutes of Health, IBM, and other members of CTC's Corporate Partnership Program.

OXYGEN-17 MRI AND MRS: OLD AND NEW

G. D. Mateescu
Department of Chemistry, Case Western Reserve University
Cleveland, Ohio 44106, USA

There are ten years since the publication of the first oxygen-17 magnetic resonance images (OMRI).[1] For those new to the "Heidelberg Conferences," the first part of the lecture will consist of a brief historical outlook highlighting some of the most important applications: *in vivo* determination of the rate of oxygen consumption (mitochondrial metabolism);[2-4] combined $^{17}O/^{31}P$ MRS for investigation of factors leading to degenerative diseases (Alzheimer, Parkinson, ischemic heart, late onset diabetes, aging);[5] performance of time release porous polymers; *in vivo* temperature determination.[6] Work in progress, within the frame of a project entitled "Fundamental Chemistry of MRI" will be reported in the second part. In particular, preliminary results on water diffusion through protein gels demonstrate the unique tracer property of ^{17}O. As seen in the Figure, a simple time dependent measurement in a selected gel slice can yield diffusion coefficients for the displacement of water within the protein column ("water chromatography"). We are currently collecting comparative data with pure gelatin and gels containing various amounts of sugars and phosphates. Washout experiments show that there are, indeed, water molecules so tightly bound, that they have very long residence time. This may explain our previously reported results which show comparatively higher ^{17}O-labeled metabolic water concentration in tissues with higher oxygen consumption (e.g., brain). This will be illustrated with ^{17}O-images of larvae after breathing ^{17}O-enriched air. Quite surprising results are obtained in experiments on proton hydration in hydrophobic media. Specifically, in a heterogeneous system comprising $H_2{}^{17}O$ monomers dissolved in chloroform and bulk $H_2{}^{17}O$ on the walls of the nmr tube, proton (HCl) hydration yields, over an unexpectedly long time scale, a series of time dependent spectra that may be assigned to a number of stable and metastable hydration clusters. Thus, correlation with gas-phase hydration becomes possible.

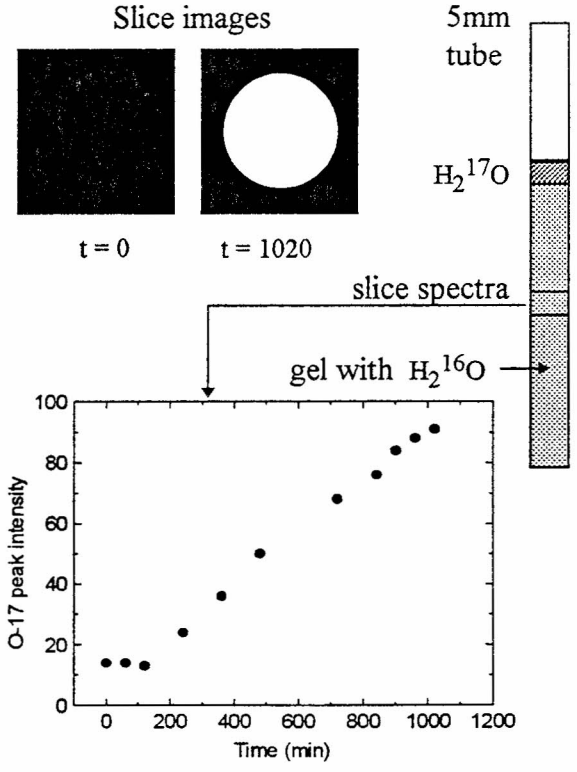

References

1. Mateescu GD, Yvars GM and Dular T, SMRM **1987**, *6*, 929.
2. Mateescu GD, LaManna JC, Lust WD, Mars L and Tseng J, SMRM **1991**, *10*, 1031.
3. Pekar J, Ligeti L, Lyon R, Ruttner Z, Gelderen vP, Moonen C, Fiat D, McLaughlin AC, SMRM , **1991**, *10*, 302.
4. Fiat D, Dolinsek J, Hankiewicz J, Dujovny M, Ausman J, Neurol. Res., **1993**, *15*, 237-248.
5. Mateescu GD and Fercu D, Adv. Exp. Biol. **1994**, *361*, 234.
6. Mateescu GD and Cabrera ME, Adv. Exp. Biol. **1997**, *411*, 585-590.

RELAXATION-DIFFUSION PROCESSES AND LOCAL MAGNETIC FIELD DISTRIBUTIONS IN NATURAL POROUS MEDIA

DELIA PEREZ, ALFONSO BENAVIDES* AND MIGUEL MARTIN-LANDROVE

Departamento de Fisica and Centro de Resonancia Magnetica
Facultad de Ciencias, Universidad Central de Venezuela,
A.P. 47586, Caracas 1041-A, Venezuela and
***Instituto de Ciencias de la Tierra**
Facultad de Ciencias, Universidad Central de Venezuela
A.P. 47586, Caracas 1041-A, Venezuela

In heterogeneous systems, it is well known thet the transversal relaxation rate is dependent on the time spacing between rf pulses in a CPMG experiment, due to the quenching of different relaxation channels. Particularly in sedimentary rocks there has been some evidence of strong relaxation rate dispersion possibly associated to resticted diffusion through the porous material. In the present work we developed a simple method to determine the evolution of the mean local magnetic field by the careful measurement of the spin-echo signal for different time spacing. The experiments were performed for different echo times and time spacing so a two dimensional array of data could be obtained for each sample. Proper analysis of the experimental data showed a general tendency of the average second moment to decrease with the time spacing and to propose a simple model to describe this particular trend. For short time spacing the experimental data showed a behavior possibly related to the spatial correlation between grains in the sedimentary rock. Some numerical simulations were performed to quantify the experimental results.

GAS PHASE IMAGING USING A RAPID SPI METHOD (SPRITE)

P.J. PRADO, B.J. BALCOM AND R.L. ARMSTRONG
MRI Centre, Department of Physics
University of New Brunswick
Fredericton, NB, E3B 5A3, Canada

Assessment of density distribution for dilute systems such as noble gases has been achieved by hyperpolarization of the specimen prior to MR imaging (1). For long T_1 relaxation times, the spin polarization increment yields a considerable SNR improvement.

Due to spin rotation relaxation, and wall collisions most gases present short MR relaxation times. This will quickly deplete any non-equilibrium hyper polarization. Furthermore, non-adsorbed molecules in porous media typically have fast relaxation mechanisms which limit T_1 to the order of several msec and T_2* to hundreds of μ sec. Such systems require a non-standard imaging method. We have implemented a time efficient Single Point Imaging (2) pulse sequence (Single Point Ramped Imaging with T_1 Enhancement, SPRITE) with a stepwise field gradient evolution (3) that allows us to visualize fluorine and proton distribution for a series of gases (chlorodifluoromethane, freon, benzene and methane). In addition, we study the adsorption of benzene in zeolites by observing fast relaxation components that are otherwise invisible to regular imaging procedures. These methods are also applicable to the determination of lung volume as will be outlined in the presentation.

1. M.S. Albert, G.D. Cates, B. Driehuys, W. Happer, B. Saam, C.S. Springer Jr and A. Wishnia, Nature 370, 199 (1994).
2. S. Gravina and D.G. Cory, J. Mag. Reson. B 104, 53 (1994)
3. B.J. Balcom, R.P. MacGregor, S.D. Beyea, D.P. Green, R.L. Armstrong and T.W. Bremner, J. Mag. Reson. A 123, 131 (1996)

Fast spatially resolved displacement-imaging in (bio)systems

T.W.J. Scheenen, D. van Dusschoten, P.A. de Jager, H. Van As
Wageningen Agricultural University
Dept. of Molecular Physics
Dreyenlaan 3, 6703 HA Wageningen, The Netherlands

Flow and/or diffusion in heterogeneous (bio)systems can be measured with Pulsed Field Gradient (PFG) experiments. In a PFG experiment two magnetic field gradient pulses of duration δ and of amplitude G, separated in time by Δ, applied to an ensemble of spins result in an echo attenuation of the NMR-signal. This attenuation of the signal is caused by a randomly distributed displacement of the spins in the observation Δ time between the two PFG's. If the displacement of the spins is a net flow in the gradient direction then also a net phase shift ϕ can be observed, proportional to the product $\gamma\delta G$ and the displacement R of the spins in the observation time.
Without a prior knowledge of the flow-profile within the pixel flow is difficult to quantify in a single shot experiment at fixed values of G, δ, and Δ (1,2). The solution to this quantification problem is to measure the signal intensity S as a function of G. A Fourier transformation of S (G) results in the average propagator P. P gives the probability that a spin at any initial position is displaced by R in the observation time. By division of P by Δ the flow-profile is obtained. This type of measurement is called displacement or q-space imaging and can be done localised but spatially unresolved, spatially resolved on a line through the sample (3) or spatially resolved in two dimensions (4), though this takes a lot of time (several hours). Here a method is presented which is able to record a full 2D spatially resolved q-space-image within short acquisition times (around 20 minutes). Two PFG's were incorporated in a turbo spin echo sequence which phase-encodes even and odd spin-echoes separately to two sets of q-space-images.

This new sequence proved its worth on a phantom with a small tube (i.d. 3 mm) of flowing water which passes the slice (thickness 3 mm) flowing up and down inside a test tube with stationary water and an air gap. 32 Images (128 * 128 pixels) obtained at 20 MHz with a turbofactor of 16 were used to sample Q-space. The forthcoming propagators were fitted to a Gaussian of which the position of the maximum gives the displacement of the spins in time Δ which is plotted in the figure. The total acquisition time was 16.30 min.

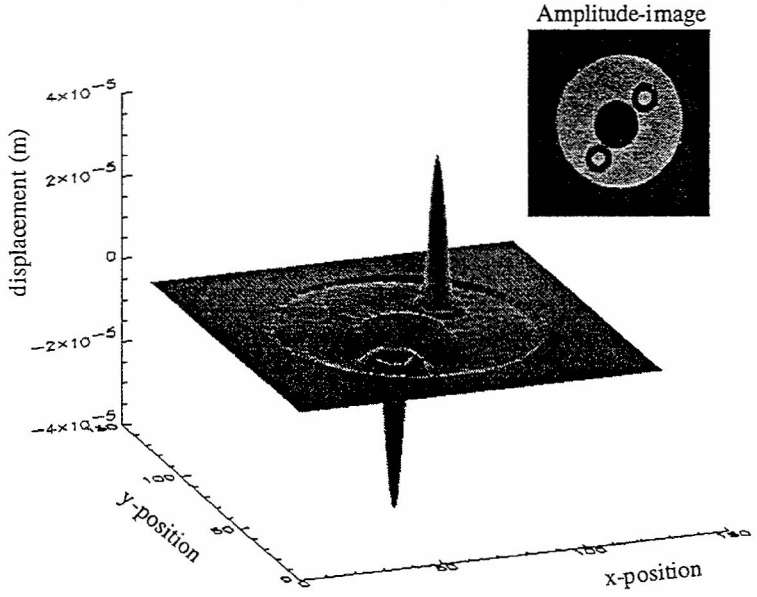

The spatially localised displacement of water in the phantom. Field of view 40 mm, Δ 6.96 ms, mean flow-velocity 2.4 mm/s.

More difficult flow-profiles were measured in an artificial kidney consisting of a glass tube with 1000 capillaries with permeable walls with an i.d. of around 200 µm, that clearly showed a non-uniform flow-pattern over the bundle of capillaries. Finally measurements were performed on whole plants which show diffusion-constants and flow-velocities within 10 % accuracy in physiologically acceptable acquisition times.

References:
1. Snaar, J.E.M. and Van As, H., 1990. Discrimination of different types of motion by modified stimulated-echo NMR. J. Magn. Reson. 87: 132-140.
2. Mansfield, P. and Issa, B., 1994. Studies of fluid transport in porous rocks by echo-planar MRI. Magn. Reson. Imag., 12: 275-278.
3. van Dusschoten, D., van Noort, J. and Van As, H., 1997. Displacement imaging in porous media using the linescan NMR technique. Geoderma, in press.
4. Callaghan, P.T., 1991. Principles of Nuclear Magnetic Resonance Microscopy. Clarendon Press, Oxford.

Diffusion Imaging with Hyper-Polarized ^{3}He Gas

D. M. Schmidt[1], J. S. George[1], S. I. Penttila[1], A. Caprihan[2], and E.F. Fukushima[2]

[1]Los Alamos National Laboratory, Los Alamos, NM 87545

[2]Lovelace Respiratory Research Institute, Albuquerque, NM 87108

In this work we demonstrate some novel aspects of diffusion with MRI and hyper-polarized ^{3}He gas. We have obtained one-dimensional images of ^{3}He gas diffusing in a slice marked by inversion of its magnetization, a technique previously used for observing diffusion of thermally polarized ^{129}Xe gas. Next the pulsed-gradient technique of Stejskal and Tanner was used for making a one-dimensional diffusion image of the gas with and without a temperature gradient present. The diffusion constant with the two methods agreed with each other and in a gas cell at 7 atm pressure it was 12 mm^2/s. In addition, we demonstrated that temperature changes can be dynamically monitored by diffusion images of ^{3}He gas.

EFFICIENT SIMULATION OF NMR IMAGING SEQUENCES BY ISOCHROMAT SUMMATION

PAVEL SHKARIN AND RICHARD G. S. SPENCER
National Institutes of Health, National Institute on Aging
4940 Eastern Avenue, Baltimore, MD 21224

Introduction: A number of computational methods are available to simulate complex imaging sequences. One of the earliest, introduced over a decade ago, is based upon following the time evolution of spin isochromats as they evolve in response to rf pulses and periods of free precession. While this, in some sense, permits an exact simulation, application of this method has been limited by the enormous numbers of isochromats required to achieve accurate results, resulting in excessively long computation times. We have re-examined this approach, and have developed an efficient, flexible, and accurate isochromat summation algorithm which permits the simulation of the time-domain signal resulting from arbitrary two-dimensional Fourier imaging sequences. The number of isochromats required to achieve a specified degree of precision as compared with the exact image is calculated, taking into account transverse relaxation and the potential for artifactual refocussing due to finite isochromat spacing. No assumptions are made regarding transverse dephasing, so that complicated sequences of direct and stimulated echoes are fully modeled. Thus, modern single–shot methods such as Burst may be simulated in a natural fashion. Our time-domain simulation readily permits the incorporation of T_1 and T_2 effects and analysis of a wide range of artifacts. Stimulated echo formation is fully incorporated into the formalism with no restrictions. The effects of inhomogeneous line broadening in spin-echo as compared with gradient-echo based sequences are clearly seen.

Methods: We model the complete time-domain signal as a finite Fourier series, where each term corresponds to an isochromat at a location (x_i, y_j) within the imaging plane. The number of isochromats required per pixel is calculated as a function of the required accuracy. The coefficients of the Fourier series evolve in response to pulses and periods of free precession. The frequency of $v_{i,j}$ of an isochromat is given by

$$v_{i,j}(t,x_i,y_j) = v_i^0{}_{,j}(x_i,y_j)+x_iG_x(t)+y_jG_y(t), \qquad (1)$$

where $v_i^0{}_{,j}(x_i,y_j)$ is a local frequency in the absence of gradients, and $G_x(t)$ and $G_y(t)$ are read and phase gradients, respectively. The signal for a specified rf and gradient sequence is reconstructed by summation of all isochromats. In the simplest case of Fourier imaging, signals from each of the appropriate phase steps are simulated, and the full image then follows by 2D-FT. The results of more complex sequences, such as EPI, BURST and QUEST are likewise reconstructed from simulations incorporating results obtained by specification of exact rf and gradient timings.

Results: We have applied our simulation to computer–defined objects with specified distributions of T_1, T_2, p, and inhomogeneous linewidth. Simple spin warp results are obtained, for a 64x64 pixel matrix size, within one minute on a Silicon Graphics Challenge XL system. With incomplete relaxation, the CPU time increased to approximately 20 minutes. Results from a 32-echo Burst sequence are obtained within approximately 3 minutes. Aliasing in the read and phase directions and its elimination by parameter adjustment is demonstrated. The stripe artifact due to pulse imperfections and the zipper artifact due to incomplete transverse dephasing between phase encode steps in spin warp imaging are recreated. The removal of these artifacts with appropriate homospoil pulses is demonstrated. Distortions in Burst imaging resulting from increasing excitation pulse angle and from short T2 effects are simulated.

References

1. Shkarin P. and Spencer R.G.S. Direct Simulation of Spin Echoes by Summation of Isochromats. Concepts in Magnetic Resonance 8(4):253-268, 1996.
2. Shkarin P. and Spencer R.G.S. Time Domain Simulation of Fourier Imaging by Imaging by Summation of Isochromats. International J. Imaging Systems and Technology (in press, 1997).

INDEX and ADDRESSES

Index

Name	Affiliation	Address	Phone	E-mail
Ailion, David	Department of Physics University of Utah	218 James Fletcher Building Salt Lake City, UT 84112	(801) 581-6973 (801) 581-4801 Fax	ailion@mail.physics.utah.edu
Airey, David	Centre for Medical and Health Physics	Queensland University of Technology P.O. Box 2434 Brisbane QLD 4001 Australia	61 7 3864 4206 61 7 3864 2924 61 7 3864 1521 FAX	d.airey@qut.edu.au
Altobelli, Steve	New Mexico Resonance	2425 Ridgecrest Drive SE Albuquerque, NM 87108	(505)262-7155 ext 5025 (505)262-7043 FAX	salto@nmr.org
Andrew, E. Raymond	University of Florida Department of Physics	215 Williamson Hall Gainesville, FL 32611	(352) 392-6691 (352) 392-8863	andrew@phys.ufl.edu
Balcom, Bruce J.	Physics Dept University of New Brunswick	P.O. Box 4400 Fredericton, N.B., Canada E3B 5A3	(506) 453-4723 (506) 453-4581	bjb@unb.ca
Baldwin, Bernie	Phillips Petroleum Co.	103GB, Bartlesville, OK 74004	(918)661-9518 (918)662-2047	babaldw@bvemx.ppco.com
Bartusek, Karel,	Academy of Sciences of the Czech Republic Institute of Scientific Instruments	Kralovopolska 147 Brno, Czech Republic 61264	420 5 41514243 420 5 41514402 FAX	bar@isibrno.cz
Baumann, Herbert	Pharmacia Upjohn	Uppsala, Sweden S-75182	46 18 164220 46 18 166387 FAX	herbert.baumann@eu.pnu.com
Berliner, Lawrence J.	Department of Chemistry Ohio State University	Newman-Wolfrom 1118 100 West 18th Avenue Columbus, OH 43210	(614) 292-0134 (614) 292-1532 FAX	Berliner@chemistry.MPS.OHIO-STATE.EDU
Beyea, Steven D.	Physics Dept University of New Brunswick	P.O. Box 4400 Fredericton, N.B., Canada E3B 5A3	(506) 453-4723 (506) 453-4581	z56c@unb.ca
Blackband, Stephen J.	Center for Structural Biology University of Florida	Box 100245 Gainesville, FL 32610-0245	(352) 846-2854 (352) 392-3422 FAX	blackie@abbot.health.ufl.edu
Blazek, Almira	Dept of Chemistry University of British Columbia	2036 Main Mall Vancouver, BC V6T 1Z1 Canada	(604) 822-2293 (604) 822-2847	ablazek@chem.ubc.ca
Bluemich, Bernhard	Societe d'Ampere Institut fur Makromolekulare Chemie	Worringer Weg 1 Aachen, 52056, Germany	49 241 806420 49 241 8888185 FAX	bluemich@erato.mc.rwth-aachen.de
Bluemler, Peter	Institut fur Makromolekulare Chemie	Worringer Weg 1 Aachen, 52056, Germany	49 241 806971 49 241 8888185 FAX	bluemler@rwth-aachen.de

Name	Affiliation	Address	Phone	E-mail
Bohris, Alexander J.	Department of Physics University of Surrey	Guildford, Surrey, UK GU2 5XH	44 1483 300800 xt 2694 44 1483 259501 FAX	A.Bohris@surrey.ac.uk
Botto, Robert	Chemistry Division/Bldg.200, Argonne National Laboratory	9700 South Cass Ave., Argonne, IL 60439	(630)252 3524 (630)252 9288 fax	robert_botto@qmgate.anl.gov
Bowtell, Richard	Magnetic Resonance Centre Department of Physics University of Nottingham	University Park Nottingham NG7 2RD UK	44 115 9514751 44 115 9515166 FAX	ppzrwb@ppn1.physics.nottingham.ac.uk
Britton, Melanie	Massey University Physics Department	Palmerston North, New Zealand	64 6 350 5333 64 6 354 0207 FAX	m.m.britton@massey.ac.nz
Burnett, Lowell J.	Quantum Magnetics	7740 Kenamar Court San Diego, CA 92121	(619) 566-9200 (619) 566-9388 FAX	ljb@qm.com
Callaghan, Paul T.	Department of Physics Massey University	Palmerston North, New Zealand	64 63 690 99 64 63 540 207 FAX	p.callaghan@massey.ac.nz
Caprihan, Arvind	New Mexico Resonance	2425 Ridgecrest Drive SE Albuquerque, NM 87108	(505)262-7155 ext 5025 (505)262-7043 FAX	arvind@nmr.org
Codd, Sarah	Massey University Physics Department	Palmerston North, New Zealand	64 6 350 5333 64 6 354 0207 FAX	S.L.Codd@Massey.ac.nz
Cory, David G.	Massachusetts Institute of Technology	NW14-4111 150 Albany Street Cambridge, MA 02139	(617) 253-3806 (617) 253-5405 FAX	dcory@mit.edu
Crozier, Stuart	Centre for Magnetic Resonance, The University of Queensland	St. Lucia, Qld 4072, Australia	61 7 3365 4100	stuart.crozier@cmr.uq.edu.au
Davies, Gareth R.	University of Aberdeen Biomedical Physics	Forester Hill Aberdeen, Scotland AB25 2ZD	44 224 681 818, ext 53192 & 52861 44 224 685 645 FAX	g.r.davies@biomed.abdn.ac.uk
De Los Santos, Armando	Southwest Research Institute	P.O. Drawer 28510 San Antonio, TX 78228-0510	(210) 522-2363 (210) 520-9935	adlsantos@swri.edu
Doty, F. David	Doty Scientific, Inc.	700 Clemson Rd., Columbia, SC 29223	(803)788-6497 (803)736-5495	
Doughty, Daryl A.	BDM Petroleum Technologies	P. O. Box 2543, Bartlesville, OK 74005	(918)338-4474 (918)338-4544fax	ddoughty@bdm.com

Name	Affiliation	Address	Phone	E-mail
Duh, Andrej	Institute of Mathematics and Physics, University of Maribor	Smetanova 17, 2000 Maribor, Slovenia		andrej@fiz.uni-lj.si
Eaton, Gareth	Department of Chemistry and Biochemistry University of Denver	Denver, CO 80208	(303) 871-2980 (303) 871-2254 FAX	geaton@du.edu
Erofeev, Leonid	Institute for Chemical Physics	Chernogolovka, Moscow, Russia	7 095 913 23 10 7 096 515 35 88 FAX	erofeev@icp.ac.ru
Fink, Gerhard	Institut fur Makromolekulare Chemie	Worringer Weg 1 Aachen, 52056, Germany	49 241 806425 49 241 8888185 FAX	gerd@erato.mc.rwth-aachen.de
Fordham, Edmund	Schlumberger-Doll Research	Old Quarry Road Ridgefield, CT 06877-4108	(203) 431-5208 (203) 438-3819 FAX	fordham@ridgefield.sdr.slb.com
Foris, Anthony	DuPont Company	Jackson Lab/Chambers Works Deepwater, NJ 08023	(609) 540-2034	
Fukushima, Eiichi	New Mexico Resonance	2425 Ridgecrest Drive SE Albuquerque, NM 87108	(505)262-7155 ext 5025 (505)262-7043 FAX	eiichi@nmr.org
Garroway, Allen N.	Naval Research Laboratory Code 6122	Washington, DC 20375-5342	(202) 767-2323 (202) 767-0594 FAX	garroway@nrl.navy.mil
Gasper, Lothar	Institut fur Makromolekulare Chemie	Worringer Weg 1 Aachen, 52056, Germany	49 241 806425 49 241 8888185 FAX	lothar@erato.mc.rwth-aachen.de
Gerald, Rex	Chemical Technology Argonne National Laboratory	9700 South Cass Avenue Argonne, IL 60439	(630) 252-4214	Gerald@cmt.anl.gov
Giesen, Roland	Institut fur Makromolekulare Chemie	Worringer Weg 1 Aachen, 52056, Germany	49 241 806425 49 241 8888185 FAX	giesen@erato.mc.rwth-aachen.de
Goerke, Ute	University of Surrey	Guildford, Surrey, UK GU2 5XH		ute.goerke@physik.uni-ulm.de
Golightly, John	Physical Chemistry Dept., Nottingham University, University Park	Nottingham, England, UK NG7 2RD	44 115 9513558 44 115 9513562fax	pcxjag@unix.ccc.nottingham.ac.uk
Gordon, Roy	Bruker Instruments	19 Fortune Drive, Manning Park, Billerica, MA 01821	(508)667-9580; (508)667-0985fax	ca@bruker.com
Grondey, Hiltrud	Dept of Chemistry University of British Columbia	2036 Main Mall Vancouver, BC V6T 1Z1 Canada	(604) 822-2293 (604) 822-2847	hgrondey@chem.ubc.ca

Name	Affiliation	Address	Phone	E-mail
Gross, Dieter	Bruker Analytische Messtechnik GMBH	Silberstreifen Rheinstetten D-76287 Germany	49 721 5161 167 49 721 5161 297 FAX	dgr@bruker.de
Guthausen, Andreas	Institut fur Makromolekulare Chemie	Worringer Weg 1 Aachen, 52056, Germany	49 241 806430 49 241 8888185 FAX	goody@erato.mc.rwth-aachen.de
Haacke, Mark	Malinckrodt Inst. of Radiology Washington University	510 S. Kingshighway St. Louis, MO 63110	(314) 362-2737 (314) 362-2350	haacke@mirlink.wustl.edu
Haase, Axel	Institute of Physics University of Wuerzburg	Am Hubland D-97074 Wuerzburg Germany	49 931 888 5868 49 931 888 5851 FAX	haase@physik.uni-wuerzburg.de
Hafner, Siegfried	Max-Planck-Institut fur Polymerforschung	Ackermannweg 10 55128 Mainz, Germany	49 6131 379 126 49 6131 379 100	hafner@mpip-mainz.mpg.de
Haishi, Tomoyuki	Institute of Applied Physics Univ of Tsukuba	1-1-1 Tennoudai Tsukuba, Ibaraki 305, Japan	0298 53 5214 0298 53 5205 FAX	haishi@mrlab.bk.tsukuba.ac.jp
Haken, Rolf	Institut fur Makromolekulare Chemie	Worringer Weg 1 Aachen, 52056, Germany	49 241 806430 49 241 8888185 FAX	rolf@erato.mc.rwth-aachen.de
Hall, Laurance D.	Herchel Smith Lab. for Med. Chem. University of Cambridge	Robinson Way GB-Cambridge, CB2 2PZ UK	44 223 336 805 44 223 336 748 FAX	ldh11@hslmc.cam.ac.uk
Hammel, Chris	Condensed Matter and Thermal Physics	MST 10 MS K764 Los Alamos National Laboratory Los Alamos, NM 87545	(505) 665-0759 (505) 665-7652 FAX	pch@lanl.gov
Han, Song-I	Institut fur Makromolekulare Chemie	Worringer Weg 1 Aachen, 52056, Germany	49 241 806425 49 241 8888185 FAX	songi@erato.mc.rwth-aachen.de
Hedlund, Laurence W.	Center for In Vivo Microscopy Department of Radiology	Duke University Medical Center Durham, NC 27710	(919) 684-7767 (919) 970-4213 FAX	lwh@orion.mc.duke.edu
Heuert, Uwe	Uni Halle, Dept of Physics	Friedemann-Bach-Pl.6 D-06108 Halle, Germany	49 345 5525595 49 345 5527161 FAX	heuert@physik.uni-halle.de
Hudson, Alex	Magnetic Resonance Centre Department of Physics University of Nottingham	University Park Nottingham NG7 2RD UK	44 115 9514751 44 115 9515166 FAX	Hudson@magres.nottingham.ac.uk
Hunter, Geoffrey	University of Dundee Dept of Chemistry	Dundee DD1 4HN Scotland UK	44 1382 344305 44 1382 345517 FAX	G.Hunter@Dundee.ac.uk
Iwamiya, Joseph H.	Lockheed Martin Missiles & Space, O/H1-32, B/204	3251 Hanover Street, Palo Alto, CA 94304	(650) 424-3480; (650) 354-5795fax	joe.iwamiya@lmco.com

Name	Affiliation	Address	Phone	E-mail
Jackson, Jasper	New Mexico Resonance	2425 Ridgecrest Drive SE Albuquerque, NM 87108	(505)262-7155 ext 5025 (505)262-7043 FAX	jjackson@lrri.org
Jacobs, Russell E.	California Institute of Technology	139-74 Beckman Institute Pasedena, CA 91125	(818) 395-2849 (818) 448-5163	rjacobs@caltech.edu
Jonsen, Paul	General Manager, OEE Chemagnetics NMR Instruments Otsuka Electronics Ltd.	7 Claro Court Business Centre Claro Road Harrogate HG1 4BA England	44 1423 531 645 44 1423 531 647 FAX	pj@otsuka.com; pj@otsuka.demon.co.uk
Kamei, Hirotake	Dept of Biomedical Engineering Graduate School of Medicine University of Tokyo	7-3-1 Hongo, Bunkyo-ku Tokyo 113, Japan	81 3 3812 2111 81 3 5689 7215 FAX	kamei@medes.m.u-tokyo.ac.jp
Kanazawa, Yoko	Faculty of Pharmaceutical Sciences, Kyushu University	Maidashi, Higashi-ku, Fukuoka 812-82 Japan	81 92 642 6622 81 92 642 6545 FAX	kanazawa@pch.phar.kyushu-u-ac.jp
Kimmich, Rainer	University of Ulm Sektion Kernresonanz	89069 Ulm Germany	731 5023140 731 5023150 FAX	rainer.kimmich@physik.uni-ulm.de
Kleinberg, Robert	Schlumberger	Old Quarry Road Ridgefield, CT 06877	(203) 431-5410 (203) 438-3819 FAX	KLEINBERG@SLB.COM
Knoergen, Manfred	Uni Halle, Dept of Physics	Friedemann-Bach-Pl.6 D-06108 Halle, Germany	49 345 5525595 49 345 5527161 FAX	knoergen@physik.uni-halle.de
Kockenberger, Walter	Magnetic Resonance Centre Department of Physics University of Nottingham	University Park Nottingham NG7 2RD UK	44 115 9514751 44 115 9515166 FAX	kocken@magres.nottingham.ac.uk
Komlosh, Michal	Massey University Physics Department	Palmerston North, New Zealand	64 6 350 5333 64 6 354 0207 FAX	M.E.Komlosh@Massey.ac.nz
Komoroski, Richard A.	University of Arkansas for Medical Sciences, NMR Lab	Slot 582 4301 West Markham Street Little Rock, AR 72205	(501) 686-6267 (501) 686-5406	rakomoroski@life.uams.edu
Koptyug, Igor V.	International Tomography Center	Institutskaya str. 3A Novosibirsk, 630090, Russia	7 3832 356216 7 3832 352366 FAX	koptyug@tomo.nsc.ru
Kose, Katsumi	Institute of Applied Physics University of Tsukuba	Tennoudai 1-1-1 Tsukuba-City, Ibaraki, 305, Japan	81 298 53 5335 81 298 53 5205 FAX	kose@bukko.bk.tsukuba.ac.jp
Kuethe, Dean	Lovelace Respiratory Research Inst.	2425 Ridgecrest Drive SE Albuquerque, NM 87108	(505)262-7155 ext 5025 (505)262-7043 FAX	dkuethe@lrri.org

Name	Affiliation	Address	Phone	E-mail
Kuhn, Winfried	IIC Innovative Imaging Corp.	Langental 18 D-66440 Blieskastel Germany	49 6842 3448 49 6842 3449 FAX	wpk01@t-online.de
Lane, Deirdre	Department of Physics University of Surrey	Guildford, Surrey, UK GU2 5XH	44 1483 300800 xt 2722 44 1483 259501 FAX	D.Lane@surrey.ac.uk
Larson, Gary	ISOTEC, Inc.	3858 Benner Road, Miamisburg, OH 45342	937-859-1808	
Lauterbur, Paul	University of Illinois Biomedical Magnetic Resonance Lab	1307 West Park Street Urbana, IL 61801	(217) 244-0600 (217) 244-1330 FAX	pcl@bmrl.med.uiuc.edu
Lee, John Joowon	U of Illinois Urbana Biomed Mag Res Lab	1307 West Park Street Urbana, IL 61801 USA	(217) 244-0600 (217) 244-1330 FAX	jlee@bmrl.med.uiuc.edu
Leisen, Johannes	Georgia Institute of Technology School of Textile & Fiber Engineering	801 Ferst Drive Atlanta, GA 30332-0295	404-894-9241 404-894-9766 FAX	johannes.leisen@textiles.gatech.edu
Lindquist, Diana	University of Arkansas at Little Rock Department of Applied Science	2801 South University Little Rock, AR 72204	(501) 686-6105 (501) 686-5406 FAX	DMLINDQUIST@UALR.EDU
Liu, Haiying	University of Minnesota	Box 292, 420 Delaware, Minneapolis, MN 55455	612-626-0951 612-625-9611fax	liu@sparky.drad.umn.edu
Lloyd, Charles	University of Dundee Dental School	University of Dundee Dundee DD1 4HN Scotland, UK	44 1382 635979 44 1382 225163fax	c.h.lloyd@dundee.ac.uk
Lonergan, Andrew	Magnex Scientific	970 Howe Road, Martinez, CA 96553	(510) 229-8000 (510) 229-8100fax	nmr magnex@aol.com
Mair, Ross W.	Harvard-Smithsonian Centre for Astrophysics Brigham & Women's Hospital	60 Garden Street, MS 59 Cambridge, MA 02138	(617) 495-7213 (617) 496-7690fax	rmair@cfa.harvard.edu
Martin-Landrove, Miguel	Centro de Resonancia Magnetica Universidad Central de Venezuela	Apartado Postal 47586 Caracas 1041-A, Venezuela	582-6052194 582-928903 582 2188 FAX 582-928903 FAX	landrove@neblina.reacciun.ve mmartin@tierra.ciens.ucv.ve
Mastikhin, Igor				mast@tomosoft.nsk.su

Name	Affiliation	Address	Phone	E-mail
Mateescu, G.D.	Department of Chemistry Case Western Reserve University	Cleveland, OH 44106-7078	(216) 368-2589 (216) 368-3006fax	gdm2@po.cwru.edu
Mattingly, Mark	Bruker Instruments, Inc.	19 Fortune Drive Manning Park Billerica, MA 01821	(508) 667-9580 (508) 667-0985fax	mm@bruker.com
McConville, Patrick	MRI Group Centre for Medical & Health Physics	School of Physical Sciences Queensland Univ of Technology GPO 2434 Brisbane, QLD, Australia 4001	617 3864 4206 617 3864 1521	b.moffat@qut.edu.au
McDonald, Peter J.	Department of Physics University of Surrey	Guildford, Surrey, UK GU2 5XH	44 1483 300800 xt 2722 44 1483 259501 FAX	P.McDonald@surrey.ac.uk
Miller, Joel B.	Naval Research Laboratory Chemistry Division, Code 6120	Washington, DC 20375-5342	(202) 767-2337 (202) 767-0594 FAX	joel.b.miller@nrl.navy.mil
Miyata, Masafumi	Structural Division Port and Harbour Research Institute	Ministry of Transport, 3-1-1 Nagase, Yokosuka, Kanagawa 239, Japan	81 468 44 5029 81 468 44 0839 FAX	miyata@cc.phri.go.jp
Moffat, Brad	Centre for Medical & Health Physics Queensland Univ of Technology	G.P.O. Box 2434 Brisbane, Qld 4001 Australia	61 7 3864 4205 61 7 3870 2019 FAX	b.moffat@qut.edu.au
Mohoric, Ales	Faculty of Mathematics and Physics University of Ljubljana	Jadranska 19 1000 Ljubljana, Slovenia	386 61 1766 591 386 61 217 281 FAX	ales@fiz.uni-lj.si
Morita, Toshikazu	Structural Division Port and Harbour Research Institute	Ministry of Transport, 3-1-1 Nagase, Yokosuka, Kanagawa 239, Japan	81 468 44 5029 81 468 44 0839 FAX	morita@cc.phri.go.jp
Morris, H. Douglas	U of Illinois Urbana Biomed Mag Res Lab	1307 West Park Street Urbana, IL 61801 USA	(217) 244-0600 (217) 244-1330 FAX	dmorris@bmrl.med.uiuc.edu
Mueller, Detlef	Bruker Analytik	Silberstreifen Rheinstetten D-76278 Germany	49 721 51610 49 721 5161 297 FAX	drm@bruker.de
Mullins, Paul	Smithkline Beecham	The Frythe, Welwyn Hertz ALG 9AR, UK	44 1438 782744 44 1279 627427 FAX	
Murphy-Bosch, Joe	Institute for Cancer Research	7701 Burholme Avenue Philadelphia, PA 19111	(215) 728-3156 (215) 728-3105FAX	jmurphy@abel.nmr.fccc.edu

Name	Affiliation	Address	Phone	E-mail
Naruse, Satoru	Department of Internal Medicine II Nagoya University School of Medicine	65 Tsurumaicho Showaku Nagoya, 466 Japan	81 52 744 2170 81 52 744 2179	snaruse@tsuru.med.nagoya-u.ac.jp
Navon, Gil	Tel Aviv University	Ramat Aviv Tel Aviv, 69978 Israel	972 3 6408156 972 3 6410665 FAX	navon@post.tau.ac.il
Newling, B.	Department of Physics University of Surrey	Guildford, Surrey, UK GU2 5XH	44 1483 300800 xt 2694 44 1483 259501 FAX	B.Newling@surrey.ac.uk
Nunes, Teresa G.	ICTPOL/IST Departamento de Engenharia de Materiais	Av. Rovisco Pais, 1 1096 Lisboa Codex, Portugal	351 1 8418101 351 1 8418101 FAX	pcteresa@alfa.ist.utl.pt
Ogawa, Kuniyasu	Research Center for Carbon Recycling & Utilization, Tokyo Institute of Technology	2-12-1 Ookayama Meguro-ku, Tokyo 152 Japan	81 3 5734 3553 81 3 5499 3974 FAX	ogawak@mep.titech.ac.jp
Oh, Hwan	Division of Engineering, Colorado School of Mines	Golden, CO 80401-1887	(303)384-2040	hoh@slate.mines.edu
Okerlund, Linda	Bruker Instruments	47697 Westinghouse Dr., Fremont, CA 94539	510-683-4300 510-490-6586fax	lso@bruker.com
Pan, Yong	Procter and Gamble Miami Valley Lab	P.O. Box 538707 Cincinnati, OH 45253-8707	(513) 627-0123 (513) 627-1233	pany@pg.com
Peacock, Evan	Central Science Laboratory University of Tasmania	GPO Box 252-74 Sandy Bay Tasmania, Australia 7001	61 362267821 61 362262494 FAX	e.peacock@utas.edu.au
Planinsic, Gorazd	Department of Physics, University of Ljubljana	Jadranska 19, 61111 Ljubljana, Slovenija	386 61 1766 500 386 61 217 281 FAX	gorazd@fiz.uni-lj.si
Pope, Jim	School of Physical Sciences Queensland University of Technology	GPO Box 2434 Queensland, Australia 4001	61 7 3864 2325 61 7 3864 1804 FAX	j.pope@qut.edu.au
Potter, Kimberlee	Gerontology Research Center NIH/NIA	4940 Eastern Avenue Baltimore, MD 21224	(410) 558-8519 (410) 558-8173	potterk@vax.grc.nia.nih.gov
Randall, E.W.	Department of Chemistry Queen Mary and Westfield College	Mile End Road London E1 4NS England	44 171 775 3258 44 181 981 8745 FAX	E.W.Randall@qmw.ac.uk
Rayner, Tim	Quantum Magnetics	7740 Kenamar Ct. San Diego, CA 92121	(619) 566-7200 (619) 566-7388	timr@news.cts.com

Name	Affiliation	Address	Phone	E-mail
Ripmeester, John	National Research Council of Canada	100 Sussex Drive Ottawa, Ontario, Canada K1A OR6	(613) 993-2011 (613) 998-7833	jar@ned1.sims.nrc.ca
Robert, Hector	FaMAF - Universidad Nacional de Cordoba	Ciudad Universitaria (5000) Cordoba Argentina	54 51 334054	robert@famaf.fis.uncor.edu
Ruff, Jan	Physicalisches Inst., Uni Wuerzburg	Med. Universitatsklinik, 97074 Wuerzburg, Germany	49 931 888-5113 49 931 888-5851 fax	ruff@physik.uni-wuerzburg.de
Saito, Koji	c/o Prof. Dr. Bernhard Bluemich Institute of Macromolecular Chemistry	RWTH - Aachen Melaten, SB Chemie, Worringer Weg 1 D-52056, Aachen, Germany	49 241 80 6479 49 241 8888 185 FAX	saito@erato.mc.rwth-aachen.de
Sarkar, Susanta	Smithkline Beecham, L-940	709 Swedeland Rd., King of Prussia, PA 19496	(610)270 6652 (610)270 6608 fax	sarkar@sbphrd.com
Savelsberg, Ralf	Institut fur Makromolekulare Chemie	Worringer Weg 1 Aachen, 52056, Germany	49 241 806421 49 241 8888185 FAX	ralf.savelsberg@post.rwth aachen.de
Scheenen, T.W.J.	Department of Molecular Physics Wageningen Agricultural University	Dreijenlaan 3 6703 HA Wageningen, The Netherlands	31 317 482723 31 317 482725	tom.scheenen@water.mf.wau.nl
Schlick, Shulamith	Department of Chemistry, University of Detroit Mercy	Detroit, MI 48219-0900	(313)993-1012 (Office) (313)993-3324 (Lab) (313)993-1144 FAX	schlicks@udmercy.edu
Schmidt, David	MS D454, Los Alamos National Laboratory	Los Alamos, NM 87545	(505)665-3584 (505)665-4507	dschmidt@lanl.gov
Scrimgeour, Sheelagh N.	Dental School University of Dundee	Dundee DD1 4HN Scotland, UK	44 1382 635979 44 1382 225163 FAX	s.z.scrimgeour@dundee.ac.uk
Seki, Yasunaga	Internal Medicine II Nagoya University	65 Tsuruma-cho, Skowa-ku Nagoya, Japan 466	81 52 744 2170 81 52 744 2179 FAX	yseki@tsuru.med.nogoya-u.ac.jp
Seo, Yoshiteru	Dept. of Physiology Kyoto Prefectural Univ. of Medicine	465 Kajii-cho, Kawaramachi-Hirokoji Agaru Kamigyo-ku, Kyoto, 444 Japan	81 75 251 5311 81 75 251 0295 FAX	yseo@phys.phys.kpu-m.ac.jp
Seymour, Joseph D.	New Mexico Resonance	2425 Ridgecrest Drive SE Albuquerque, NM 87108	(505)262-7155 ext 5025 (505)262-7043 FAX	jseymour@nmr.org
Shukla, Rajesh	Bracco Research USA	305 College Road East Princeton, NJ 08540	(609) 514-2409 (609) 514-2446	R.Shukla@Research.Bracco.com

Name	Affiliation	Address	Phone	E-mail
Shushakov, Oleg	Russian Acad. Sci. Inst. of Chem. Kinet. & Combust.	3, Institutskaya St. Novosibirsk, 630090, Russia	7 383 2 35 24 77 7 383 2 35 23 50 FAX	hydro@kinetics.nsk.su
Spencer, Richard	NIH/NIA Gerentology Research Center	4940 Eastern Avenue Baltimore, MD 21224	(410) 558-8226 (410) 558-8323fax	spencer@helix.nih.gov
Spyros, Apostolos	Sektion Kernresonanzspektroskopie Universitat Ulm	Albert Einstein Allee 11 89 069 Ulm, Germany	49 731 502 3142 49 731 502 3150 FAX	Apostolos.Spyros@physik.uni-ulm.de
Stepisnik, Janez	Department of Physics University of Ljubljana	Jadranska 19 1000 Ljubljana, Slovenia	386 61 1788563 386 61 217 181 FAX	Janez.Stepisnik@fiz.uni-lj.si
Stilbs, Peter	Department of Chemistry Physical Chemistry Kungl Tekniska Hogskolan	Royal Inst. of Technology s-100 44 Stockholm Sweden	46 8 7908201 46 8 7908207 FAX	peter@physchem.kth.se
Stoddard, R. Dean	Department of Physics, Washington University	1 Brookings Drive St. Louis, MO 63130	(314) 935-6292	rds@howdy.wustl.edu
Sugano, Takahiro	Structural Division, Port and Harbour Research Institute	Ministry of Transport, 3-1-1 Nagase, Yokosuka, Kanagawa 239, Japan	81 468 44 5029 81 468 44 0839	sugano@cc.phri.go.jp
Suh, Byoung Jin	Los Alamos National Laboratory	Mail Stop K764/MST-10 Los Alamos, NM 87545	(505) 665-0364 (505) 665-7652	suh@lanl.gov
Sukumar, Subramaniam	Varian NMR Instruments	3120 Hansen Way Palo Alto, CA 94304-1030	(415) 424-4623 (415) 852-9688 FAX	ssukumar@nmr.varian.com
Szayna, Malgorzata	Dept. ZKM - Bldg. G 201 BASF Aktiengesellschaft	AK/C - Tagungen, B 1 67056 Ludwigshafen, F.R.G.	49 621 60 41949 49 621 60 21863 FAX	malgorzata.szayna@zkm.x400.basf-ag.de
Szeles, J. Constantin	Dept. of Vascular Surgery, University of Vienna Medical School	Waehringer Guertel 18-20, A-1090 Vienna, Austria	43 1 40400 5620 43 1 40400 6958fax	
Takamiya, Hisatake	Orthop. Surgery, Kyoto Prefectural Univ. of Medicine	465 Kajii-cho, Kawaramachi-Hirokoji, Agaru, Kamigyo-ku, Kyoto, 444 Japan	81 75 251 5549 81 75 251 5841fax	takamiya@phys. phys.kpum.ac.jp
Traub, Bernd	Max Planck Institut fur Polymerforschung	Ackermannweg 10 55128 Mainz, Germany	49 6131 379 217 49 6131 379 100 FAX	traub@mpip-mainz.mpg.de
Van der Weerd, L.	Department of Molecular Physics Wageningen Agricultural University	Dreijenlaan 3 6703 HA Wageningen, The Netherlands	31 317 482026 31 317 482725 FAX	louise.meulenkamp@water.mf.wau.nl

Name	Affiliation	Address	Phone	E-mail
Vasina, Elena	Department of Molecular Physics Kazan State University	Kremlevskaya Street, 18 Russia, Kazan, 420008	8432 31 51 71 8432 38 83 95 FAX	Elena.Vasina@ksu.ru
von Kienlin, Markus	Institute of Physics University of Wuerzburg	Am Hubland D-97074 Wuerzburg Germany	49 931 888 5109 49 931 706297 FAX	kienlin@physik.uni-wuerzburg.de
Walton, Jeffrey H.	University of California UCD NMR Facility	Davis, CA 95616	(916) 752-7794 (916) 752-3516	jhwalton@ucdavis.edu
Warren, Warren S.	Department of Chemistry Princeton University	Princeton, NJ 08544-1009	(609) 258-3910 (609) 258-6746 FAX	wwarren@princeton.edu
Weingarten, Klaus	Institut fur Makromolekulare Chemie	Worringer Weg 1 Aachen, 52056, Germany	49 241 806425 49 241 8888185 FAX	klaus@erato.mc.rwth-aachen.de
Wind, Robert A.	Pacific Northwest National Laboratory	P.O Box 999, P7-55 Richland, WA 99352	(509) 376-1115 (509) 376-2303 FAX	ra_wind@pnl.gov
Woelk, Klaus	Inst. Phys. Chem University of Bonn	Wegelerstr. 12 D-53115 Bonn, Germany	49 228 737871 49 228 732551 FAX	woelk@rs1.thch.uni-bonn.de
Xia, Yang	Physics Department Oakland University	274 Hannah Hall Rochester, MI 48309	(248) 370-3420 (248) 370-3408 FAX	xia@oakland.edu
Xu, Su	National Institutes of Health	Bldg. 10, BIN-256, LDRR Bethesda, MD 20892	(301) 402-1981 (301) 402-3216	sxu@helix.nih.gov
Zimmer, Gisela	Institut fur Makromolekulare Chemie	Worringer Weg 1 Aachen, 52056, Germany	49 241 806430 49 241 8888185 FAX	zimmer@erato.mc.rwth-aachen.de
Zweier, Jay L.	The EPR Center, Johns Hopkins Univ., Sch. of Med.	5501 Hopkins Bayview Circle, Baltimore, MD 21224	410-558-8202 410-558-2448 fax	jzweier@welchlink.welch.jhu.edu